Project Acronym:

FUSVET (SEED/1221/0080)

Focused Ultrasound System for Veterinary Chemotherapeutic Applications for Oncology

Deliverable number: 3.4

Title: Evaluation of the MR compatibility and functionality of the robotic system/transducer

Prepared by:

Nikolas Evripidou (CUT)
Anastasia Antoniou (CUT)
Antria Filippou (VET-EX MACHINA)
Kyriakos Spanoudes (VET-EX MACHINA)
Christakis Damianou (CUT)

Date: 31/01/2025

Funded by the European Union NextGenerationEU

Cyprus tomorrow RECOVERY AND RESILIENCE PLAN

Republic of Cyprus

RESEARCH & INNOVATION FOUNDATION

The FUSVET project is funded by the Recovery and Resilience Facility of the NextGenerationEU instrument, through the Research and Innovation Foundation (RIF) of Cyprus.

Table of Contents

Executive Summary

In this deliverable, the evaluation of the 5 degrees of freedom (DOF) robotic device that was developed in the framework of the FUSVET project is presented. The robotic device is integrated with a single-element focused ultrasound (FUS) transducer that is actuated within a conical water container. The developed robotic system and the transducer are fully described in Deliverable 3.1 and Deliverable 3.2, respectively. Initially, both the robotic system and the transducer were extensively evaluated in laboratory and Magnetic Resonance Imaging (MRI) settings on excised pork tissues, agar-based phantoms, and thin polymer plastic films.

Primarily, the motion range of the PC-controlled stages of the robotic device was determined by performing sonications on thin polymer plastic films. Motion of the device was executed along the origin and end points of each axis, where sonications were performed with low acoustical power, resulting in local lesion formation on the plastic film. The motion range of the robotic system was found by measuring distances between the formed lesions. Sonications were then executed in the laboratory on phantoms and excised tissue. Primarily, the focal point of the transducer was localised within the phantom or excised tissue using motion of the device and sonications at low acoustical power. Thereafter, sonications were performed at varied acoustical power to examine the effect of applied sonication parameters on the temperature increase induced within the agar-based phantoms or excised tissue, and determine whether the transducer produces ablative temperatures within the tissue sufficient for lesion formation.

After confirming that the transducer was able to produce ablative temperatures within tissue, motion of the robotic device and the integrated transducer was initiated for the ablation of excised tissue. Sonications were performed using a constant protocol (acoustical power, sonication time, and focal depth) and motion was executed along various grid patterns with varied step sizes to examine the formation of discrete or overlapping lesions. Overlapping lesions were formed on the tissue and the dimensions of the formed lesions were measured to assess the ability of the system to create sufficiently large ablative areas.

Additionally, a series of experiments were performed within a clinical 3 T MRI scanner (Magnetom Vida, Siemens Healthineers, Erlangen, Germany) to assess the MRI compatibility of the robotic device and the transducer and to evaluate the thermal heating abilities of the transducer. The MRI compatibility of the robotic system and the transducer was assessed on an agar-based phantom. MRI magnitude and phase images of the phantom were consecutively acquired during various activation configurations of the robotic system and the transducer using a Fast low angle shot (FLASH) sequence. Signal to noise ratio (SNR) was measured at a specific location on the agar-based phantom on magnitude images, while signal intensity was calculated in the phantom on phase images for the various activation states of the robotic system and the transducer.

A series of sonications were then executed on excised pork tissue and agar-based phantoms to assess the thermal heating abilities of the system. Initially, sonications on excised tissue and agar-based phantoms were executed with varied sonication parameters to evaluate the ability to monitor sonications with MR thermometry. Sonications were also executed on excised tissue to assess the ability to detect inflicted lesions using high resolution T2-Weighted (T2-W) and

T1-Weighted (T1-W) sequences. T2-W sequences were utilised with varied echo time (TE) values to image the tissue at specific timeframes after sonications to assess the effect of the TE on the optimal detection of lesions.

The developed 5 DOF robotic system integrating FUS technology was also evaluated for its *in-vivo* safety and efficacy on tumorgraft murine models. Ten male adult C57BL/6 mice were inoculated with MCA205 mouse fibrosarcoma cells, developing sarcoma tumours, and 7 days after transplantation were employed in experiments to evaluate the response of the tumour growth to FUS sonications delivered with the robotic system. Specifically, the mice were divided in an experimental group ("FUS group", n=5) wherein the tumour grafts were treated with FUS, and a control group ("Control group", n=5) in which no treatment was delivered to the murine models.

An appropriate experimental procedure was followed for each group to ensure that all mice were ethically manipulated, thus guaranteeing animal safety. Mice from both groups were anaesthetised and measurements of tumour diameters were acquired. Tumours on mice of the "FUS group" were sonicated in a grid manner using a constant high-power FUS therapeutic protocol that was appropriately generated based on baseline tumour size. Thereafter, mice from the "Control group" and "FUS group" were allowed to recover from anaesthesia and were monitored for a 7-day period to assess the occurrence of any adverse events arising from natural tumour growth and application of FUS treatment, respectively. FUS was consistently applied over 3 treatment sessions that were delivered at 7, 14 and 21 days following transplantation, while tumour diameter measurements acquired in both groups at 10, 14, and 21 days served as endpoints for evaluating any FUS-related therapeutic effects on tumour growth.

While gross examination of mice of the "FUS group" revealed the successful formation of discrete lesions on targeted tumour areas after each FUS treatment session revealing the system's efficacy in inducing consistent *in-vivo* coagulative tumour necrosis, tumour diameter measurements indicated that tumour growth was significantly ($p<0.1$) suppressed by FUS one week after application of the 2nd FUS treatment session. No acute or long-term FUS-related therapeutic effects were reported from repetitive FUS sessions indicating the *in-vivo* safety of the system, with mice from both groups humanely euthanised shortly after the 21st day due to tumour-related adverse events.

Finally, the safety and efficacy of the robotic system was evaluated on pets (dogs and cats) with naturally occurring tumours. Pets were recruited following a targeted recruitment campaign wherein specific veterinarians across Cyprus were contacted in order to be informed about the project and examine the potential of them providing dog or cat cases for the veterinary clinical trials. Animals were enrolled according to specific eligibility criteria following conscious informed consent from their owners. Veterinary trials lasted 24 months with a total of 18 pets, namely 2 cats and 16 dogs, enrolled in the study.

Sonications were executed with the robotic system following a treat and resect approach. Various sizes and types of tumours were treated with FUS following therapeutic protocols that were appropriately generated based on the size of the tumour. Coagulative necrosis of targeted tumour cells was evidenced by histopathological examination of the resected tumours, while in some cases inflicted lesions were visible by tumour gross examination.

Materials and Methods

Focused Ultrasound (FUS) system

The developed 5 degrees of freedom (DOF) robotic device was connected to several peripheral devices to assemble the FUS system required for ablations. Specifically, the FUS system comprised of the single-element focused transducer that was integrated within the robotic system. The transducer was developed in-house using a non-magnetic piezoceramic element (Hubei Hannas Tech Co., Hubei, Wuhan, China) that was housed in a 3D-printed (F270, Stratasys, Minnesota, USA) Acrylonitrile Styrene Acrylate (ASA) thermoplastic enclosure. The manufactured transducer operates at a nominal frequency (F) of 2.75 MHz, has a diameter (D) of 50 mm and a radius of curvature (ROC) of 65 mm. The fabricated transducer, as integrated within the robotic system, was connected, and tuned to a radiofrequency (RF) amplifier (AG1016, T & C Power Conversion Inc., Rochester, NY, USA) that generated and supplied an amplified electrical signal to the FUS transducer for operation. The manufactured transducer converts electrical power to acoustic power with an efficiency of 30 % as estimated using a precision ultrasound power meter (UPM-DT100N, Ohmic Instruments Co., Missouri, USA). Accordingly, the robotic device was connected to an electronic driving system, which is fully described in Deliverable 3.3, for controlling motion in the 3 PC-controlled stages of the robotic system (X, Y, and Z). The developed treatment planning, control, and monitoring software (Deliverable 3.3) was connected to the hardware to automatically control the robotic motion and the FUS sonication protocols. Figure 1 shows a schematic diagram of the FUS system.

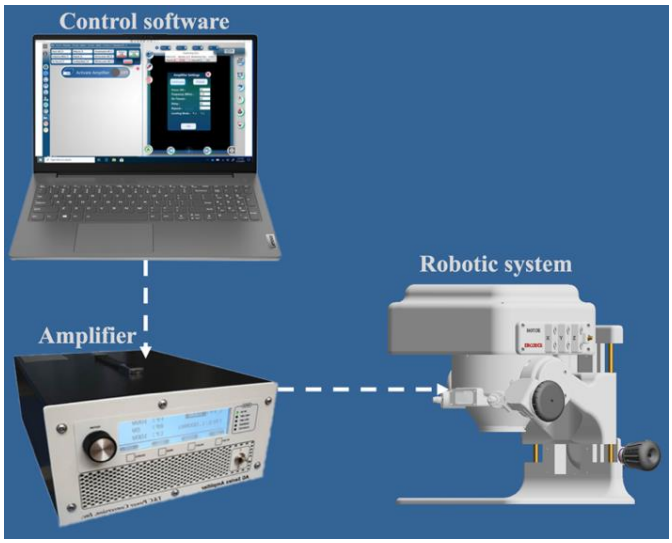

Figure 1: Schematic diagram of the FUS system.

Evaluation on agar-based phantoms, excised pork tissues, and plastic films

Agar-based phantoms

Agar-based phantoms were employed as sonication targets for evaluating the Magnetic Resonance Imaging (MRI) compatibility of the robotic system and assessing the thermal heating capabilities of the manufactured FUS transducer (F=2.75 MHz). The phantoms were manufactured using low-cost inclusion materials and following an easy preparation procedure.

Specifically, the phantoms were developed using deionised and degassed water in appropriate volumes and a constant concentration (6 % w/v) of granulated agar (10164, Merck, Darmstadt, Germany) which is accountable for forming hydrogen bonds between the inclusions and the aqueous solution. In some cases, silicon dioxide in a fine granular form (S5631, Sigma-Aldrich, St. Louis, Missouri, USA), was added in a 4 % w/v concentration to enhance the ultrasonic scattering properties of the fabricated agar-based (6 % w/v) phantoms. The agar-based or agar-based doped with silicon dioxide phantoms were developed in rectangular molds that were designed with a computer-aided design (CAD) software (Inventor Professional, Autodesk, California, USA) and 3D-printed using an industrial rapid prototyping machine (F270, Stratasys) and ASA thermoplastic material. The molds were designed and printed with appropriate dimensions to allow accommodation of the final produced phantoms under the acoustic cone of the robotic system for evaluation purposes. The developed phantoms closely emulate the thermal (conductivity, diffusivity and specific heat), acoustic (propagation speed and attenuation) and magnetic (T1 and T2 relaxation times) properties of specific human soft tissues, thus being ideal for employment as sonication targets during the evaluation experiments.

Excised tissue

Excised pork tissue was also employed in the evaluation experiments of the system. Large pieces of freshly excised pork tissue were acquired from a butcher shop and employed as sonication targets to assess the ability of the transducer to generate ablative temperatures and successfully form demarcated thermal lesions. The employed tissue pieces were selected to have minimal fat layers or other non-homogeneous structures to reduce to a feasible extent the reflection of the ultrasonic beam and allow maximum transmission of acoustic energy.

Polymer Polyvinyl Chloride (PVC) films

Polymer PVC films were also utilised as sonication targets in the evaluation experiments to determine the motion range of the developed robot. The employed PVC films are print plates of an industrial 3D printer (Fortus FDM400mc, Stratasys) that have a minimal thickness (0.7 mm) that does not greatly attenuate ultrasonic beam. The polymer PVC films were utilised since when sonicated they deform and locally form white lesions, thus visually indicating the exact sonication location. The size and shape of the formed lesions correspond somehow to the ultrasonic beam.

Laboratory Experiments

Sonications on thin polymer PVC films

The motion range of the manufactured robotic system was investigated in the laboratory setting through sonications executed on thin polymer PVC films (Fortus FDM400mc print plates, Stratasys) using the transducer of the system. A single PVC film was enclosed within a 3D-printed (CR-10 S4, Creality, Shenzhen, China) Polylactic Acrylate (PLA) plastic film holder as shown in Figure 2A. The PLA holder was developed with dimensions of 83 mm (l) × 83 mm (w) × 113 mm (h) and had a 1 mm thick gap below its top surface allowing secure placement of the PVC film, while a circular aperture with a radius of 83 mm was allowed on

the top surface of the holder, acting as an acoustic window, permitting sonications of the enclosed PVC film. The PLA plastic film holder with the enclosed PVC film was accommodated below the robotic system as shown in Figure 2B, with the PVC film, through the circular aperture of the film holder, in direct contact with the thin membrane that covers the conical water container of the robotic device.

Figure 2: A) Photo of the PLA plastic film holder that was used to secure the PVC films during sonications, and B) Experimental set-up used for sonications on thin PVC films with the plastic film holder accommodated below the acoustic window of the robotic system.

Figure 3 shows the schematic diagram of the experimental set-up. The conical water container of the robotic system was entirely filled with deionised and degassed water, while a thin layer of ultrasound gel (Quick-Eco Gel, AB Medica Group S.A., Barcelona, Spain) was applied between the membrane and the PVC film interface offering optimal acoustic coupling. Noteworthy, lesioning on the PVC films after ultrasonic exposures is attributed to reflection effects of the ultrasound beam arising as a result of significant differences between the acoustic impedances of water (enclosed within the conical water container of the robotic system), and air (present below the bottom surface of the PVC film). Ultimately, to allow lesion formation on the PVC films, the distance between the transducer and the upper surface of the PVC film was set at 60 mm, so that the PVC film was directly placed at the focus of the transducer.

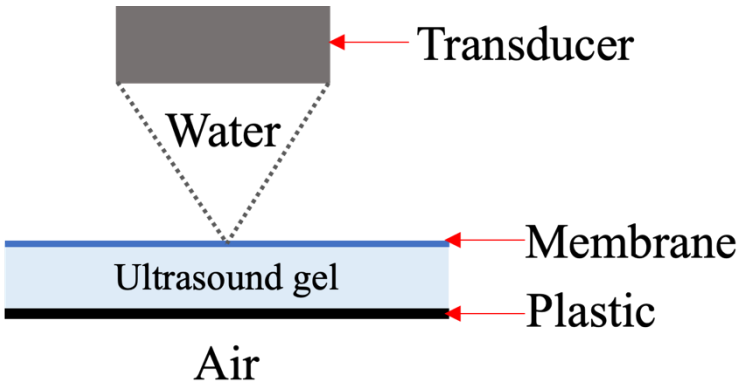

Figure 3: Schematic diagram of the experimental set-up used for sonications on thin PVC films using the robotic system and the transducer.

Manual transducer motion was independently commanded through the developed control software along the PC-controlled X and Y axes of the robotic system, and the origin and end

points of each axis were determined using feedback from the software. At each respective location (origin and end points of X and Y axes) single sonications were executed using an acoustic power of 20 W for a sonication time of 15 s, to determine the motion range on each positioning stage.

Temperature increase in phantom and excised tissue

Temperature measurements were recorded in the laboratory during single sonications executed at varied acoustical power on an agar-based phantom (6 % w/v agar) and on pieces of excised pork tissue using the robotic system and the transducer.

Prior to sonications, a portable X-ray system (IMS001, Shenzhen Browiner Tech Co. Ltd, Shenzhen, China) and a diagnostic ultrasound device (DP-50, Mindray, Shenzhen, China) with a linear probe with a frequency range of 5-10 MHz were used to image the robotic system. The purpose of imaging was to visualize the enclosed contents of the robotic system in order to measure from images the distance between the transducer and the thin membrane that covers the water container of the robotic system. In this manner, for X-ray imaging, the robotic system was laterally accommodated on top of a computed radiography (CR) cassette and X-ray exposure was executed using a tube voltage of 50 kV and a current of 45 mA for an exposure time of 45 ms. After exposure, a CR reader (Vita Flex, Carestream Health Inc., Rochester, NY, USA) was used to digitize the data of the latent image, with the distance between the transducer and the membrane measured using a medical imaging software (Image Suite, Carestream Health Inc.) as indicatively shown in Figure 4.

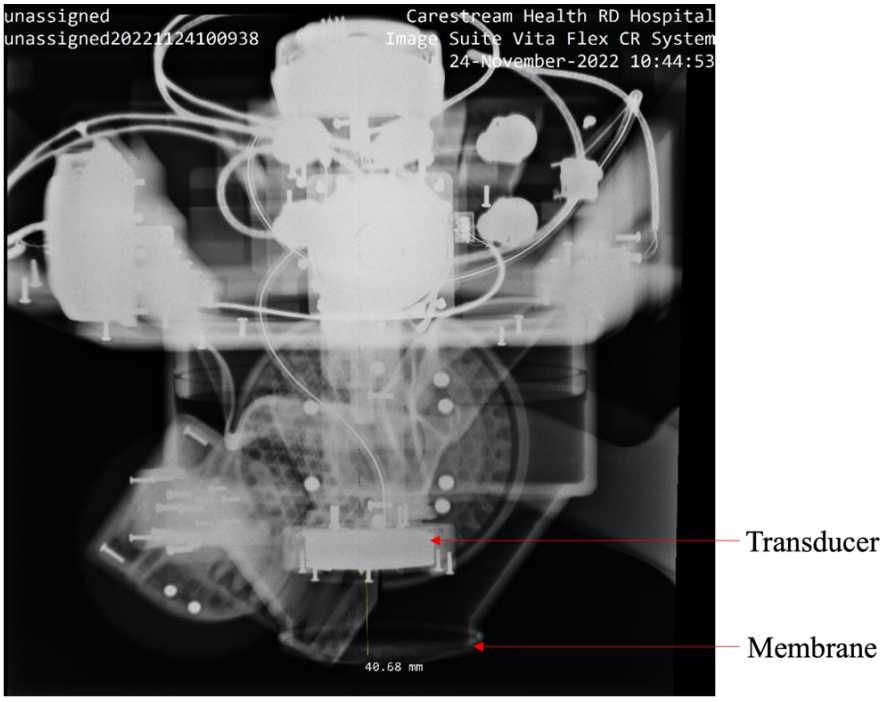

Figure 4: X-ray image of the robotic system acquired to enable measurements of the transducer-membrane distance. For this image a distance of 40.68 mm was measured.

Correspondingly, for ultrasound imaging, the linear probe of the ultrasound system (DP-50, Mindray) was placed on the acoustic membrane of the robotic system and the distance between the transducer and the membrane was estimated as shown in Figure 5.

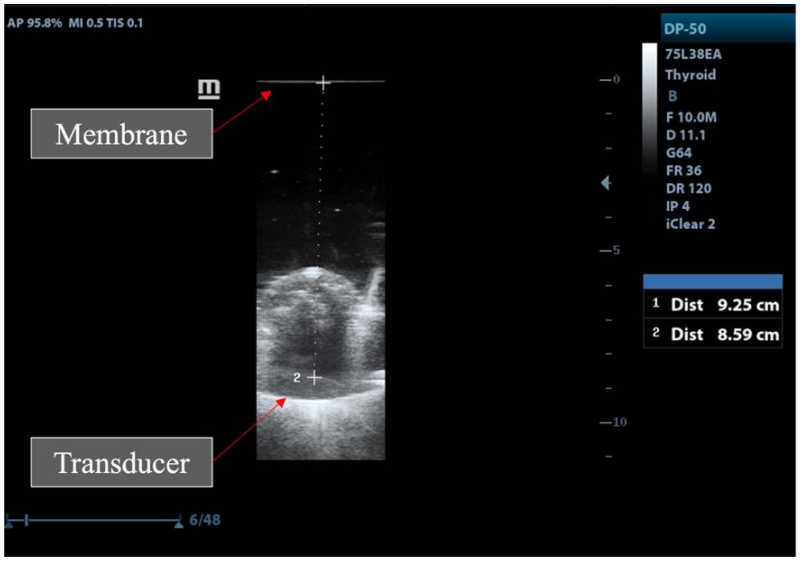

Figure 5: Ultrasound image of the robotic system acquired to enable measurements of the transducer-membrane distance. A distance of 8.59 cm was measured for this image.

Following X-Ray and ultrasound imaging of the robotic device and measurements of the transducer-membrane distance, movement in the Z-axis of the robotic system, which moves the transducer up and down, was commanded with the software to appropriately set the position of the transducer at the required location for sonications. After motion, correct positioning of the transducer at the required location was evidenced by performing X-ray and ultrasound imaging of the robotic system as described above (Figure 4 and Figure 5). Sonications on the agar-based phantom (6 % w/v agar) and excised tissue were executed with the transducer-membrane distance set at 40 mm, resulting in a 25 mm focal depth.

Initially, the agar-based phantom (6 % w/v agar) was positioned under the acoustic membrane of the robotic device with a thin layer of ultrasound gel (Quick-Eco Gel, AB Medica Group S.A.) accommodated in-between to minimise air and achieve acoustic coupling. A 100 μm thin thermocouple (5SC-TT-K-30-36, type K insulated beaded wire, Omega Engineering, Norwalk, Connecticut, USA), which was connected to a digital thermometer (HH806AU, Omega Engineering), was inserted within the phantom at a 25 mm depth, to record temperatures during sonications as shown in Figure 6.

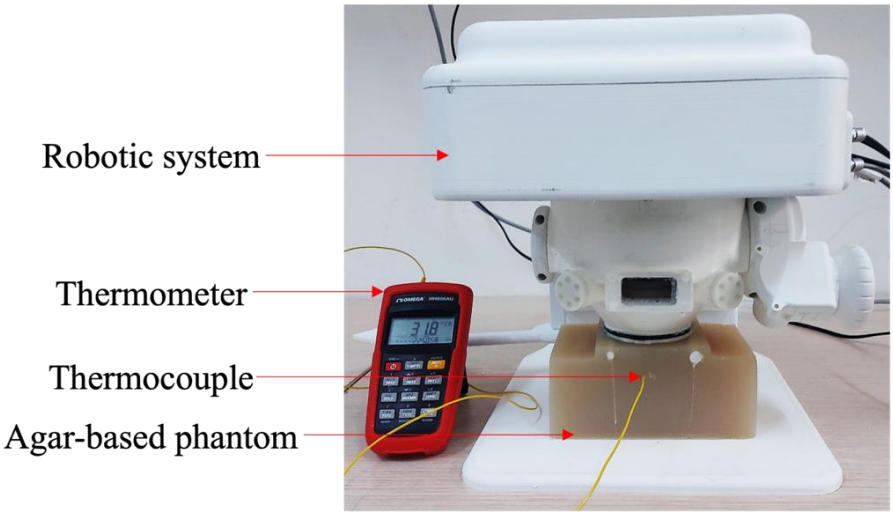

Figure 6: Experimental set-up used for temperature measurements within an agar-based phantom.

After insertion of the thermocouple, the centre of the transducer was set above the thermocouple by executing low power sonications and appropriately moving the transducer in the X and Y axes. Correct positioning of the centre of the transducer directly above the thermocouple was determined at the location where the highest temperature was recorded with the thermocouple. Sonications were then executed at varied acoustical power for a sonication time of 60 s to investigate the effect of power on temperature change.

For sonications on excised tissue, pieces of tissue were individually placed in an identical manner below the membrane of the robotic system, with ultrasound gel (Quick-Eco Gel, AB Medica Group S.A.) added on the membrane-tissue interface for coupling purposes. Accordingly, the thermocouple was inserted at the same 25 mm depth from the upper surface of the tissue to record temperatures during sonications. Similarly, the centre of the transducer was positioned above the thermocouple, and sonications of 60 s duration were performed to record the temperature change at the focal point and observe the effect of power on the induced temperature change.

Ablations of excised tissue in a laboratory setting

Ablations were executed within the laboratory on several pieces of excised tissue to evaluate the ability of the robotic system and transducer to create multiple discrete or overlapping lesions. The robotic system utilises a top-to-bottom approach to ultrasonic delivery, with a thin membrane covering the water container of the device which was filled with deionised and degassed water. The excised pork tissue was accommodated below the acoustic window of the robotic device with ultrasound gel (Quick-Eco Gel, AB Medica Group S.A.) added between the tissue surface and the membrane to serve as an acoustic coupling medium. In this manner, the ability of the system to successfully form lesions with this configuration was investigated. The robotic system was connected through cables with the electronic driving system, the RF amplifier, and the developed software. The software was used to plan the sonication trajectory, control the sonication parameters (acoustic power, sonication time, and time delay between sonications) and the motion of the robotic device through commands that adjust the grid size and the step size between sonications points. Figure 7 shows the experimental set-up used in the laboratory for ablations of excised tissue. Multiple grid sonications in different grid patterns and varied grid step sizes were performed with the software, to assess the ability of the system to inflict either discrete or overlapping lesions on the excised tissue target. Grid sonications, irrespective of the commanded trajectory (grid size and step) were performed at an acoustic power of 60 W for a sonication time of 20 s, and a time delay of 60 s between successive sonications. All sonications were executed with the distance between the transducer and the membrane set at 40 mm, thus resulting in a focal depth of 25 mm within the targeted excised tissue.

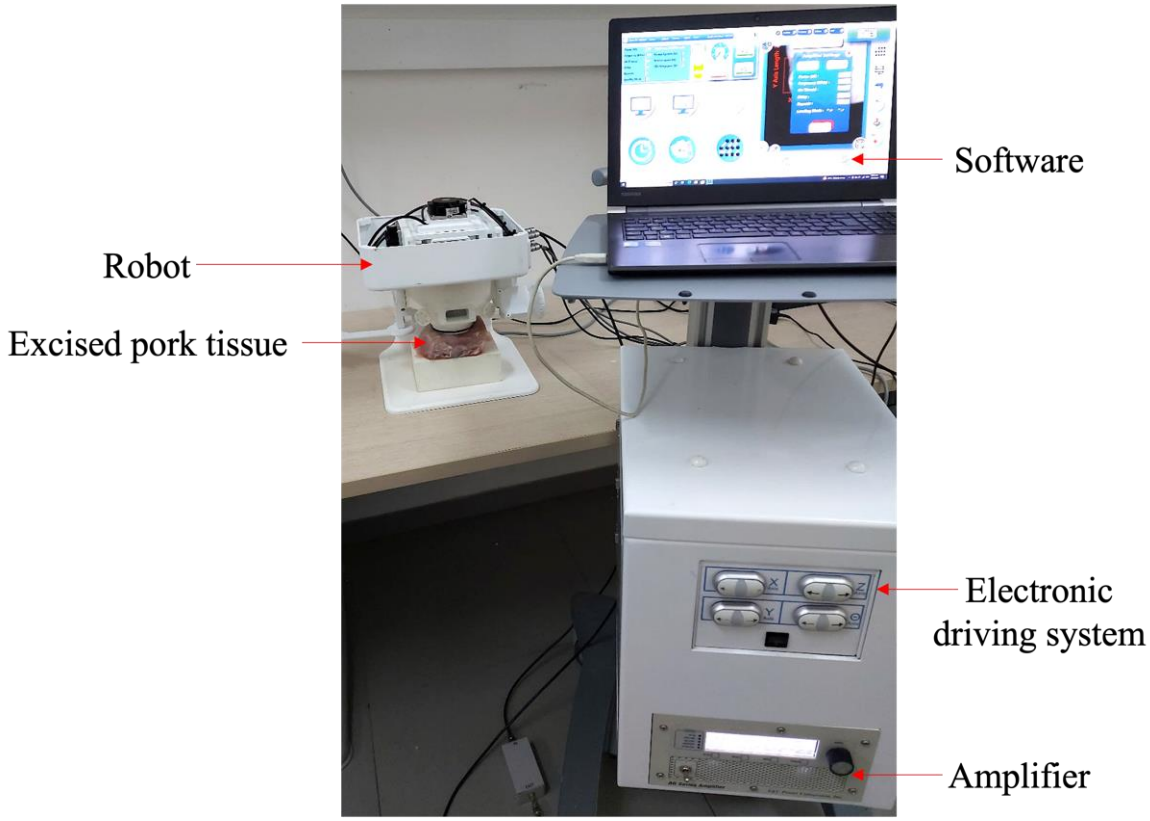

Figure 7: Experimental set-up used for ablation of excised tissue within the laboratory using the robotic device.

MRI Experiments

Experimental setting for MRI experiments

The developed 5 DOF robotic system and the transducer were evaluated for their MRI compatibility and thermal heating abilities within a clinical 3 T MRI scanner (Magnetom Vida, Siemens Healthineers, Erlangen, Germany). The FUSVET robotic system was simply placed on the patient table of the 3 T MRI scanner (Magnetom Vida, Siemens Healthineers). Agar-based phantoms developed with dimensions of 90 mm (l) × 75 mm (w) × 80 mm (h) and pieces of excised pork tissue were employed as sonication targets during the MRI experiments. For each experiment, the employed sonication target (agar-based phantom, or excised tissue) was positioned under the acoustic window of the robotic system. A thin layer of ultrasound gel (Quick-Eco Gel, AB Medica Group S.A.) was applied between the upper surface of the employed sonication target (phantom or excised tissue) and the thin membrane that covers the conical water container of the robot. Ultrasound gel acts as a coupling medium offering maximal transmission of acoustic energy to the target during activation of the transducer. Figure 8 shows the experimental setting used for the MRI experiments, with the system accommodated in the MRI scanner and the agar-based phantom (Figure 8A) or excised pork tissue (Figure 8B) positioned below the acoustic window of the system.

Figure 8: Experimental set-up inside the 3 T MRI scanner with the robotic system positioned on the MRI table and A) an agar-based phantom, or B) excised pork tissue, accommodated beneath the conical acoustic window of the robotic system.

An 18-channel MRI body coil (Body18, Siemens Healthineers) was positioned around the FUSVET system for imaging purposes. The coil was accommodated on the front end, around the sonication target (agar-based phantom or excised tissue) to enhance the detected MRI signal as illustrated by the photo of the experimental setting shown in Figure 9. The FUSVET system was connected to the developed electronic driving system and RF amplifier. Notably, both the electronic driving system and RF amplifier were accommodated in the MRI control room and were connected with the robot through waveguides. Connection of the transducer as integrated within the robot, with the RF amplifier was executed through a low-pass RF filter which was employed to prevent imaging artifacts.

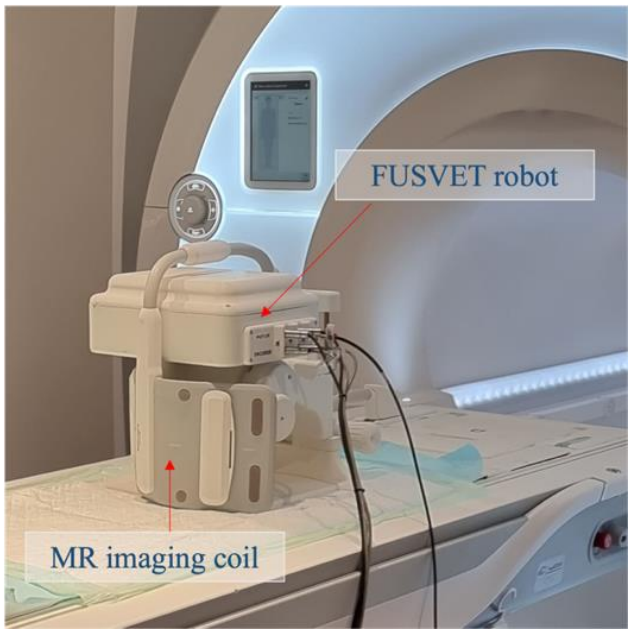

Figure 9: Experimental set-up inside the 3 T MRI scanner with the system positioned on the MRI table and an MR imaging coil accommodated around it for imaging purposes.

MRI compatibility of the robot and transducer

Experiments were executed inside the 3 T MRI scanner (Magnetom Vida, Siemens Healthineers) to assess the MRI compatibility of the FUSVET robot and the integrated transducer. For the MRI compatibility experiments, an agar phantom doped with silicon dioxide (6 % w/v agar, and 4 % w/v silicon dioxide) was positioned under the acoustic window of the system and surrounded by a body coil (Body18, Siemens Healthineers) (Figure 9) that was employed for imaging purposes.

The MRI compatibility of the robotic system, and the ultrasonic transducer was assessed by evaluating the effect of various activation states of the individual components of the system (robotic device, driving electronics, RF amplifier, and transducer) on the Signal to Noise Ratio (SNR) of the acquired MR images. In this manner, the agar-based phantom was sequentially imaged in the coronal plane for a series of different system configurations using a 2D Fast Low Angle Shot (FLASH) sequence with the following parameters: Repetition time (TR) = 25 ms, Echo time (TE) = 10 ms, Field of view (FOV) = 280×280 mm^2, Slice thickness = 3 mm, Acquisition matrix = 96×96, Number of excitations (NEX) = 1, Echo train length (ETL) = 1, Flip angle = 30^o, and Pixel Bandwidth = 501 Hz/pixel. Since the FLASH sequence is normally utilised for Magnetic Resonance (MR) thermometry purposes, it was specifically employed for imaging to assess the impact of the system on the signal loss of the acquired images (magnitude and phase), ultimately evaluating whether the system will severely affect the quality of MR thermometry.

For each activation state, SNR calculations were executed on the acquired magnitude FLASH image of the phantom, thus allowing estimations regarding the impact of the corresponding activation state on the quality of imaging. Specifically, circular regions of interest (ROIs) were chosen on the image at specific locations within the phantom and at the air background (noise). Noise in the air background was assumed to follow a Gaussian distribution. The average signal of the phantom ROI ($SI_{phantom}$) and the standard deviation of the signals from the air ROI (σ_{noise}) were substituted in equation 1 resulting in estimations of the SNR.

$$SNR = {SI_{phantom}}/{\sigma_{noise}} \quad (1)$$

Additionally, for each activation condition, average signal intensities were measured at specific ROIs within the phantom on acquired FLASH phase images (which are used for MR thermometry calculations) to investigate the effect of the corresponding activation on signal loss and thus the sufficient quality of these images for use in MR thermometry.

MRI compatibility of the robotic system

The MRI compatibility of the robotic system was assessed for different configurations of the robotic and electronic driving systems. The electronic driving system requires DC power in order to control the non-magnetic piezoelectric motors (USR60-S3N, Shinsei Kogyo Corp., Tokyo, Japan) and optical encoders (EM1-0-500-I, US Digital Corporation, Vancouver, Washington, USA) that actuate motion in the 3 PC-controlled stages. In this manner, MR imaging, SNR and signal intensity calculations were executed for the three activation states listed in Table 1. Initially, imaging was performed with only the robotic system present in the

MRI bore (i.e., cables not connected), upon connection of the robotic system with the motion cables and the electronic driving system (i.e., cables connected), as well as upon activation of the electronic driving system and the motor drivers (i.e., DC ON).

Table 1: Activation states used to assess the MRI compatibility of the robotic system.

No.	Activation state
1	Cables not connected
2	Cables connected
3	DC ON

MRI compatibility of the transducer

Accordingly, the MRI compatibility of the transducer was evaluated for various activation conditions of the transducer and RF amplifier. MR imaging on which SNR and signal intensity calculations were performed, was executed for the activation states listed in Table 2. Primarily, coronal FLASH images were acquired at the reference condition with solely the robotic system accommodated on the table with no cables connected (i.e., cables not connected). Thereafter, imaging was executed upon connection of the RF cables and the amplifier (i.e., cables connected), upon activation of the amplifier with no power applied to the transducer (i.e., Amplifier ON), as well as upon activation of the transducer at varied acoustical power of 15-60 W (15 W step). During transducer evaluation, the driving system of the robot was removed.

Table 2: Activation states used to assess the MRI compatibility of the transducer.

No.	Activation state
1	Cables not connected
2	Cables connected
3	Amplifier ON
4	Power = 15 W
5	Power = 30 W
6	Power = 45 W
7	Power = 60 W

Ablations of excised tissue in the MRI environment

Experiments were executed on excised pork tissue inside the 3 T MRI scanner (Magnetom Vida, Siemens Healthineers) to assess the thermal heating of the system and the integrated transducer. Pieces of excised tissue were accommodated under the acoustic window of the system and surrounded by the body coil (Body18, Siemens Healthineers) (Figure 9). Initially, a high-resolution T2-Weighted (T2-W) Turbo Spin Echo (TSE) sequence was employed for imaging the robotic system and the excised tissue on an axial plane to assess proper acoustic coupling and determine the focal depth of the sonications (by measuring distance between the transducer and excised tissue). Axial T2-W TSE images of the experimental set-up were acquired with the following parameters: TR = 2520 ms, TE = 51 ms, FOV = 289×280 mm^2, Slice thickness = 5 mm, Acquisition matrix = 256×265, NEX = 1, ETL = 60, Flip angle = 131^o, and Pixel Bandwidth = 150 Hz/pixel. Figure 10 shows the acquired axial T2-W TSE image of the experimental set-up, revealing an excellent coupling between the excised tissue and the robotic system.

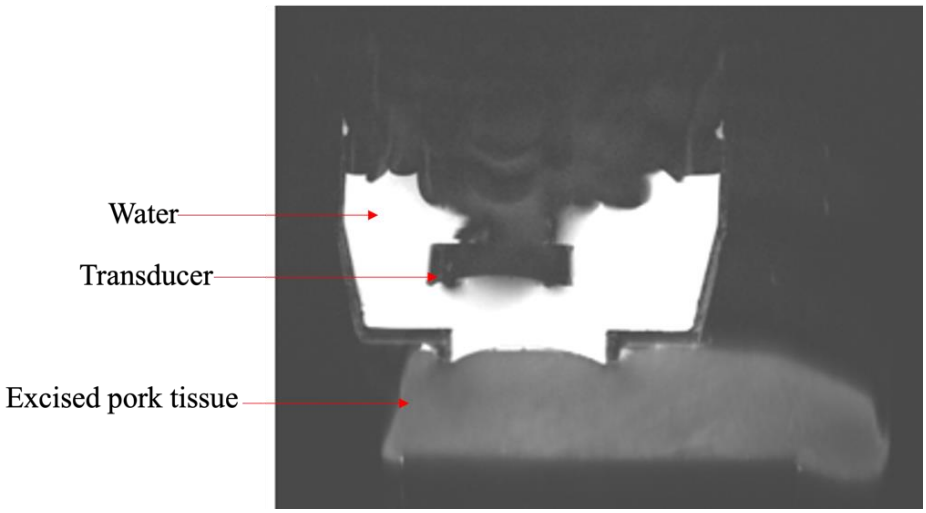

Figure 10: Axial T2-W TSE image of the experimental set-up showing the robotic system with a piece of excised pork tissue accommodated under the acoustic window.

Sonications monitored with MR thermometry

After validating good acoustic coupling, a series of single sonications were performed using varied acoustical power for a constant duration to assess the thermal heating abilities of the system. Sonications were imaged using the FLASH sequence. Acquired FLASH magnitude and phase MR images were utilised to generate MR thermometry data (thermal maps and temperature graphs) for the sonications using the developed software, thus monitoring thermal heating during ablations.

Lesion detection during sonications

Moreover, a series of single or grid sonications were executed using varied sonication parameters (acoustic power, and sonication time) to monitor and detect the formation of lesions on excised tissue. A T2-W TSE sequence was employed for detecting and imaging lesions inflicted on tissue during grid sonications, while T2-W and T1-Weighted (T1-W) TSE sequences with varied parameters were utilised to image lesions inflicted on pork tissue after single sonications.

Sonications on agar-based phantoms monitored with MR thermometry

The thermal heating of the system and the integrated transducer was also assessed inside the 3 T MRI scanner (Magnetom Vida, Siemens Healthineers) on agar-based phantoms doped with silicon dioxide (6 % w/v agar, and 4 % w/v silicon dioxide). The agar-based phantom was positioned below the robotic system following the experimental setting shown in Figure 8. The phantom and system were surrounded by the body coil (Body18, Siemens Healthineers) as shown in Figure 9. Primarily, a T2-W TSE sequence was utilised for imaging the experimental setting on an axial plane. The axial T2-W TSE images of the experimental setting were acquired with the following acquisition parameters: TR = 2300 ms, TE = 49 ms, FOV = 275×280 mm^2, Slice thickness = 10 mm, Acquisition matrix = 208×204, NEX = 1, ETL = 16, Flip angle = 110^o, and Pixel Bandwidth = 150 Hz/pixel. The acquired T2-W TSE image of the experimental setting is shown in Figure 11, indicating good coupling between the acoustic membrane and the agar-based phantom. Single sonications were then executed on the agar-based phantom using varied acoustical power for a constant duration of 30 s, to assess the thermal heating of

the system. The FLASH sequence was used for imaging during sonications with the acquired coronal FLASH images employed for MR thermometry calculations using the developed software.

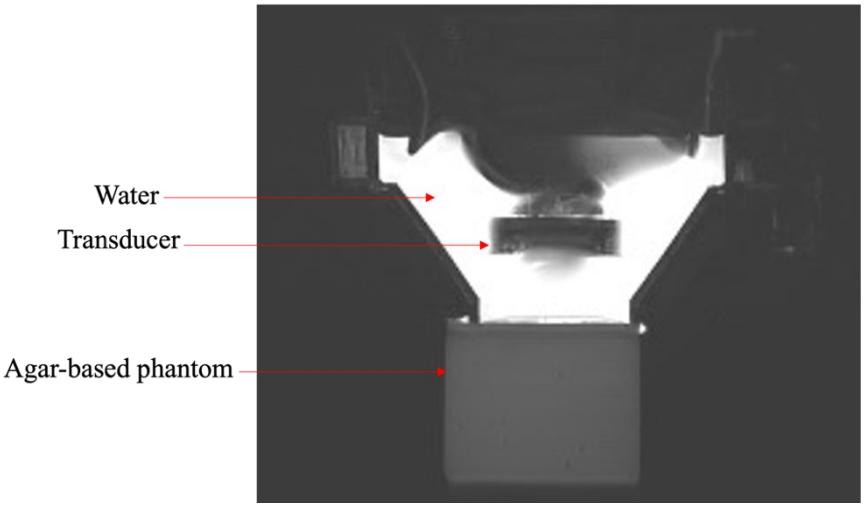

Figure 11: Axial T2-W TSE image of the experimental set-up showing the robotic system with an agar-based phantom accommodated under the acoustic window.

Evaluation on tumorgraft murine models

Mice type and handling

The fabricated 5 DOF robotic system and the integrated transducer were also employed for delivering FUS to tumorgraft mice. All experimental procedures involving mice were performed at the premises of the Cyprus Institute of Neurology and Genetics (CING) (Nicosia, Cyprus) in accordance with the granted study license (CY/EXP/PR.L09/2022) and the guidelines and protocols established by the Veterinary Services of Cyprus (Ministry of Agriculture, Rural Development and Environment, Nicosia, Cyprus). C57BL/6 mice were used in the experiments since these constitute the most common strain of genetically engineered mice employed for biomedical research. Ten male inbred adult (aged more than 6 weeks) C57BL/6 mice were acquired from the controlled facilities of the CING (Cyprus). Water and food were provided to the mice ad libitum.

Tumorgraft mouse model

The tumorgraft mouse models were attained by inoculating all mice with sarcoma cells of the MCA205 mouse fibrosarcoma cell line. Cancerous cells were acquired from Sigma-Aldrich. Cells were expanded with standard cell culture media, supplemented with 10 % fetal bovine serum and 1 % penicillin/streptomycin. Each mouse was injected at a single site in the shoulder with 2.5×10^5 cells and remained in cage for 1 week to allow tumour development so that the response of the tumour transplant to FUS therapy delivered with the robotic system could be studied.

FUS ablation of tumorgraft mouse models

The tumorgraft mouse models (n=10) were employed to test the efficacy of consistent delivery of FUS therapy on the development and growth of the tumour transplants. In this sense, the 10 mice were randomly divided directly after transplantation into the following 2 subgroups:

1) Group A (n=5): Experimental group consecutively treated with FUS to assess the effects of FUS therapy on tumour development and the occurrence of any adverse events. Referred to as "FUS group".
2) Group B (n=5): Negative control group wherein FUS was not delivered to evaluate the natural course of tumour growth and mice behaviour with no treatment applied. Referred to as "Control group".

The mice appointed to each group were assigned with specific ID tags. Specifically, mice in the "FUS group" were given the tag "FUS" followed by a number from 1 to 5 (FUS1, FUS2, FUS3, FUS4 and FUS5), while the mice of the "Control group" were allotted the "CTR" tag followed by the corresponding numbers (CTR1, CTR2, CTR3, CTR4, and CTR5).

Experiments were initiated one week (7 days) after transplantation. Before execution of any experimental procedure, mice were anaesthetised by the principal investigator and veterinarian (DVM Kyriakos Spanoudes, VET-EX MACHINA) using Avertin (Sigma-Aldrich). Anaesthesia was delivered via injection to ensure the mice's insensitivity to pain. Anaesthesia was cautiously supplied to each mouse using a weight-based administered dose (15 μL/g). Following anaesthesia, any hair existing on the surface of the tumour and surrounding areas were shaved. Thereafter, each mouse was differently manipulated depending on its designated subgroup following the set experimental workflow of the corresponding mice group (FUS or control).

"Control group" procedure workflow

The anaesthetised control mice (n=5) were placed in a prone position on the examination table and measurements of the tumour diameters were acquired using a vernier caliper. To ensure that anaesthesia did not impact the welfare of the animals, the ability of each mouse to respire normally was examined. Each mouse was then placed back in its cage wherein it was allowed to naturally emerge from anaesthesia. After recovery from anaesthesia, movement, breathing, drinking, and eating patterns of murines were regularly monitored to evaluate the ability of the mice to behave normally, thus ensuring the welfare of the tumorgraft animals. The anaesthesia and abovementioned experimental process were repeated on all mice at 7, 10, 14 and 21 days following transplantation. The timeline of the procedure workflow on the control tumorgraft mice is shown in Figure 12.

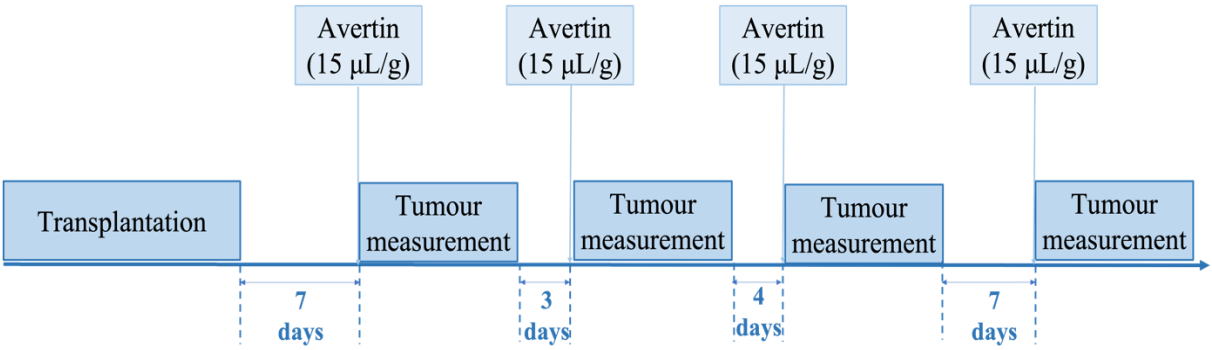

Figure 12: Timeline of the experimental procedure on tumorgraft mice of the "Control group".

"FUS group" procedure workflow

The diameters of the sarcoma tumour grafts on the anaesthetised mice of the "FUS group" (n=5) were measured using the caliper. Following tumour size measurements, anaesthetised

mice were individually positioned on the base of the robotic system. Figure 13 shows a photo of the experimental set-up.

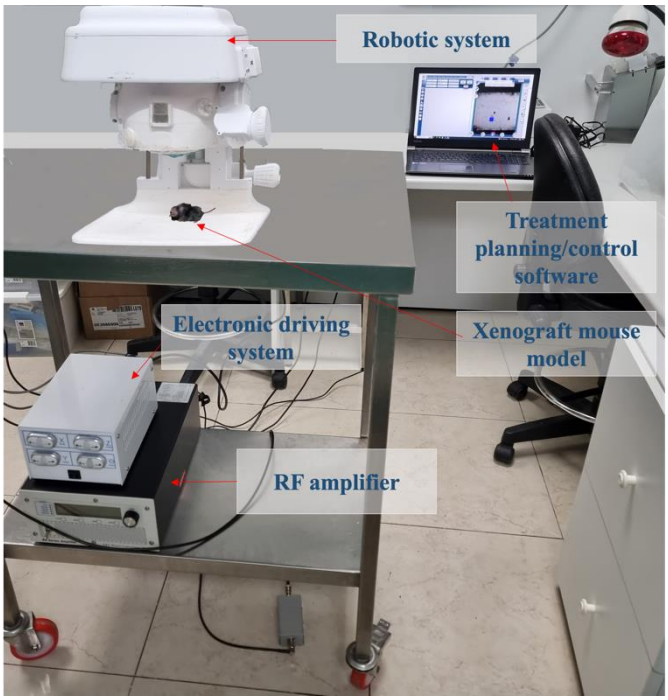

Figure 13: Photo of the experimental setting used for ablation of tumorgraft mice of the "FUS group".

The conical water container of the robotic system was filled with degassed/deionised water to create an environment for efficient transmission of ultrasound. A 3D-printed (F270, Stratasys) Acrylonitrile Butadiene Styrene (ABS) platform having a height of 10 cm was employed to raise the mouse to the level of the acoustic window of the robotic system, thus allowing contact of the tumour with the thin membrane film covering the acoustic window. A layer of ultrasound gel (Quick-Eco Gel, AB Medica Group S.A.) was applied on the tumour to achieve efficient acoustic coupling with the membrane film cover. This configuration ensured efficient delivery of acoustic energy from the ultrasonic transducer to the targeted area of the tumour. A schematic diagram indicating the configuration of the tumorgraft mice of the "FUS group" on the robotic system is shown in Figure 14.

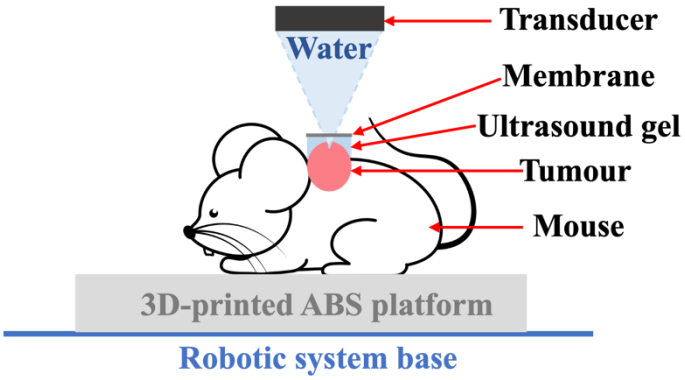

Figure 14: Schematic diagram of the configuration of the tumorgraft mice of the "FUS group" on the robotic system.

After appropriate arrangement under the acoustic window of the robotic system, tumour grafts on all mice were treated with FUS following the set therapeutic protocols. All tumours, irrespective of their size, were sonicated in an identical grid manner by commanding motion in

the PC-controlled X and Y stages of the robotic system. Specifically, multiple sonications were executed along a 3×3 grid pattern with a 4 mm step size employed between planned grid points. Each grid point was sonicated using an electric power of 250 W which, given the 30 % efficiency of the transducer, corresponds to an output acoustic power of 75 W. Sonications were performed for a sonication time of 10 s, while a 10 s time delay was applied between successive exposures. Considering the small size of the mice, all sonications were executed with the focus of the transducer positioned on the interface of the tumour grafts (transducer-membrane distance = 60 mm) to guarantee animal safety. Furthermore, during the experimental procedure, the breathing and motion patterns of the murines were monitored to evaluate any acute effects possibly induced from the FUS therapy. If there were any indications of pain or irregular breathing, the therapeutic procedure was halted to ensure animal welfare and safety.

After the end of the treatment, the ablated part of the tumour was grossly examined to assess the formation of coagulative lesions on the surface of the tumour. Moreover, following ablations, the FUS-treated mice were checked for normal breathing and were placed in their cages to recover from anaesthesia. Following anaesthesia emergence, the mice underwent a 7-day follow-up period wherein the animals were monitored for any occurrence of adverse events. After the end of the 7-day period, the procedure was repeated on all mice to evaluate any effects from consecutive FUS sessions delivered at different timepoints after transplantation on the growth of the neoplasms. Particularly, a total of 3 individual FUS treatment sessions were applied on all mice, occurring at 7, 14 and 21 days after transplantation. Notably, similar to the "Control group", 3 days after the first treatment session (10 days after transplantation), the mice were anaesthetised, and their tumour diameters were measured with no FUS therapy applied on the tumours. Figure 15 shows the timeline of the experimental workflow on the tumorgraft mice of the "FUS group".

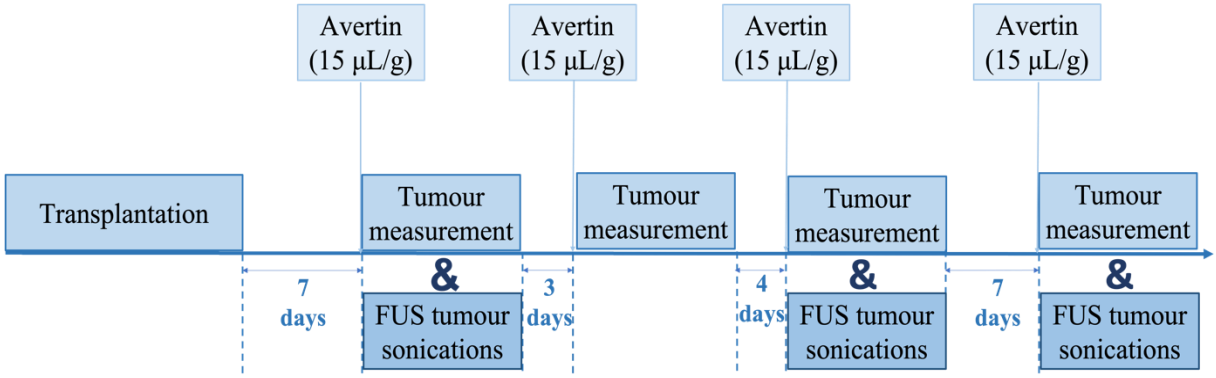

Figure 15: Timeline of the experimental procedure on tumorgraft mice of the "FUS group".

Statistical analysis

Tumour diameters as measured at 7, 10, 14, and 21 days after transplantation on the mice of the "FUS group" and the "Control group" were analysed to determine the significance of tumour size differences between the two groups. Specifically, data acquired 7 days after transplantation were compared to investigate whether significant variation existed between the average diameters of the formed tumours on the mice of the two groups. Data acquired at the subsequent timepoints (10, 14, and 21 days) were analysed to investigate whether a significantly smaller average tumour diameter was achieved in the mice of the "FUS group" as

a result of application of the FUS treatment. Particularly, data obtained at 10, 14, and 21 days were analysed to determine whether the average tumour diameter on the mice of the "FUS group" was smaller than the average tumour diameter on the mice of the "Control group" 3 days after application of the 1st FUS session, 7 days after application of the 1st FUS session and 7 days after application of the 2nd FUS session, respectively. Differences between the two groups at the 4 different timepoints (7, 10, 14, and 21 days) were tested by unpaired two-sample t-tests. All significance tests were one-tailed and those with a p value less than 0.1 (10 %) were considered statistically significant.

Evaluation on pets with naturally occurring tumours

Pet recruitment

Experiments with the 5 DOF robotic system and the integrated transducer were also executed on dogs and cats with natural neoplasia. Experiments on pets (dogs and cats) with naturally occurring tumours were granted an approval (CY/EXP/PR.L09/2022) by the Veterinary Services of Cyprus on 18/10/2022. Having obtained all necessary licenses, a search to find cases of companion animals with malignancies was launched. The primary point of contact were veterinarians receiving at their clinic cases of cats and dogs with cancer whose owners were willing to enrol their animals in our trials for targeted treatment of their tumours with FUS. Veterinary clinics in various Cypriot districts that collaborated with us in previous research grants were informed about the trials executed in the framework of this project. Phone calls were made by the research team to inform veterinarians about the trials, explain the approach and workflow of the experimental procedure and determine whether they would be interested in collaborating with us again, by referring cases of canines and felines with malignancies. Additionally, the principal investigator, a veterinarian with strong bonds with the Cyprus veterinary association and excellent relations with veterinary surgeons across Cyprus, personally contacted fellow veterinarians to examine whether they would be interested in participating in the programme. The programme was described in detail and any queries arising were answered both in person and by phone. From all veterinarians contacted, 2 clinics agreed to be involved in the programme. As shown in Figure 16, the first experiment was performed on 19/12/2022, almost 2 months after obtaining the approval, while the last experiment was executed on 11/12/2024, lasting a total period of 24 months.

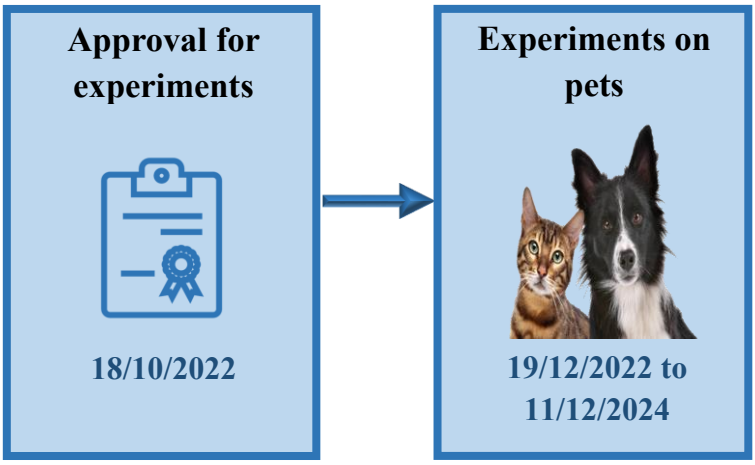

Figure 16: Schematic diagram of the duration of experiments on dogs and cats.

Notably, all pets were ethically enrolled in the veterinary trials according to specific eligibility criteria following informed consent from their human owners. Consent forms were carefully prepared and provided to veterinarians who accepted to participate in the programme. The veterinarians were responsible of giving the forms to owners who consciously decided on whether they would like to enrol their pets in the trial to undergo local tumour treatment with FUS. The consent form provided essential information relating to the study including its purpose, eligibility criteria, potential benefits of the therapeutic ultrasound application to the animal and the veterinary oncological field, possible adverse events, experimental procedure as well as the rights and obligations of owners. Consequently, owners were provided with adequate information allowing them to decide on whether to enrol their pets in the trial for cancer treatment with FUS before surgery or opt for a conventional surgical approach.

Workflow of veterinary clinical trials

Experiments were performed at the clinics of the veterinarians providing the cases, in accordance with the granted license. The robotic system was accommodated on the treatment table for execution of the FUS ablations. Figure 17 shows indicative photos of the robotic system as placed on the treatment table at various veterinary clinics. All experiments were executed with both the referring veterinarian and the project's principal investigator present to ensure the safety of the treatment and the welfare of the recruited animal, as indicatively shown in Figure 18.

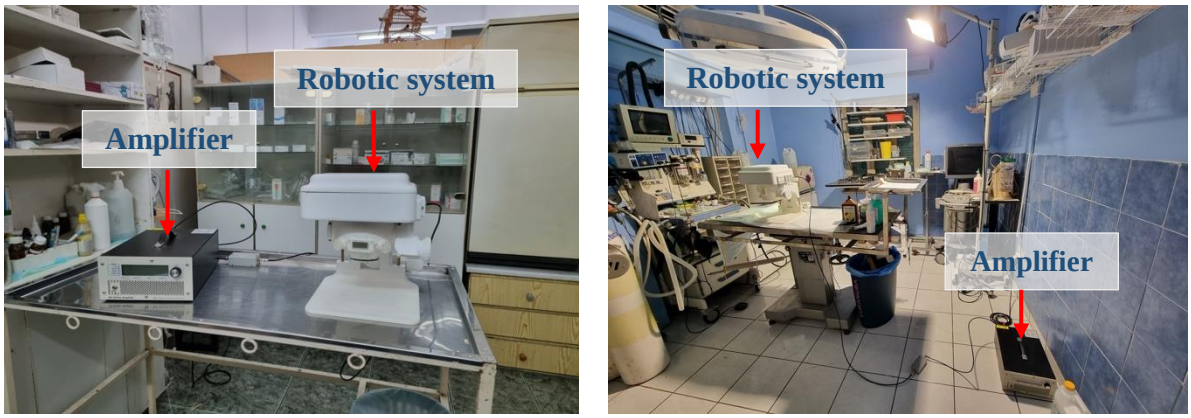

Figure 17: Photos of the system installed at various veterinary clinics.

Figure 18: Photo of the principal investigator and one of the referring veterinarians taken during one of the experiments.

Animal positioning for FUS treatment

All experiments were executed following a standard workflow. Initially, the animal was appropriately anaesthetised by the referring veterinarian, and was cautiously accommodated under the conical transducer housing of the robotic system in a recumbent position that allowed contact of the targeted area with the acoustic window. Figure 19 shows indicative examples of dogs and cats of different sizes positioned in lateral or dorsal recumbency under the robotic device for treatment of tumours at varied locations.

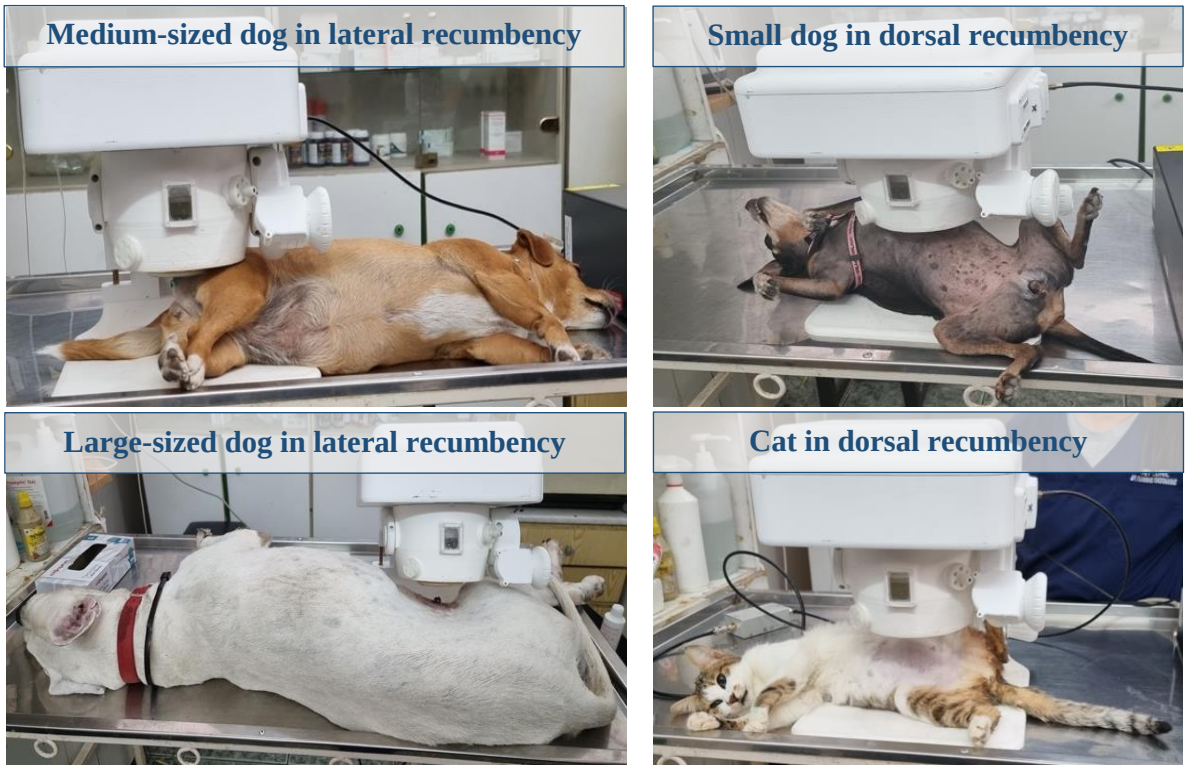

Figure 19: Configuration of recruited dogs and cats for treatment, with the animal placed in a recumbent position and the tumour arranged under the acoustic window of the robotic system.

The conical transducer housing was filled with degassed water, allowing efficient transmission of the ultrasound beam to the targeted area of the tumour. The area around the tumour was shaved, while a thin layer of ultrasound gel (Quick-Eco Gel, AB Medica Group S.A.) was applied on the tumour. With this approach, optimal acoustic coupling with the thin membrane covering the acoustic window of the conical housing was achieved, ensuring maximal transfer of acoustic energy to the targeted area.

To guarantee the safety and welfare of the pet, only cases with tumours thicker than 30 mm were recruited, while all ablations were performed with the transducer focus positioned on the tumour interface. Consequently, unintended heating of the pet's body due to far-field was avoided, ensuring that no damage in normal tissue or skin burns were induced. Figure 20 shows a schematic diagram of the configuration of the tumour under the acoustic window of the robotic system. An indicative photo of tumour placement for treatment showing the acoustic coupling between the tumour and the robotic system is shown in Figure 21.

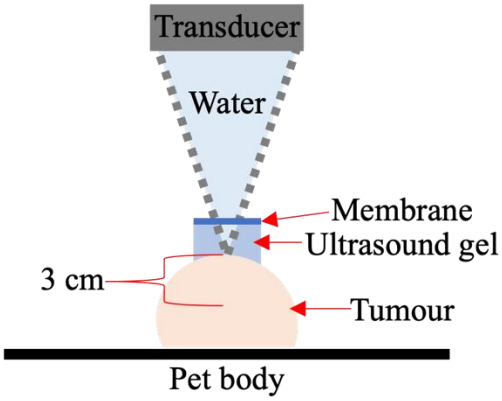

Figure 20: Schematic diagram of tumour placement under the acoustic window of the robotic system.

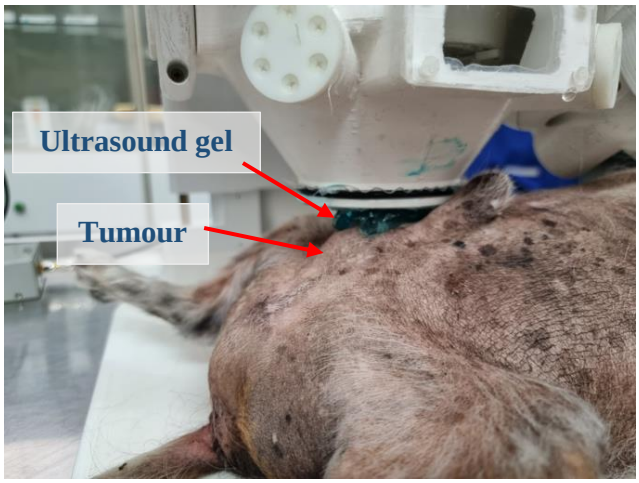

Figure 21: Tumour placement below the robotic system with efficient coupling between the tumour and the acoustic window.

FUS ablation of canine and feline tumours

Tumours on dogs and cats were ablated, with all details of the experimental procedure documented as shown in Table 3. Each experiment was provided with a study ID comprising of the project name (FUSVET) and the number of the recruited animal (e.g., 1, 2, etc.), while essential details relating to the pet, including its species, age, weight, owner, and tumour type and size were filled out. Additionally, equipment used for ablations and details of the sonication protocol were included in the description of the experimental procedure.

Ablation of tumours was performed in all animals following a similar approach. Initially, treatment safety was assessed by sonicating the tumour with low acoustic power for a short duration to evaluate the endurance of the animal to ablation. In case low energy sonications were well tolerated by the dog or cat without any pain felt, ablation of tumours with high power was performed. Tumour ablations were executed using sonication parameters (power and sonication time) that were appropriately chosen based on the size of the tumour and its location relative to sensitive areas such as nerves and bones. To maintain treatment safety and ensure the welfare of the pet, vital signs of the animal were monitored during the experimental procedure. Respiration rate, heart rate, urination level, pedal reflexes, and temperature of the animal were measured at regular intervals and recorded in the anaesthesia/monitoring record shown in Table 4.

Table 3: Template of experimental information.

Date	-
Study ID	FUSVET-X (where X is 1,2,3, etc.)
Referring veterinarian	-
Anaesthesia	-
Weight (Kg)	-
Age (years)	-
Species	-
Name of owner	-
Tumour type	-
Size of tumour	-
Procedure	1. Anaesthesia 2. Treatment with FUS 3. Surgical removal of tumour and biopsy
Robot	FUSVET
Transducer	F=2.75 MHz, R=65 mm, D=50 mm
Amplifier	AG1016 (AG Series Amplifier, T & C Power Conversion Inc.)
Focal depth	Interface (transducer to membrane distance=60 mm)
Protocol	Acoustic power, sonication time
Observation	-
Biopsy procedure	-

Table 4: Template of the anaesthesia/monitoring record.

Date			**Time**		
Animal ID			FUSVET-X (where X is 1,2,3, etc.)		
Species					
Sex					
Age					
Weight (Kg)					
Study			CY/EXP/PR.L09/2022		
Principal Investigator			K. Alexandros Spanoudes		
Anaesthesia record					
Time			**Anaesthesia**		
			Surgery ended		
Monitoring record					
Time	**Heart Rate**	**Resp. Rate**	**Urination** (0 to 3)	**Absence of Movement /Pedal Reflex**	**Temp. (°C)**

Tumour excision and histological examination

Following FUS ablations, the tumour was grossly examined to macroscopically evaluate the formation of coagulative lesions at the sonicated region. The tumour was then surgically excised by the referring veterinarian with clean margins, and the ablated area was sectioned and immediately immersed in a 10 % formaldehyde solution. Resected samples were histologically examined by an advanced histopathological and cytological centre (Dr. Stelios Panayiotou, SGS Diagnostic Centre of Histopathology and Cytology Limited, Limassol, Cyprus). Samples were sectioned, and the Haematoxylin and Eosin (H&E) stained slides were scanned and digitally saved using a dedicated brightfield scanner (VENTANA DP 200, Roche Diagnostics International AG, Rotkreuz, Switzerland). Note that in one study (study ID: FUSVET-9) histological examination was instead performed by a specialized veterinary pathology centre (N.G.N Veterinary Pathology Consulting, Meniko, Cyprus).

Results

Evaluation on agar-based phantoms, excised pork tissues, and plastic films

Laboratory Experiments

Sonications on thin polymer PVC films

Figure 22 shows the lesions formed on the interface of the PVC film after sonications (acoustic power of 20 W for a sonication time of 15 s) executed at the origin and end points of the X and Y axes of the robotic system. Distances between lesions formed at the origin and end points of each positioning stage were measured using a ruler to determine the motion range of the X and Y axes. As illustrated in Figure 22, the motion range of the X-axis was found at 45 mm, while for the Y-axis at 32 mm.

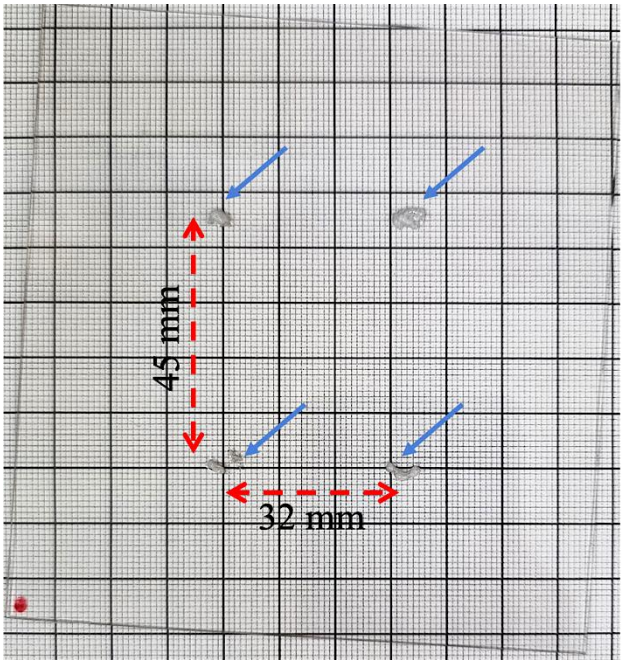

Figure 22: Lesions (blue arrows) formed on the PVC plastic film after sonications at an acoustical power of 20 W for a sonication time of 15 s using manual motion of the robotic device and the integrated 2.75 MHz transducer (D=50 mm, ROC=65 mm) along the X and Y axes.

Temperature increase in phantom and excised tissue

Temperature increase in phantom

Sonications on the agar-based phantom (6 % w/v) executed with the robotic system and the integrated 2.75 MHz transducer were performed using varied acoustical power of 30 W, 45 W and 60 W for a constant sonication time of 60 s. Figure 23, Figure 24, and Figure 25 show the rate of temperature increase recorded during sonications executed at acoustic power of 30 W, 45 W, and 60 W, respectively. Table 5 shows the temperature change (from the initial temperature of the phantom) achieved as a result of the three sonications executed at varied acoustical power.

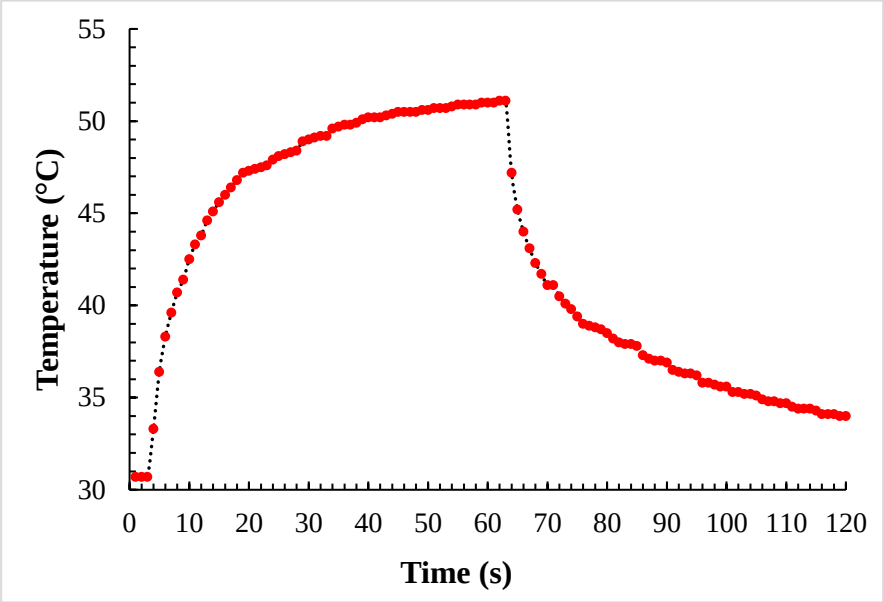

Figure 23: Temperature as a function of time recorded during sonications executed on an agar-based phantom (6 % w/v agar) using the robotic system and a 2.75 MHz transducer (D=50 mm, ROC=65 mm) at an acoustic power of 30 W for a sonication time of 60 s at a 25 mm focal depth.

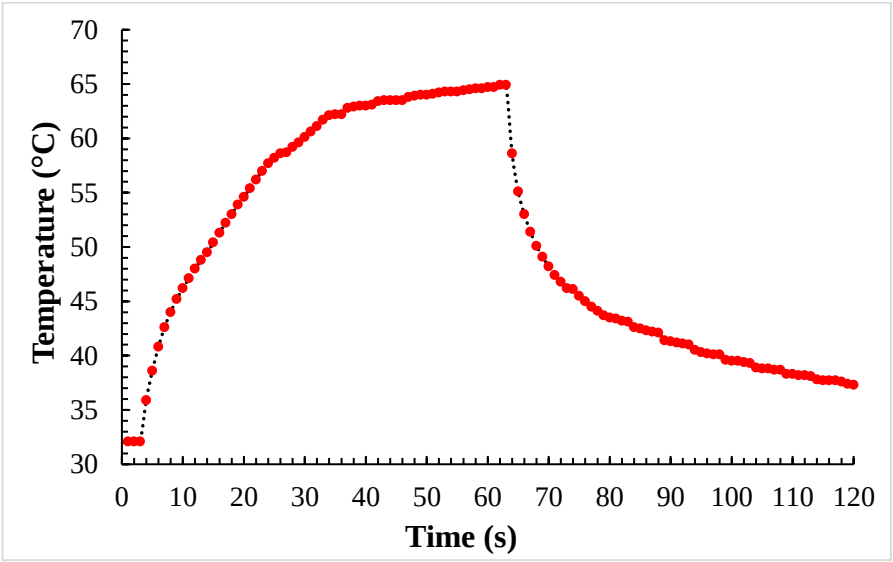

Figure 24: Temperature as a function of time recorded during sonications executed on an agar-based phantom (6 % w/v agar) using the robotic system and a 2.75 MHz transducer (D=50 mm, ROC=65 mm) at an acoustic power of 45 W for a sonication time of 60 s at a 25 mm focal depth.

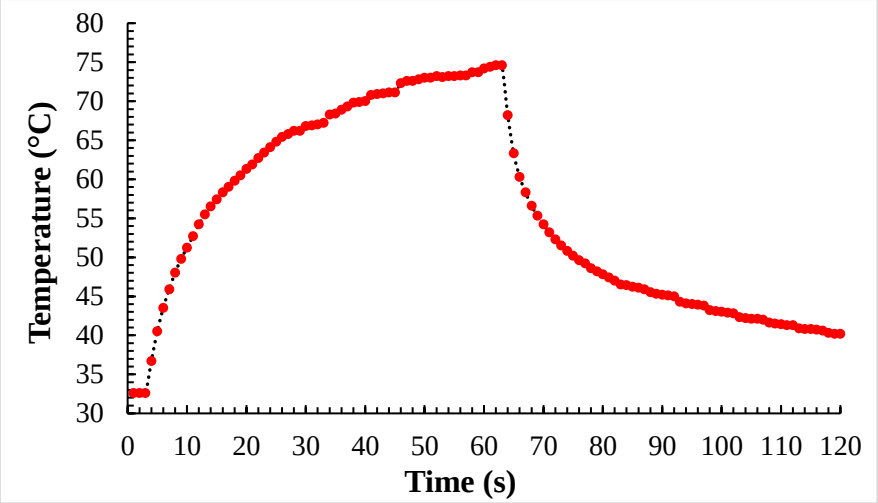

Figure 25: Temperature as a function of time recorded during sonications executed on an agar-based phantom (6 % w/v agar) using the robotic system and a 2.75 MHz transducer (D=50 mm, ROC=65 mm) at an acoustic power of 60 W for a sonication time of 60 s at a 25 mm focal depth.

Table 5: Temperature change induced resulting sonications executed on an agar-based phantom (6 % w/v agar) using the robotic system and a 2.75 MHz transducer (D=50 mm, ROC=65 mm) at varied acoustical power for a constant sonication time of 60 s at a 25 mm focal depth.

Acoustic power (W)	Sonication time (s)	Energy (J)	Temperature change (ºC)
30	60	1800	20.4
45		2700	32.8
60		3600	42

Temperature increase in excised tissue

Additionally, sonications with the FUS system were executed on pieces of excised pork tissue. Correspondingly, tissue sonications were also performed at a 25 mm focal depth using varied acoustical power of 30 W, 45 W, and 60 W for a constant duration of 60 s. Figure 26 shows the increase of temperature which was recorded with the thermocouple during sonications executed at an acoustical power of 45 W.

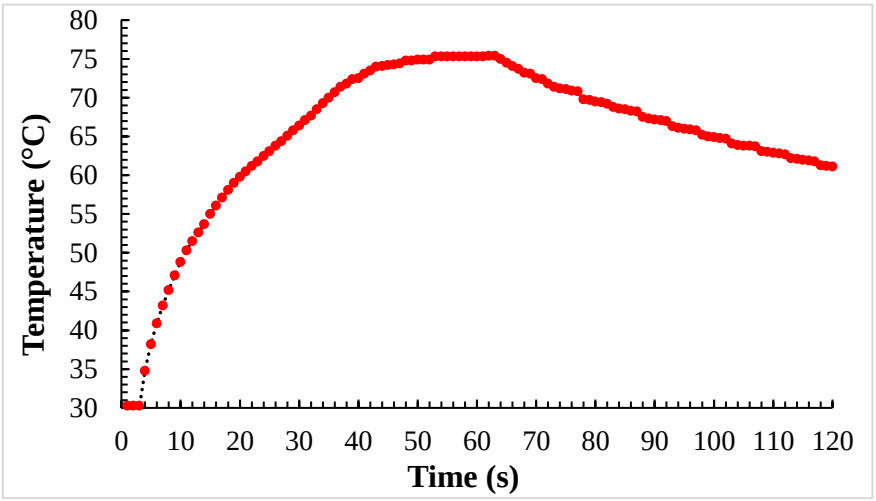

Figure 26: Temperature as a function of time recorded during sonications executed on excised pork tissue using the robotic system and a 2.75 MHz transducer (D=50 mm, ROC=65 mm) at an acoustic power of 45 W for a sonication time of 60 s at a 25 mm focal depth.

Temperature changes induced within the excised tissue pieces as a result of sonications executed at varied acoustical power of 30-60 W (15 W step) are shown in Table 6. Temperature changes achieved at each sonication protocol were sufficiently high to result in the formation of lesions on the sonicated tissue pieces. Figure 27A and Figure 27B show photos of the sliced tissue, revealing lesions formed on a plane parallel to the beam after sonications performed using an acoustic power of 30 W and 60 W, respectively.

Table 6: Temperature change induced resulting sonications executed on excised pork tissue using the robotic system and a 2.75 MHz transducer (D=50 mm, ROC=65 mm) at varied acoustical power for a constant sonication time of 60 s at a 25 mm focal depth.

Acoustic power (W)	Sonication time (s)	Energy (J)	Temperature change (°C)
30	60	1800	35.1
45		2700	45.1
60		3600	68

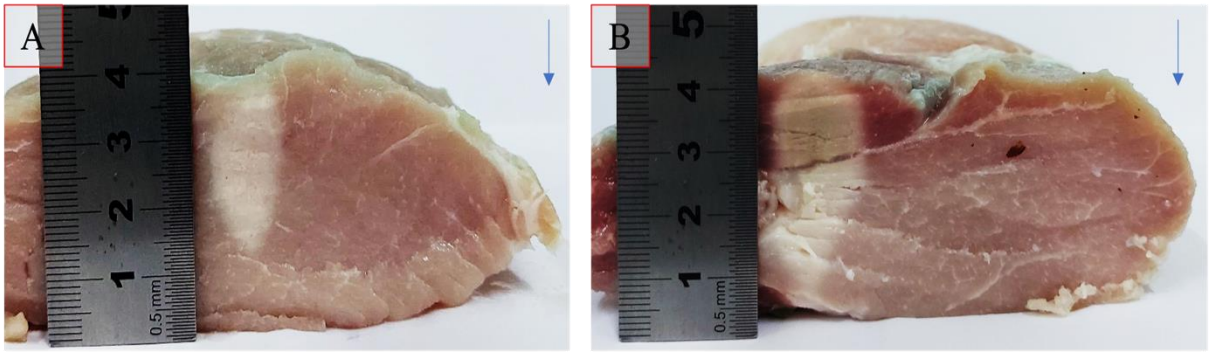

Figure 27: Lesions formed on excised pork tissue on a plane parallel to the beam after sonications executed with the robotic system and a 2.75 MHz transducer (D=50 mm, ROC=65 mm) at varied acoustical power for a sonication time of 60 s at a 25 mm focal depth. Lesions inflicted using acoustical power of A) 30 W, and B) 60 W. Blue arrows indicate the direction of the ultrasonic beam.

Ablations of excised tissue in a laboratory setting

Formation of overlapping lesions

Motion of the robotic system in a grid pattern was utilised for the formation of overlapping lesions using a constant ultrasonic protocol (acoustic power of 60 W for a sonication time of 20 s at 25 mm focal depth), with motion commanded in various grid patterns and different step sizes. Initially, grid sonications on the excised tissue using the constant sonication parameters (acoustic power of 60 W for a sonication time of 20 s) were executed in a 2×2 grid pattern with a step size of 7 mm to investigate the ability of the system to inflict overlapping lesions. After sonications, the excised tissue was sliced at 10 mm from the sonicated surface, to examine the formed lesions and measure the dimensions of the ablated area. Figure 28A shows a photo of the overlapping lesions formed on the sliced tissue on a plane perpendicular to the beam. The tissue was then vertically sliced to reveal the overlapping lesions on a plane parallel to the beam as shown in the photo of the lesions in Figure 28B. The overlapping lesions were formed with an ablated area of 23×21 mm^2 and a length of 22 mm.

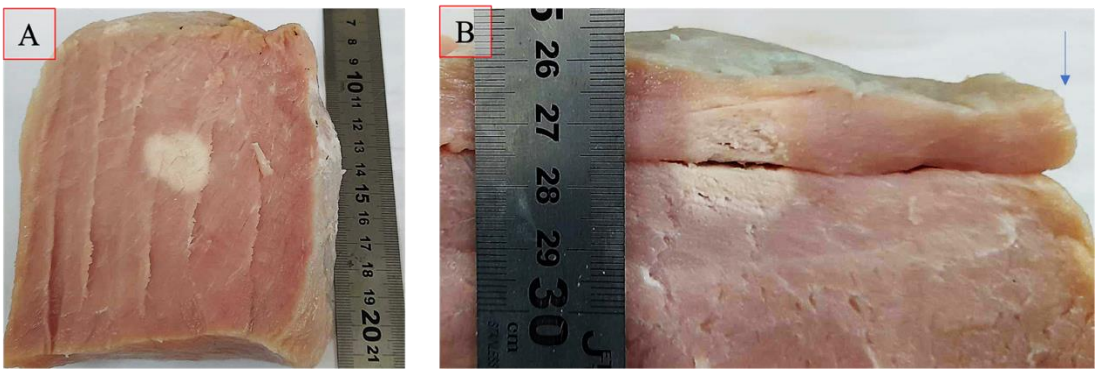

Figure 28: Photo of overlapping lesions formed on excised pork tissue after sonications executed at an acoustic power of 60 W for a sonication time of 20 s with motion of a 2.75 MHz transducer (D=50 mm, ROC=65 mm) using the robotic system in a 2×2 grid with a 7 mm step at a 25 mm focal depth. A) Lesions formed on a A) plane perpendicular to the beam, and B) plane parallel to the beam. Blue arrow indicates direction of the ultrasonic beam.

Grid sonications were then executed using the same ultrasonic protocol, with robotic motion commanded in a larger 3×3 grid pattern to investigate the ability of the system to ablate a larger area of tissue. An identical step of 7 mm was employed between each sonication point. After exposure, the tissue was horizontally sliced at 10 mm, revealing a well-demarcated area of overlapping lesions formed on a plane perpendicular to the beam as shown in Figure 29. Similarly, the tissue was appropriately cut vertically, revealing the length of the overlapping lesions as shown in Figure 30. Overlapping lesions inflicted by this protocol were formed with an area of 26×28 mm^2 and a length of 44 mm.

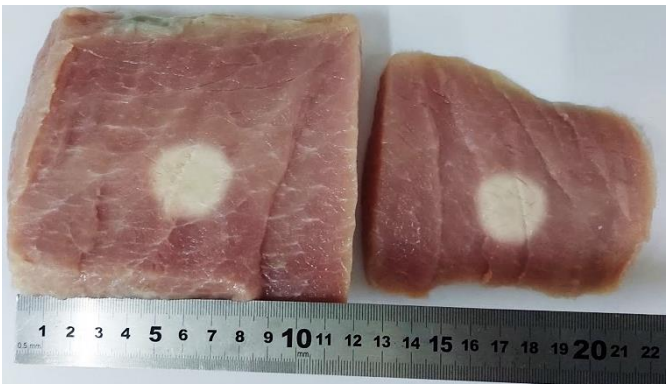

Figure 29: Overlapping lesions formed on excised pork tissue on a plane perpendicular to the beam after sonications executed at an acoustic power of 60 W for a sonication time of 20 s with motion of a 2.75 MHz transducer (D=50 mm, ROC=65 mm) using the robotic system in a 3×3 grid with a 7 mm step at a 25 mm focal depth. Slice of the tissue at 10 mm and its mirror (from right to left).

Figure 30: Overlapping lesions formed on excised pork tissue on a plane parallel to the beam after sonications executed at an acoustic power of 60 W for a sonication time of 20 s with motion of a 2.75 MHz transducer (D=50 mm, ROC=65 mm) using the robotic system in a 3×3 grid with a 7 mm step at a 25 mm focal depth. Blue arrow indicates the direction of the ultrasonic beam.

MRI Experiments

MRI compatibility of the robot and transducer

MRI compatibility of the robotic system

The magnitude FLASH images of the agar-based phantom which were acquired at the various activation states of the robotic system (cables not connected, cables connected, and DC ON) are shown in Figure 31.

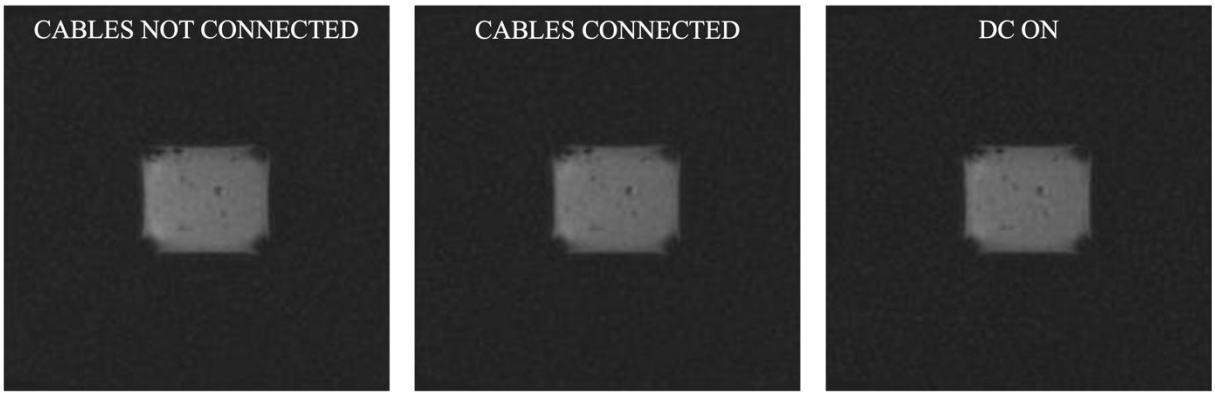

Figure 31: Coronal magnitude FLASH images of an agar-based phantom (6 % w/v) doped with silicon dioxide (4 % w/v) acquired at various activation states of the robotic system.

Figure 32 shows an indicative example of the circular ROIs that were set within the phantom and the air background for signal intensity and standard deviation calculations, respectively. Figure 32 shows signal intensity measurements executed for the magnitude MR image that was acquired with only the robotic system present in the bore (cables not connected), with the phantom and air ROIs for images acquired at subsequent activation conditions remaining at identical locations.

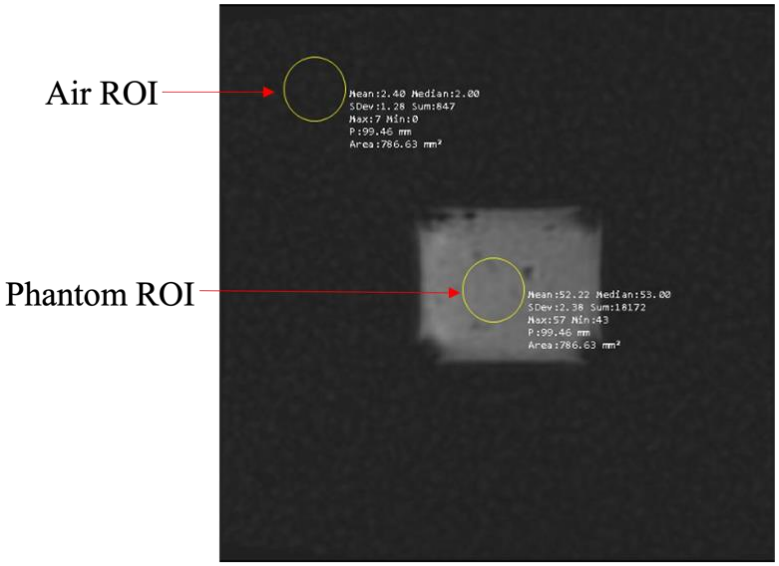

Figure 32: Measurement of signal intensities at specific ROIs in the agar-based phantom and the air background on a coronal magnitude FLASH image of the phantom acquired at reference condition (robotic system in bore and cables not connected).

Table 7 shows the average signals in the phantom ROI and the standard deviation of signals in the air ROI as measured from the magnitude FLASH images acquired at each activation state of the robotic system, while Figure 33 shows the SNR as estimated for each condition.

Table 7: Signal measurements in agar-based phantom and air ROIs and SNR calculations executed on FLASH images of the phantom acquired at different activation conditions of the robotic system.

Activation state	Average signal in phantom ROI ($SI_{phantom}$)	Standard deviation of signal in air ROI (σ_{noise})	SNR
Cables not connected	52.22	1.28	40.8
Cables connected	49.34	1.31	37.66
DC ON	47.55	1.37	34.71

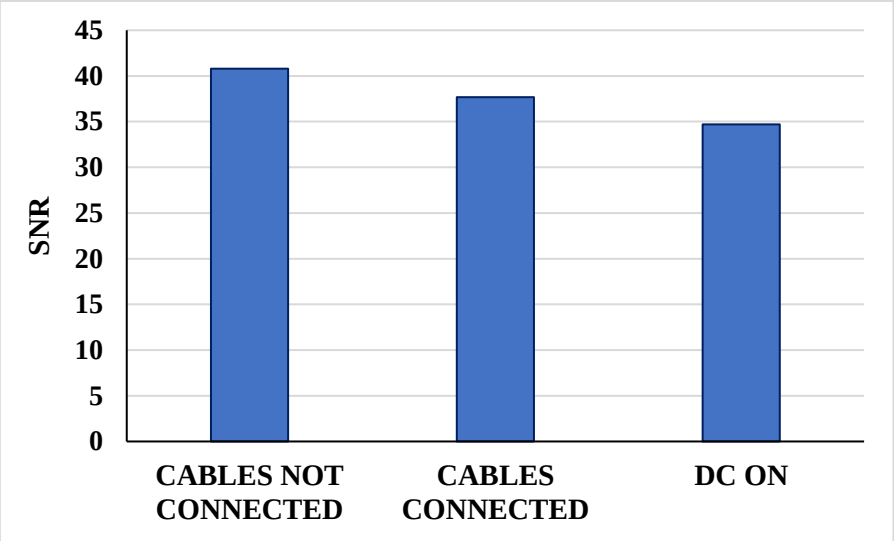

Figure 33: Bar chart of SNR as calculated from coronal magnitude FLASH images of an agar-based phantom (6 % w/v agar, and 4 % w/v silicon dioxide) acquired at various activations of the robotic system.

Accordingly, Figure 34 shows the coronal phase FLASH images of the agar-based phantom that were acquired at the corresponding configurations of the robotic system (cables not connected, cables connected, and DC ON).

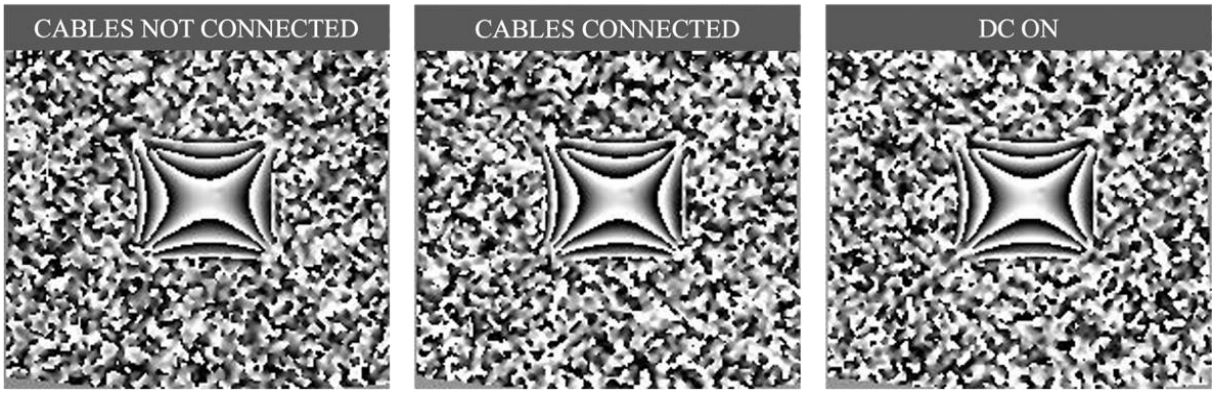

Figure 34: Coronal phase FLASH images of an agar-based phantom (6 % w/v agar, and 4 % w/v silicon dioxide) acquired at various activation states of the robotic system.

Figure 35 shows the ROI that was set at a specific location within the phantom for measuring the average signal intensity of the phase FLASH image which was acquired during the

reference condition, with the robotic system solely present on the MRI table (cables not connected). The signal measured at the reference state was translated to a percent value (100 %), with signal measurements at the same ROIs for phase FLASH images taken at subsequent activation states (cables connected, and DC ON) visualized as a percentage of the reference signal as shown in Figure 36.

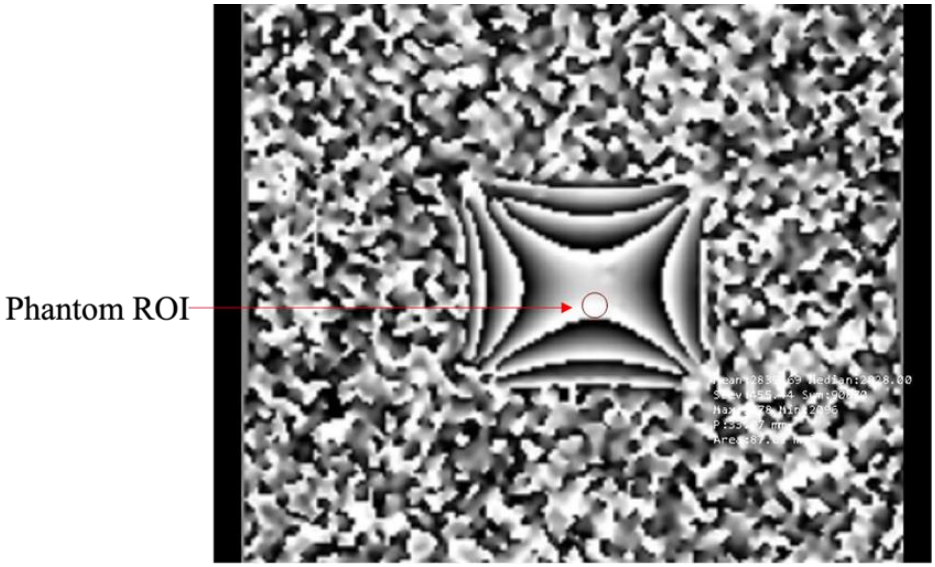

Figure 35: Measurements of signal intensity at a specific ROI in the agar-based phantom on a coronal phase FLASH image of the phantom acquired at the reference state with only the robotic system in the bore (cables not connected).

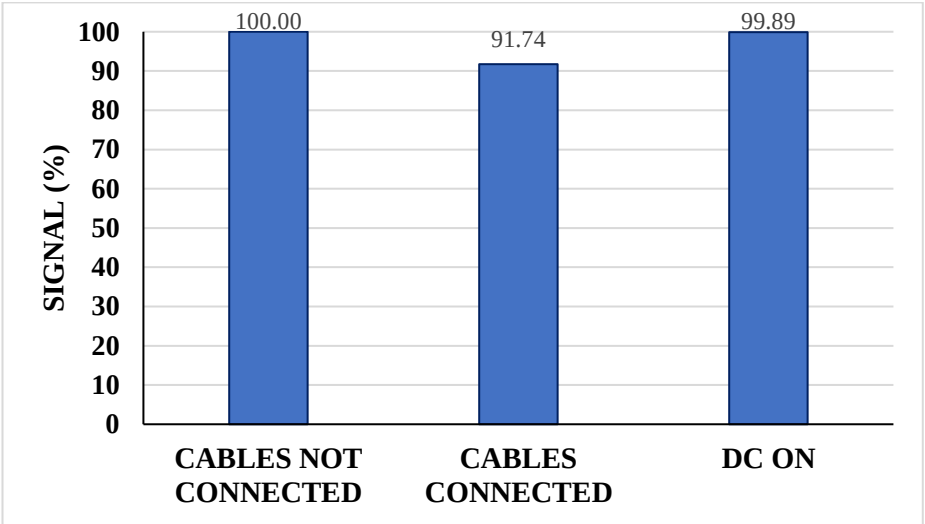

Figure 36: Bar chart of signal (%) as calculated from coronal phase FLASH images of an agar-based phantom (6 % w/v agar, and 4 % w/v silicon dioxide) acquired at various activations of the robotic system.

MRI compatibility of the transducer

Figure 37 shows the coronal magnitude images of the agar-based phantom taken with the FLASH sequence at the reference state with the sole presence of the robotic system in the MRI bore (cables not connected), upon system connection with the RF cables (cables connected), amplifier activation (amplifier ON) and transducer activation at varied acoustical power of 15-60 W (Power = 15-60 W).

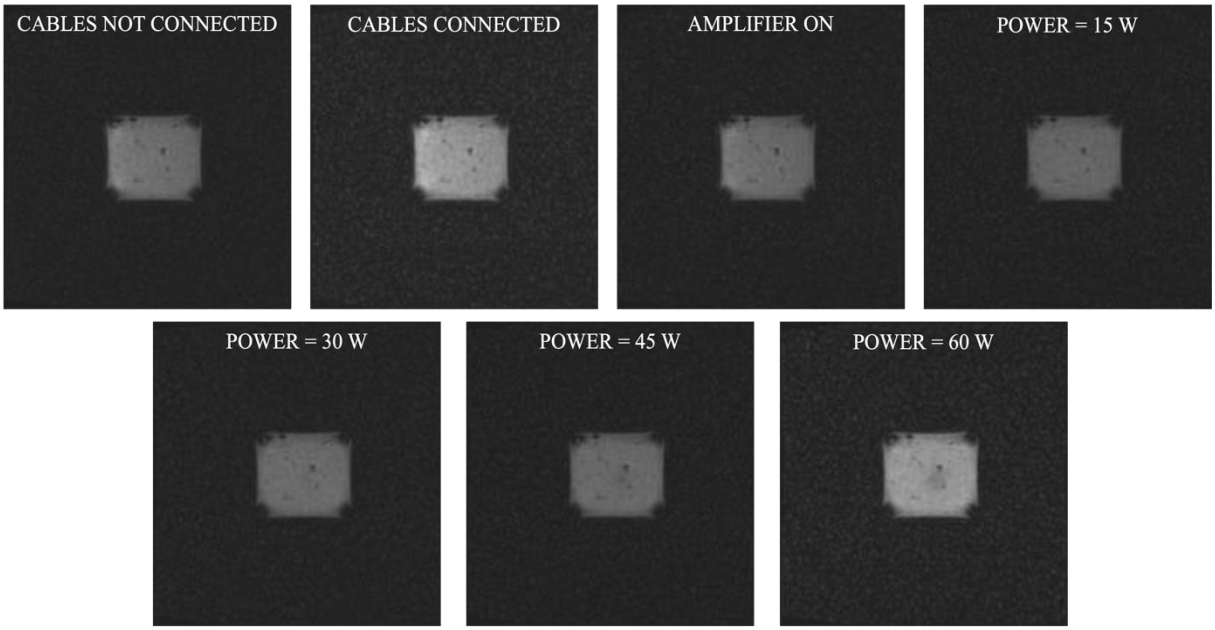

Figure 37: Coronal magnitude FLASH images of an agar-based phantom (6 % w/v agar, and 4 % w/v silicon dioxide) acquired at various activation states of the transducer.

Signal intensity measurements on magnitude FLASH images of the agar-based phantom taken at different configurations of the transducer for SNR calculations were performed at identical phantom and air ROIs as those set for assessing the compatibility of the robotic system (Figure 32), as indicatively shown in Figure 38 for an image acquired during transducer activation at an acoustical power of 30 W. Table 8 shows the signal intensity and standard deviation values measured in the agar phantom and air ROIs, respectively, for each different activation configuration of the transducer. Correspondingly, Figure 39 shows the calculated SNR for each varied transducer configuration.

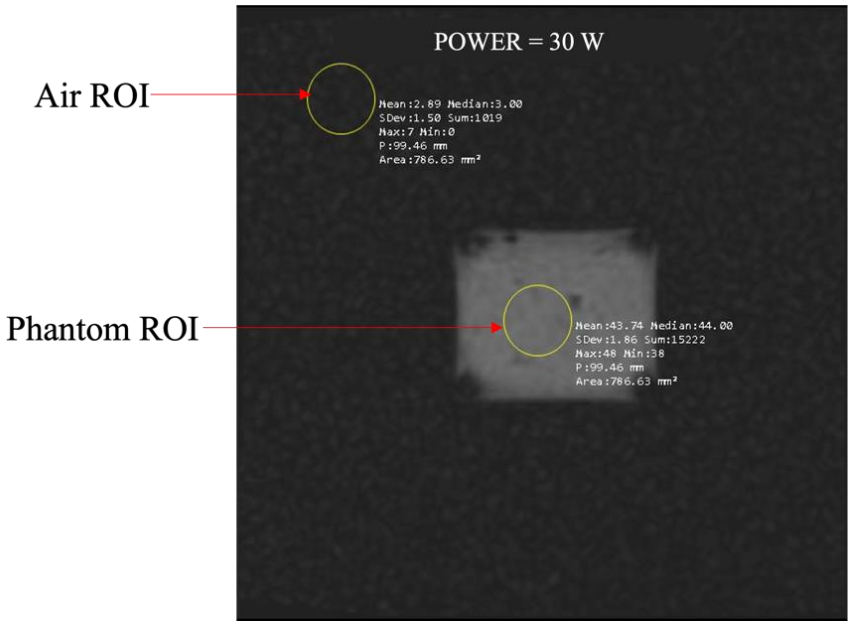

Figure 38: Signal intensity measurements at specific ROIs in the agar-based phantom and the air background on a coronal magnitude FLASH image of the phantom acquired during activation of the transducer at an acoustical power of 30 W.

Table 8: Signal measurements in agar-based phantom and air ROIs and SNR calculations performed on FLASH images of the phantom acquired at different activation conditions of the ultrasonic transducer.

Activation state	Average signal in phantom ROI ($SI_{phantom}$)	Standard deviation of signal in air ROI (σ_{noise})	SNR
Cables not connected	52.22	1.28	40.8
Cables connected	51.84	1.81	28.64
Amplifier ON	51.75	1.66	31.17
Power = 15 W	44.82	1.65	27.16
Power = 30 W	43.74	1.5	29.16
Power = 45 W	42.71	1.31	32.6
Power = 60 W	41.46	1.39	29.83

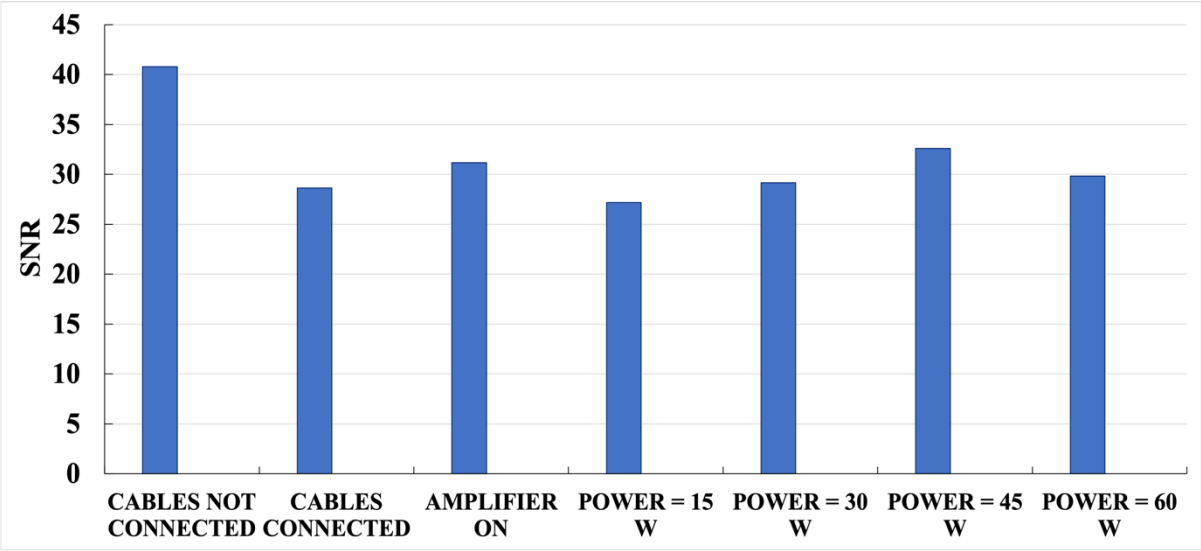

Figure 39: Bar chart of SNR as calculated from coronal magnitude FLASH images of an agar-based phantom (6 % w/v agar, and 4 % w/v silicon dioxide) acquired at various activations of the ultrasonic transducer.

Phase images taken with the FLASH sequence at each of the 7 different activation states of the ultrasonic transducer (cables not connected, cables connected, amplifier activation, and transducer activation at acoustic power of 15, 30, 45, and 60 W) are shown in Figure 40. Correspondingly, average signal measurements for coronal phase FLASH images acquired during each different transducer configuration were executed for a specific ROI within the agar-based phantom as shown in Figure 41 for an image acquired during amplifier activation. Notably, as shown in Figure 41, the ROI was set at an identical location within the phantom as the one used for signal measurements on phase FLASH images acquired during various activation states of the robotic and electronic driving systems (Figure 35).

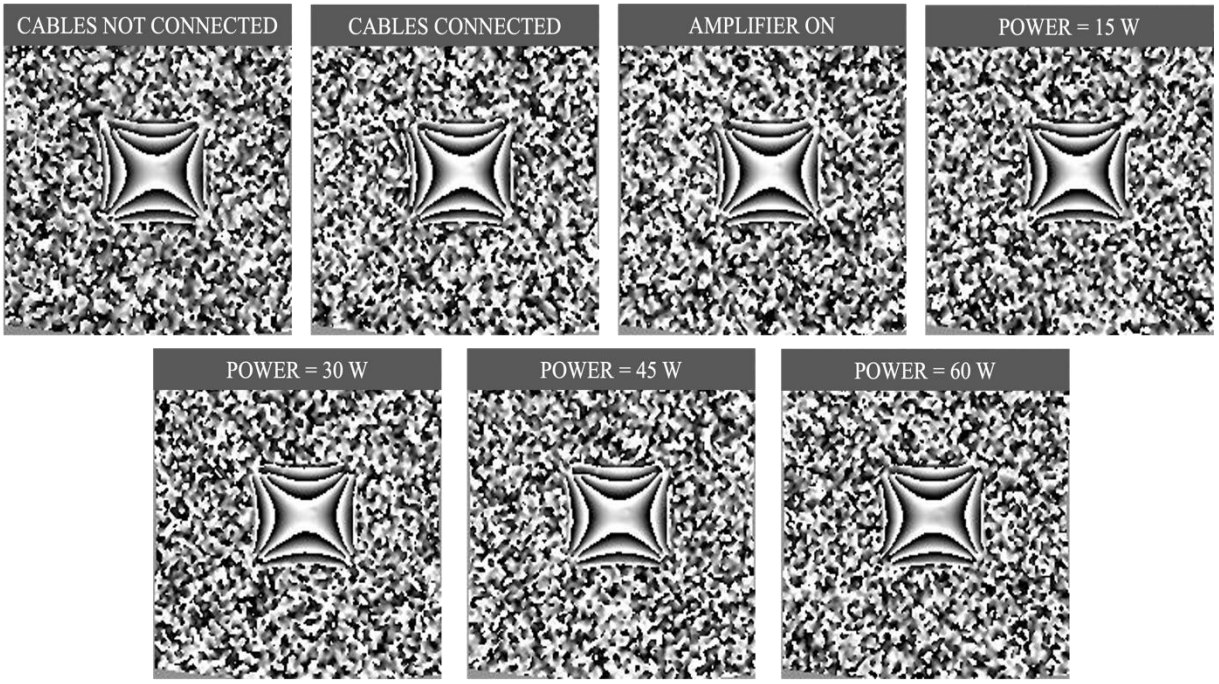

Figure 40: Coronal phase FLASH images of an agar-based phantom (6 % w/v agar, and 4 % w/v silicon dioxide) acquired at various activation states of the transducer.

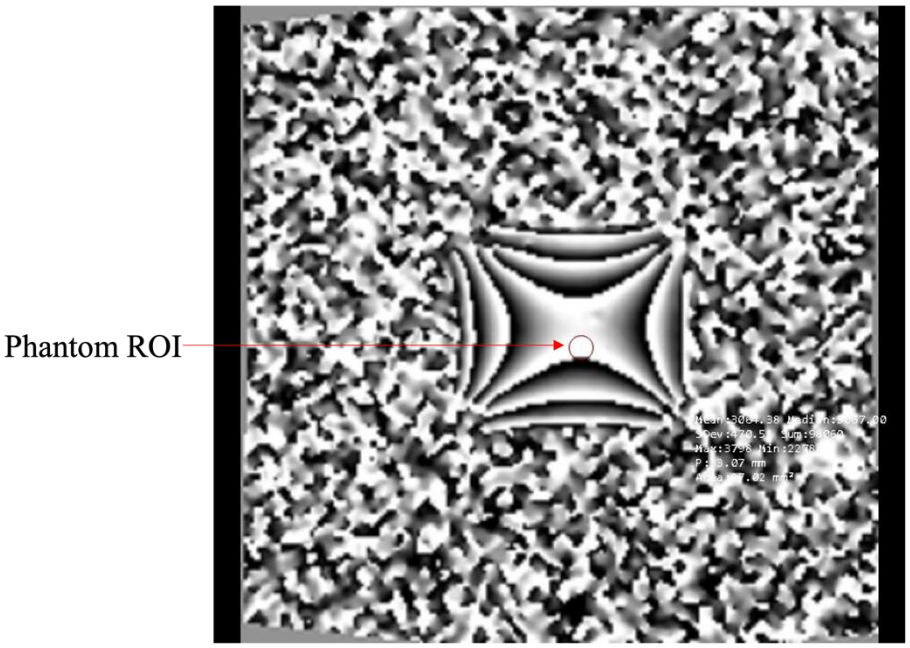

Figure 41: Measurements of average signal intensity at a specific ROI in the agar-based phantom on a coronal phase FLASH image of the phantom acquired during activation of the RF amplifier.

Accordingly, the average signal which was measured at the reference condition with sole presence of the robotic system in the MRI bore, was converted to a 100 % signal value. Signals calculated for phase FLASH images acquired at the following activation conditions (cables connected, amplifier activation, and transducer activation at acoustic power of 15, 30, 45, and 60 W) were appropriately given as percentages of the reference signal as shown in Figure 42.

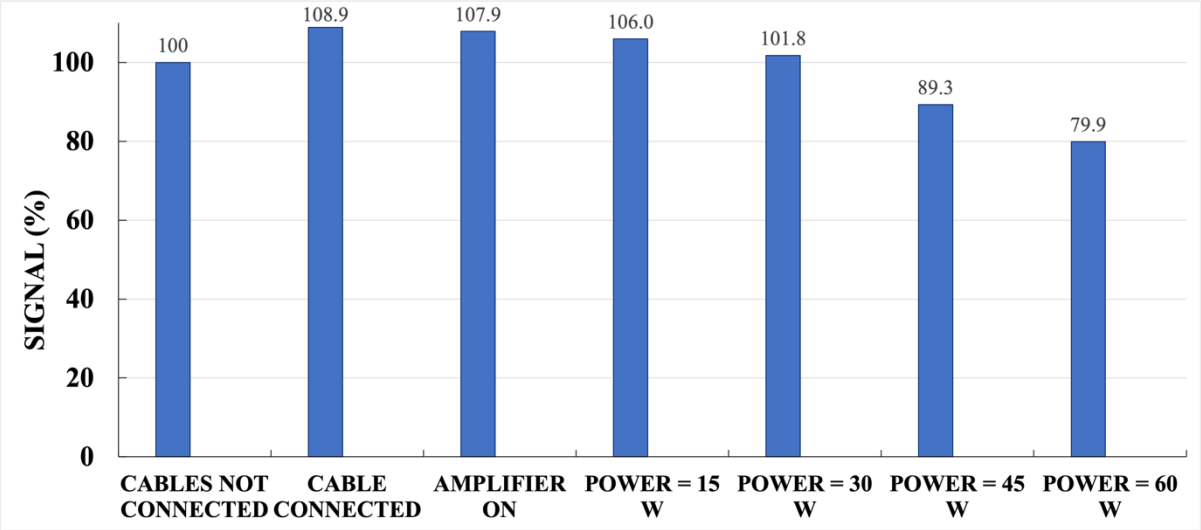

Figure 42: Bar chart of signal (%) as calculated from coronal phase FLASH images of an agar-based phantom (6 % w/v agar, and 4 % w/v silicon dioxide) acquired at various activations of the ultrasonic transducer.

Ablations of excised tissue in the MRI environment

Sonications monitored with MR thermometry

A series of sonications were executed on excised pork tissue using varied acoustical power for a constant sonication time of 60 s at a focal depth of 30 mm. Sonications were imaged with the FLASH sequence and images were processed to produce MR thermometry data. Initially, sonications were performed at an acoustical power of 45 W with FLASH images acquired in a coronal plane with a temporal resolution of 2.4 s. Figure 43 shows the coronal colour-coded thermal maps generated at certain timepoints during sonications, while Figure 44 shows the temperature increase induced in a ROI set at the focal point within the excised pork tissue. Sonications were sufficient to induce a temperature increase of 31.8 ^{o}C.

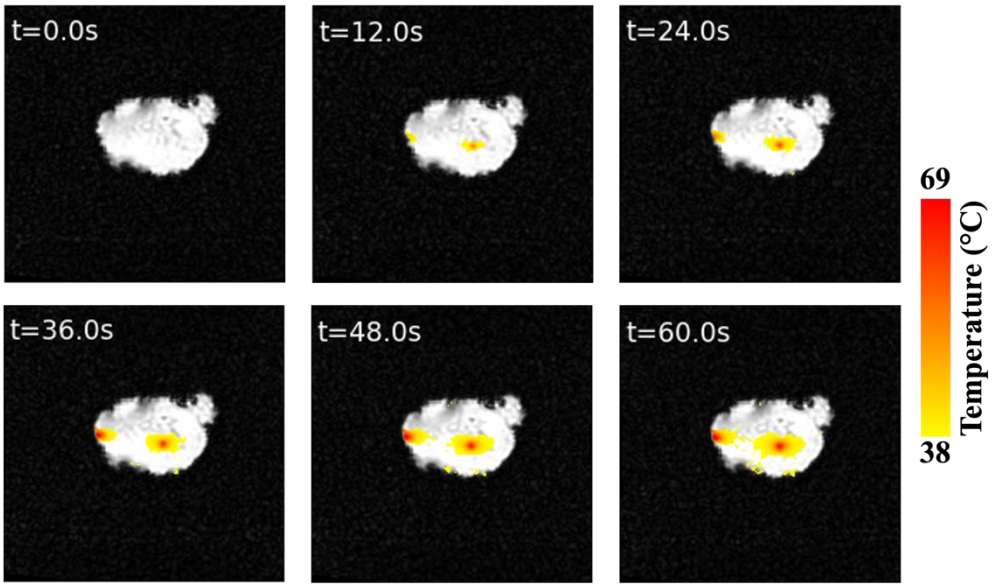

Figure 43: Coronal colour-coded thermal maps of excised pork tissue showing temperature increase at specific timepoints during sonications executed with the robotic system and a 2.75 MHz transducer (D=50 mm, ROC=65 mm) at acoustic power of 45 W for a sonication time of 60 s at a 30 mm focal depth.

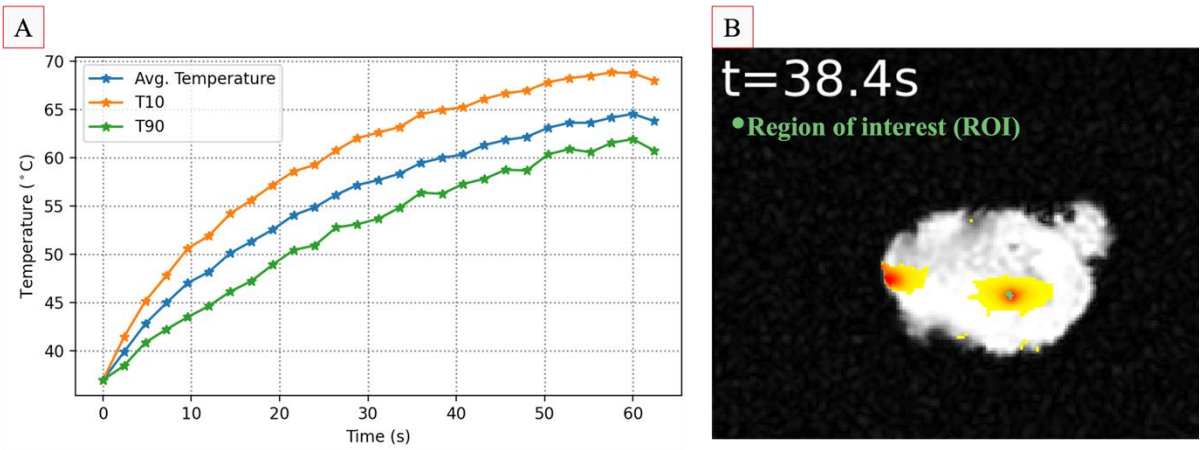

Figure 44: A) Temperature increase observed in a B) coronal ROI set at the focal spot within the excised pork tissue, during sonications executed with the robotic system and a 2.75 MHz transducer (D=50 mm, ROC=65 mm) at acoustic power of 45 W for a sonication time of 60 s at a 30 mm focal depth.

Robotic motion was then commanded to move the integrated 2.75 MHz transducer 10 mm left in the Y axis, wherein single sonications were executed on the same piece of excised tissue for an identical duration of 60 s using an increased acoustical power of 60 W. Axial FLASH images of the tissue were acquired during sonications as well as during a 60 s cooling period. Generated axial thermal maps showing the evolution of heating during sonications are shown in Figure 45. Sonications induced a temperature increase of 50.4 ^{o}C at the ROI set at the focal spot within the excised tissue as shown in Figure 46.

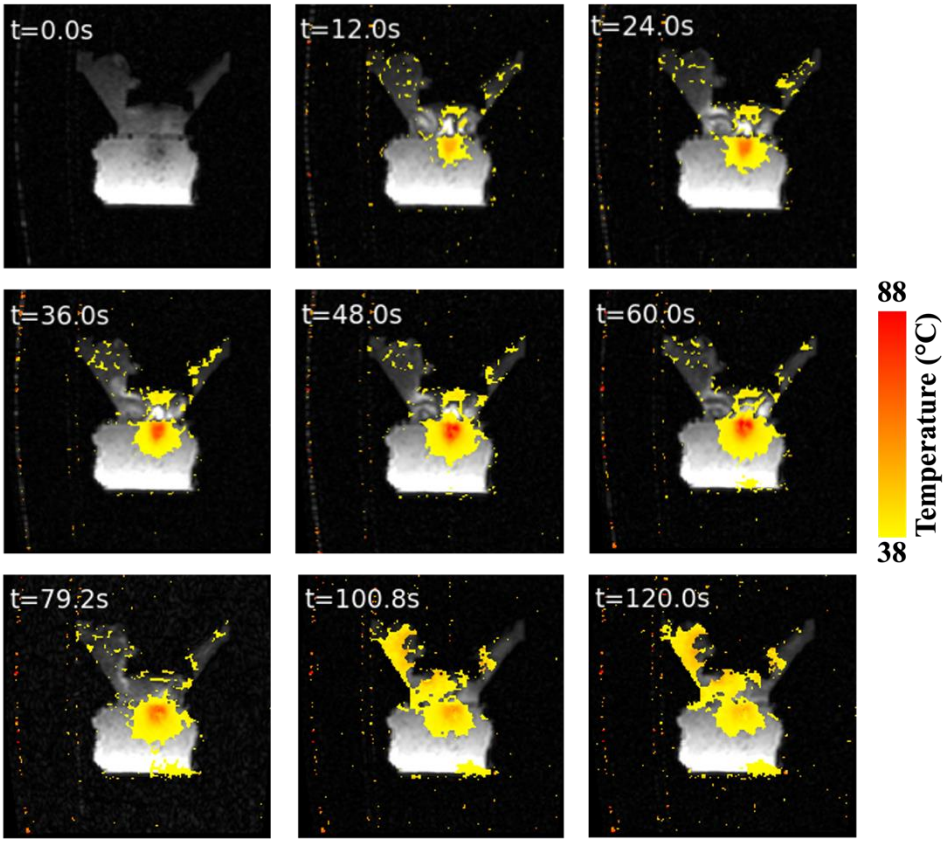

Figure 45: Axial colour-coded thermal maps of excised pork tissue showing temperature increase at specific timepoints during sonications executed with the robotic system and a 2.75 MHz transducer (D=50 mm, ROC=65 mm) at acoustic power of 60 W for a sonication time of 60 s at a 30 mm focal depth.

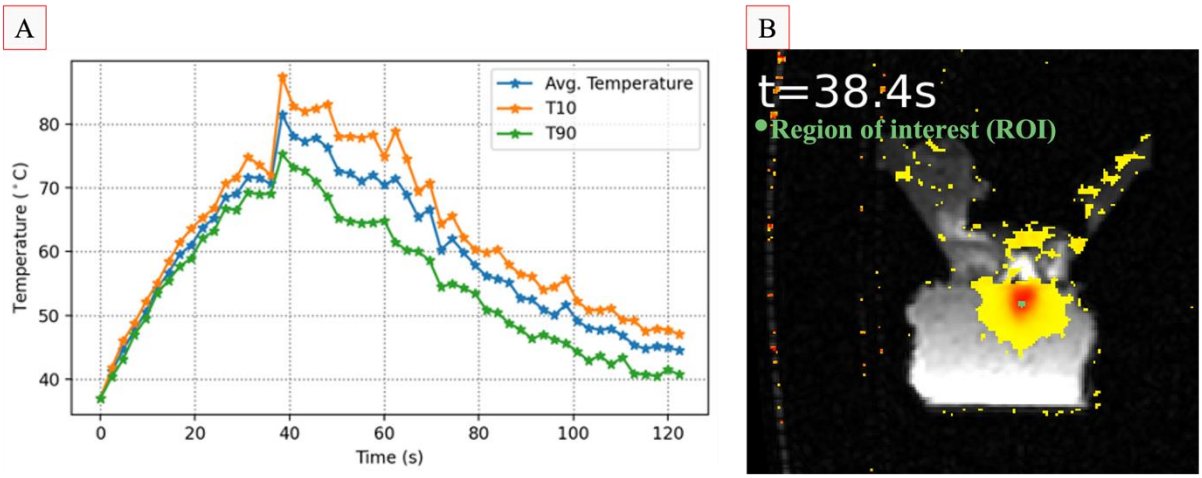

Figure 46: Temperature increase observed in an B) axial ROI set at the focal spot within the excised pork tissue, during sonications executed with the robotic system and a 2.75 MHz transducer (D=50 mm, ROC=65 mm) at acoustic power of 60 W for a sonication time of 60 s at a 30 mm focal depth.

Two sonications were then performed on a single location on a different piece of excised tissue by applying an acoustical power of 60 W for the constant duration of 60 s. Both sonications were executed at a focal depth of 30 mm and were imaged with the FLASH sequence in coronal and axial planes. The colour-coded thermal maps of the sonications generated in a coronal plane are shown in Figure 47. Sonications induced a temperature increase of 37.4 ºC in the ROI set at the focal spot within the tissue in the coronal plane as shown in Figure 48.

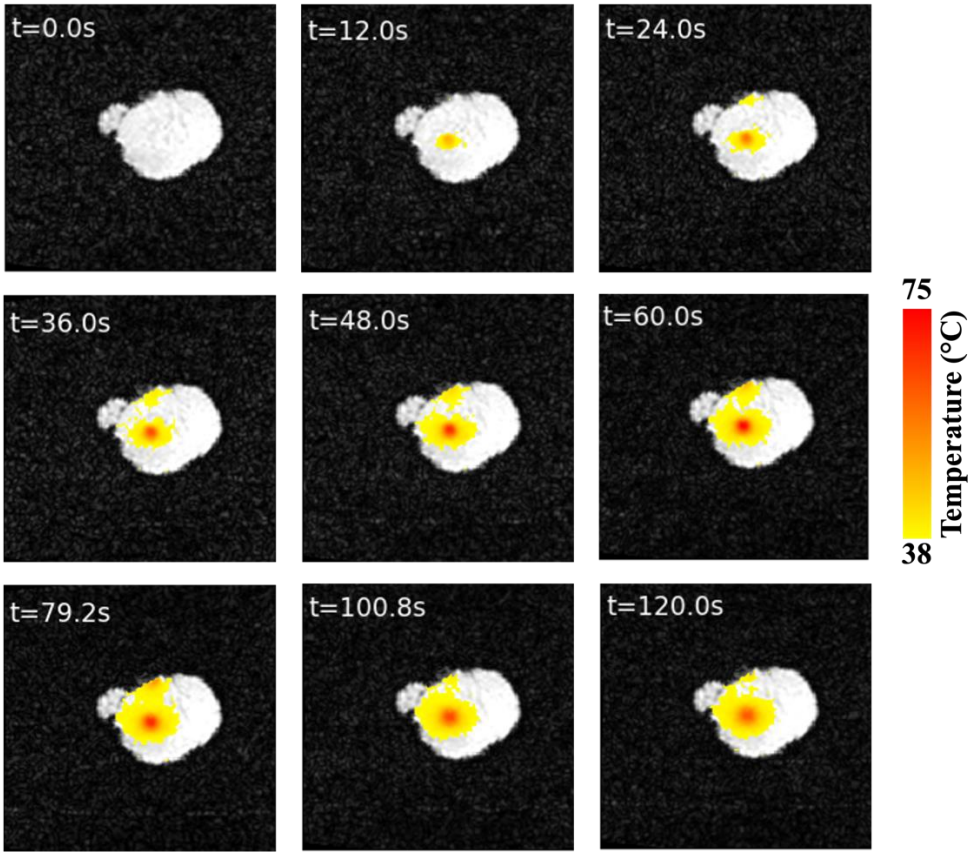

Figure 47: Coronal colour-coded thermal maps of excised pork tissue showing temperature increase at specific timepoints during sonications executed with the robotic system and a 2.75 MHz transducer (D=50 mm, ROC=65 mm) at acoustic power of 60 W for a sonication time of 60 s at a 30 mm focal depth.

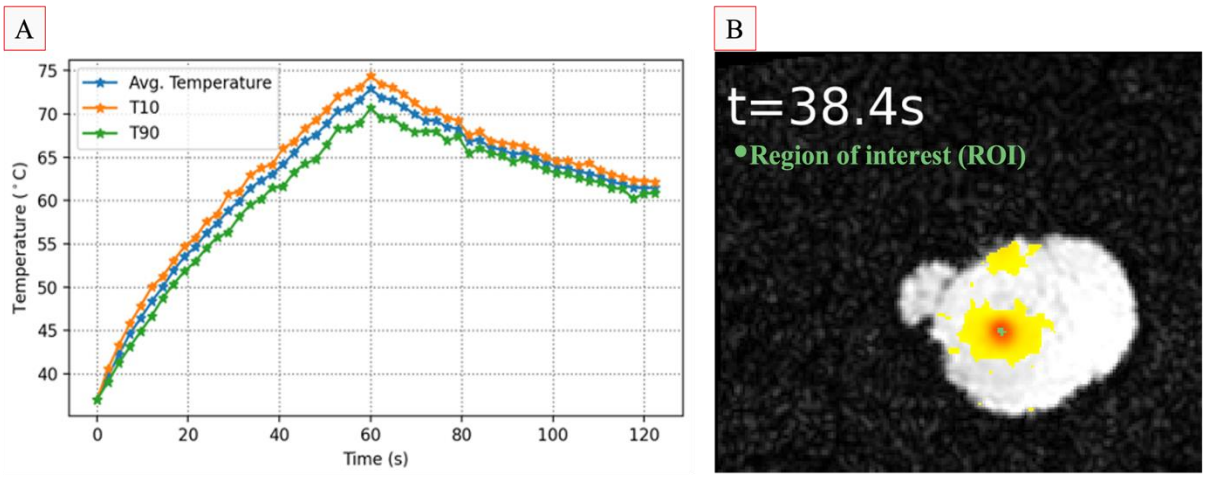

Figure 48: Temperature increase observed in a B) coronal ROI set at the focal spot within the excised pork tissue, during sonications executed with the robotic system and a 2.75 MHz transducer (D=50 mm, ROC=65 mm) at acoustic power of 60 W for a sonication time of 60 s at a 30 mm focal depth.

Figure 49 shows the colour-coded thermal maps produced in the axial plane, while Figure 50 shows the temperature increase induced within the set tissue ROI resulting sonications imaged in the axial plane. In the axial plane, a temperature increase of 32.3 ºC was induced by the sonications (Figure 50).

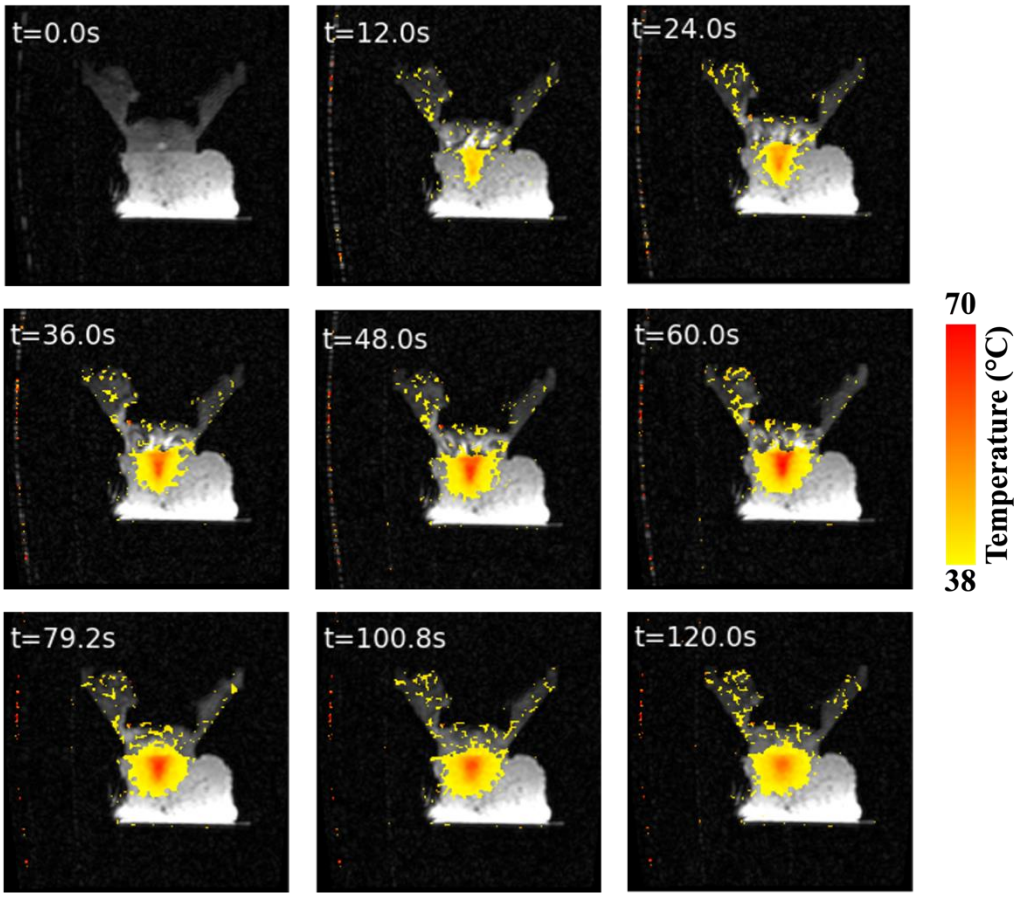

Figure 49: Axial colour-coded thermal maps of excised pork tissue showing temperature increase at specific timepoints during sonications executed with the robotic system and a 2.75 MHz transducer (D=50 mm, ROC=65 mm) at acoustic power of 60 W for a sonication time of 60 s at a 30 mm focal depth.

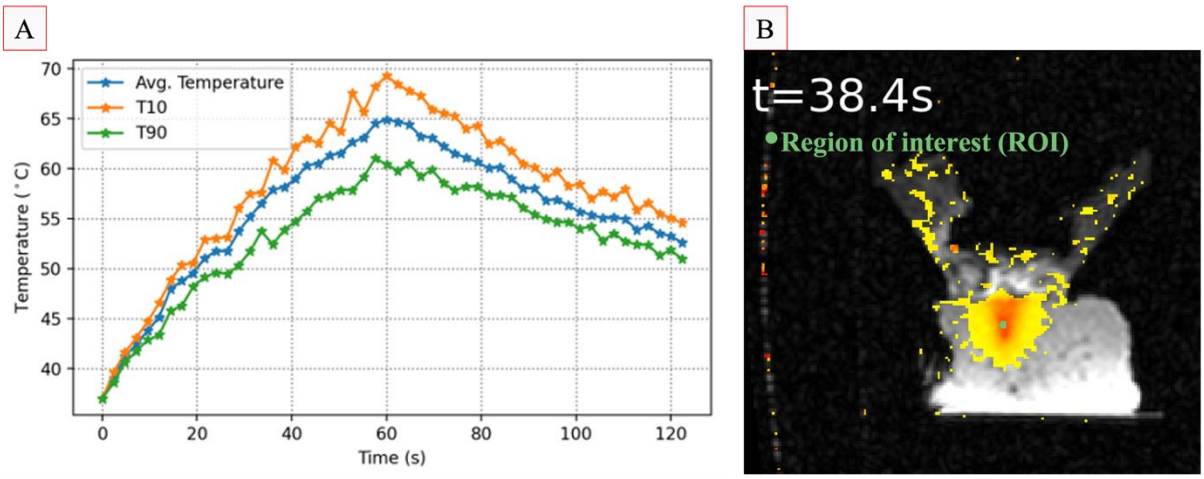

Figure 50: Temperature increase observed in an B) axial ROI set at the focal spot within the excised pork tissue, during sonications executed with the robotic system and a 2.75 MHz transducer (D=50 mm, ROC=65 mm) at acoustic power of 60 W for a sonication time of 60 s at a 30 mm focal depth.

Coronal T2-W TSE images (TR = 2300 ms, TE = 49 ms, FOV = 280×280 mm^2, Slice thickness = 10 mm, Acquisition matrix = 208×204, NEX = 1, ETL = 16, Flip angle = 110^o, and Pixel Bandwidth = 150 Hz/pixel) of the two pieces of excised pork tissue were acquired after sonications executed on each tissue piece to image the formed lesions as shown in Figure 51A and Figure 51B, respectively.

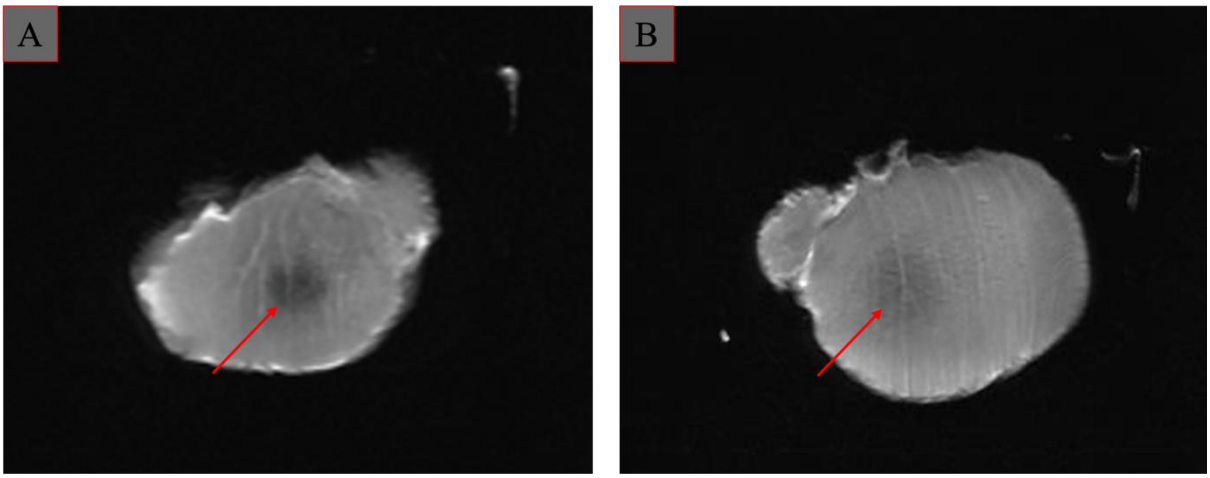

Figure 51: Coronal T2-W TSE images of lesions (red arrows) inflicted on two pieces of excised pork tissue after sonications executed using the robotic system and the 2.75 MHz transducer (D=50 mm, ROC=65 mm) at varied acoustical power for a sonication time of 60 s at a 30 mm focal depth. A) Lesions inflicted on the first piece of tissue after sonications at acoustic power of 45 W and 60 W, and B) Lesions inflicted on the second piece of tissue after sonications at acoustic power of 60 W.

Lesion detection during sonications

Initially, grid sonications were executed on a piece of excised tissue to monitor the formation of lesions during ablations, using a T2-W TSE sequence. Sonications of excised tissue were performed at an acoustical power of 60 W for a sonication time of 20 s, with motion of the robotic system and the transducer initiated in a 3×3 grid pattern with a 10 mm step. Grid sonications were executed at a focal depth of 30 mm, while a time delay of 60 s was utilised between successive sonications. Coronal T2-W TSE images (TR = 2100 ms, TE = 51 ms, FOV = 280×280 mm^2, Slice thickness = 5 mm, Acquisition matrix = 256×256, NEX = 1, ETL = 11,

Flip angle = 131°, and Pixel Bandwidth = 150 Hz/pixel) were acquired after sonications at each point of the 3×3 grid, visualising lesions formed at each sonication point as shown in Figure 52. Figure 53 and Figure 54 show photos of the excised tissue after exposure, showing discrete lesions formed in planes perpendicular and parallel to the beam, respectively. The dimensions of the individual formed lesions (as numbered in Figure 54) are shown in Table 9.

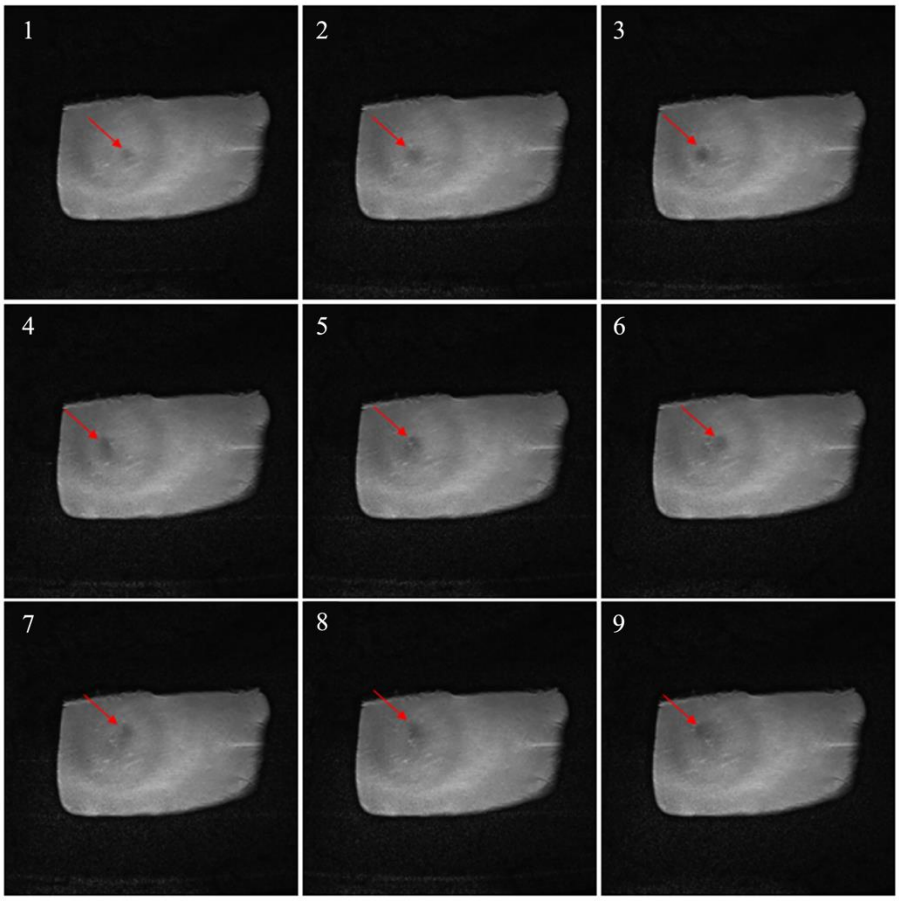

Figure 52: Coronal T2-W TSE images showing lesions (red arrow) inflicted on excised pork tissue after sonications executed at an acoustic power of 60 W for a sonication time of 20 s with motion of a 2.75 MHz transducer (D=50 mm, ROC=65 mm) using the robotic system in a 3×3 grid with a 10 mm step at a 30 mm focal depth. Numbers (1-9) represent the sonicated point of the 3×3 grid.

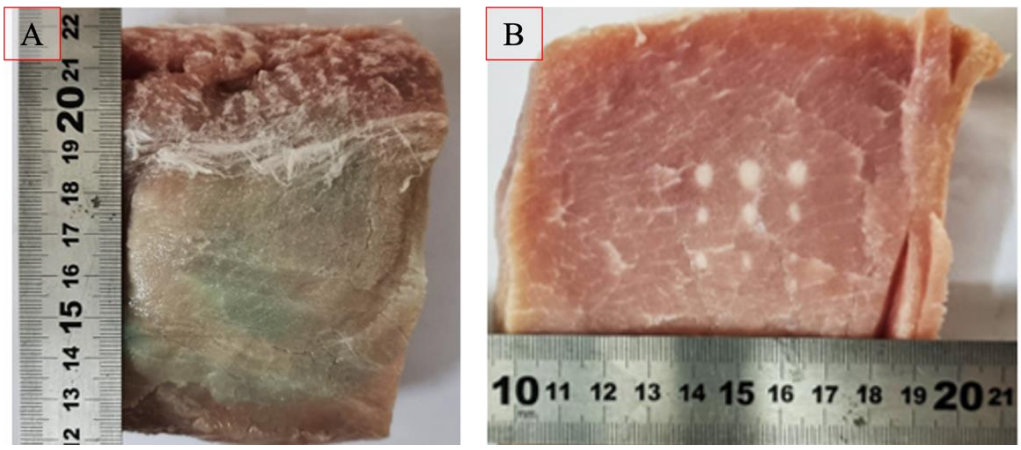

Figure 53: Photos of discrete lesions formed on excised pork tissue on a plane perpendicular to the beam after sonications in a 3×3 grid with a 10 mm step using the robotic system and a 2.75 MHz transducer (D=50 mm, ROC=65 mm) at acoustic power of 60 W for a sonication time of 20 s at a 30 mm focal depth. A) Surface of the tissue, and B) Slice of the tissue at 10 mm.

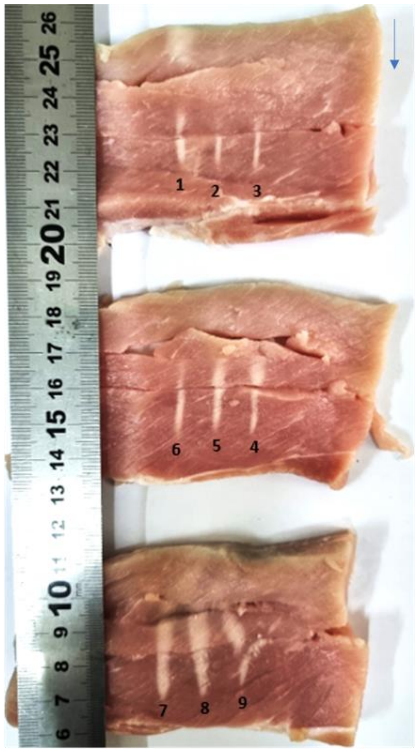

Figure 54: Photos of discrete lesions formed on excised pork tissue on a plane parallel to the beam after sonications in a 3×3 grid with a 10 mm step using the robotic system and a 2.75 MHz transducer (D=50 mm, ROC=65 mm) at acoustic power of 60 W for a sonication time of 20 s at a 30 mm focal depth. Blue arrow indicates ultrasonic beam direction.

Table 9: Dimensions of discrete lesions formed on excised pork tissue after sonications in a 3×3 grid using the robotic system and a 2.75 MHz transducer (D=50 mm, ROC=65 mm) at an acoustic power of 60 W for a sonication time of 20 s at a 30 mm focal depth.

Lesion	Diameter (mm)	Length (mm)
1	2.37	13.91
2	1.82	8.73
3	1.46	13.47
4	1.64	20.54
5	2.64	19.42
6	2.18	20.50
7	4.55	25.56
8	6.11	24.87
9	6.09	22.85
Average	***3.21***	***18.87***

Thereafter, single sonications were executed on the excised tissue to investigate the ability to detect lesions at certain timeframes post-sonications using T1-W and T2-W TSE sequences with varied parameters. Specifically, varied TE values of the T2-W TSE sequence were employed for imaging the tissue after exposures. In this regard, an increased acoustical power of 75 W was used for a sonication time of 60 s to ablate the excised tissue at a single location. Sonications were executed at the same focal depth of 30 mm. Initially, a T2-W TSE sequence

with the following imaging parameters: TR = 2100 ms, FOV = 160×160 mm^2, Slice thickness = 5 mm, Acquisition matrix = 416×416, NEX = 1, ETL = 11, Flip angle = 131^o, Pixel Bandwidth = 150 Hz/pixel, and a TE of 50 ms was employed for imaging the tissue directly after sonications and 5 minutes thereafter. Coronal T2-W TSE images, acquired directly after sonications and 5 minutes thereafter, showing the inflicted lesions on the excised tissue are shown in Figure 55A, and Figure 55B, respectively. Similarly, the T2-W TSE sequence was employed with the same imaging parameters and a decreased TE value of 48 ms for imaging the tissue 5 minutes after sonications, with the lesion clearly visible on the acquired coronal image as shown in Figure 55C.

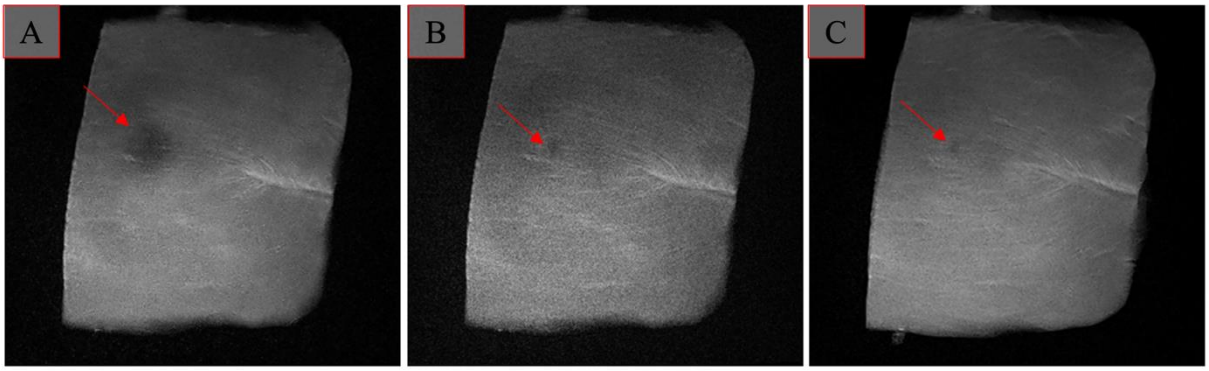

Figure 55: Coronal T2-W TSE images of lesion (red arrows) inflicted on excised pork tissue after sonications executed with the robotic system and the 2.75 MHz transducer (D=50 mm, ROC=65 mm) at an acoustic power of 75 W for a sonication time of 60 s at a 30 mm focal depth. Images acquired with A) TE=50 ms directly after sonications, B) TE=50 ms 5 minutes after sonications, and C) TE=48 ms 5 minutes after sonications.

Additionally, a T1-W TSE sequence (TE = 12 ms, TR = 1500 ms, FOV = 160×160 mm^2, Slice thickness = 8 mm, Acquisition matrix = 352×352, NEX = 1, ETL = 11, Flip angle = 131^o, and Pixel Bandwidth = 150 Hz/pixel) was utilised to image the excised tissue 5 minutes after the executed sonications. The T1-W TSE image acquired in a coronal plane, showing the lesion formed on the tissue, is shown in Figure 56. Figure 57 shows the lesion formed on the excised tissue in a plane parallel to the beam, after tissue slicing. The lesion inflicted by sonications was formed with a diameter of 12.30 mm and a length of 36.55 mm.

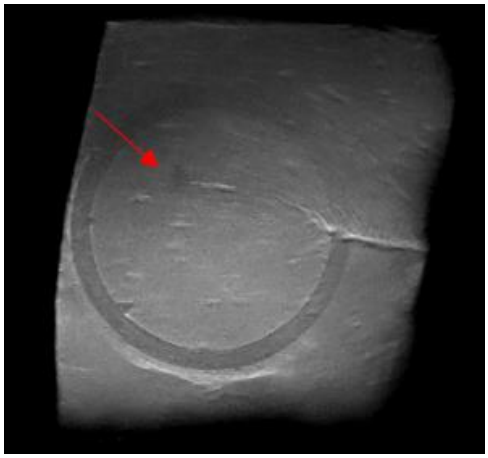

Figure 56: Coronal T1-W TSE image (TE=12 ms) of lesion (red arrow) inflicted on excised pork tissue acquired 5 minutes after sonications executed using the robotic system and the 2.75 MHz transducer (D=50 mm, ROC=65 mm) at an acoustic power of 75 W for a sonication time of 60 s at a 30 mm focal depth.

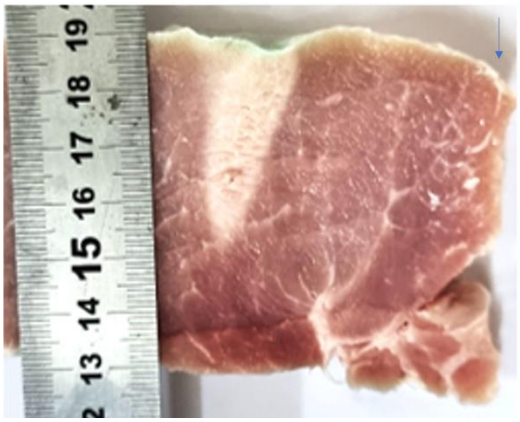

Figure 57: Lesion formed on excised pork tissue on a plane parallel to the beam after sonications executed using the robotic system and the 2.75 MHz transducer (D=50 mm, ROC=65 mm) at an acoustic power of 75 W for a sonication time of 60 s at a 30 mm focal depth. Blue arrow indicates beam direction.

Sonications on agar-based phantoms monitored with MR thermometry

A series of sonications were also performed on agar-based phantoms to assess and monitor the thermal heating of the system using MR thermometry. Sonications were executed using varied acoustic power of 15-60 W (15 W step) for a constant sonication time of 30 s at a focal depth of 30 mm. Figure 58 shows the coronal colour-coded thermal maps produced during sonications executed using an acoustical power of 45 W. Figure 59 shows the recorded temperature increase induced in the ROI set at the focal area within the agar-based phantom. Sonications executed with the acoustical power of 45 W induced a temperature increase of 32.4 ºC. Table 10 shows the temperature change recorded with MR thermometry, from a reference temperature of 37 ºC, resulting sonications performed at varied acoustical power of 15-60 W.

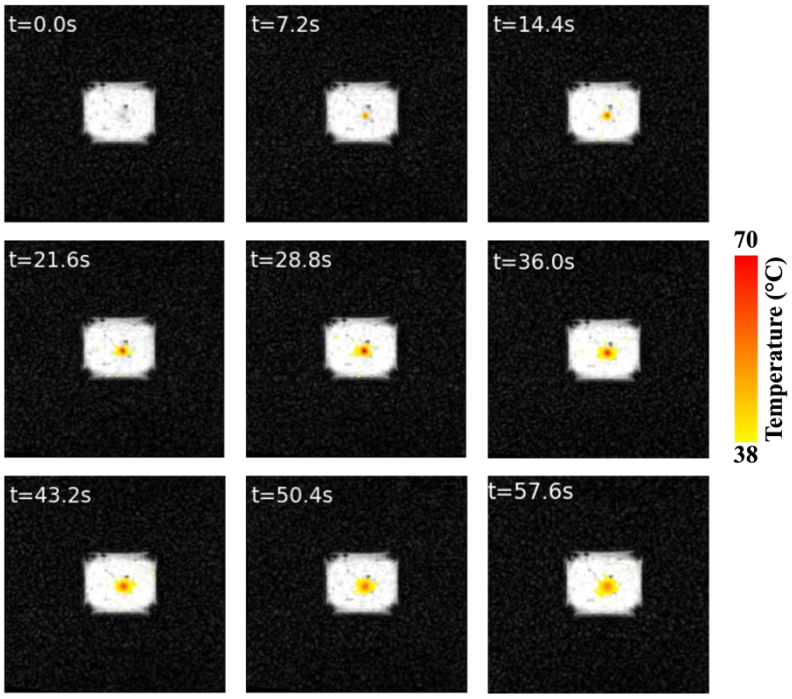

Figure 58: Coronal colour-coded thermal maps of an agar-based phantom (6 % w/v agar, and 4 % w/v silicon dioxide) showing temperature increase at specific timepoints during sonications executed with the robotic system and a 2.75 MHz transducer (D=50 mm, ROC=65 mm) at acoustic power of 45 W for a sonication time of 30 s at a 30 mm focal depth.

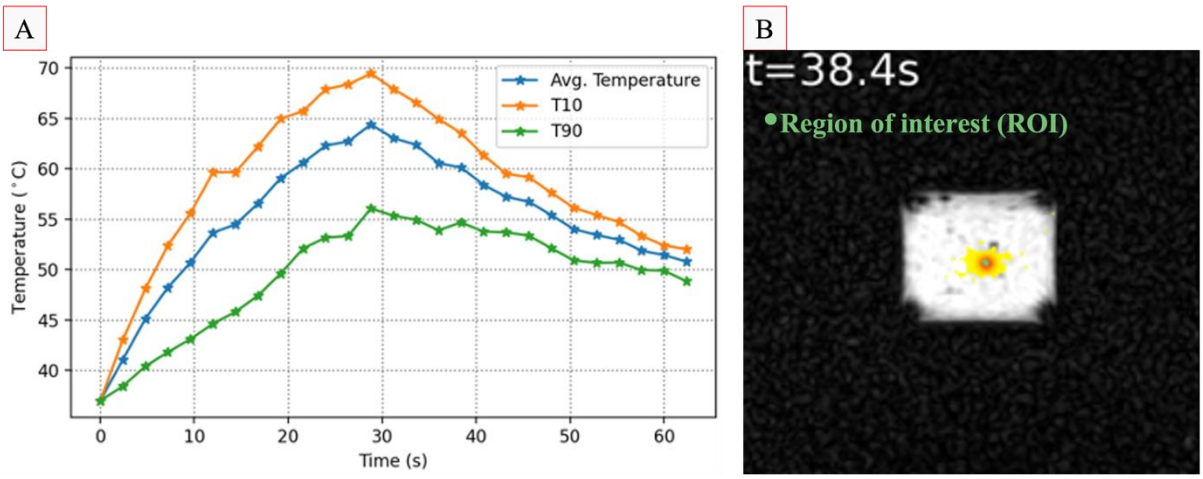

Figure 59: Temperature increase observed in a B) coronal ROI set at the focal spot within the agar-based phantom (6 % w/v agar, and 4 % w/v silicon dioxide), during sonications executed with the robotic system and a 2.75 MHz transducer (D=50 mm, ROC=65 mm) at acoustic power of 45 W for a sonication time of 30 s at a 30 mm focal depth.

Table 10: Temperature change recorded with MR thermometry resulting sonications executed on an agar-based phantom (6 % w/v agar, and 4 % w/v silicon dioxide) using the robotic system and a 2.75 MHz transducer (D=50 mm, ROC=65 mm) at varied acoustical power for a constant sonication time of 30 s at a 30 mm focal depth.

Acoustic power (W)	Sonication time (s)	Imaging plane	Temperature change (°C)
15	30	Coronal	16.4
30			28.7
45			32.4
60			34.9
		Axial	28.9

Evaluation on tumorgraft murine models

FUS ablation of tumorgraft mouse models

One week after transplantation, visual examination of the mice and palpation at the inoculation site confirmed tumour formation on all mice of both groups ("FUS group" and "Control group"). Figure 60 and Figure 61 show photos of the sarcoma tumour grafts as formed on the mice of the "Control group" (n=5) and of the "FUS group" (n=5), respectively. Visual inspection and caliper measurements of the diameters of the grown tumours revealed a variation in tumour sizes among the 10 tumorgraft mice. The diameters of the formed tumours as measured for each of the 5 mice of either the "Control" or the "FUS" groups are listed in Table 11. As shown in Table 11, differences in tumour sizes were observed within mice of the same group, as well as between the average tumour diameters of the two groups. Nevertheless, the performed t-test did not reveal a significant difference in the average diameter of formed tumours on mice of the "FUS group" (Mean (M)=2, Standard deviation (SD)=2.24) and on mice of the "Control group" (M=2.92, SD=2.69, unpaired t-test; t(8)=-0.5882, p=0.2863).

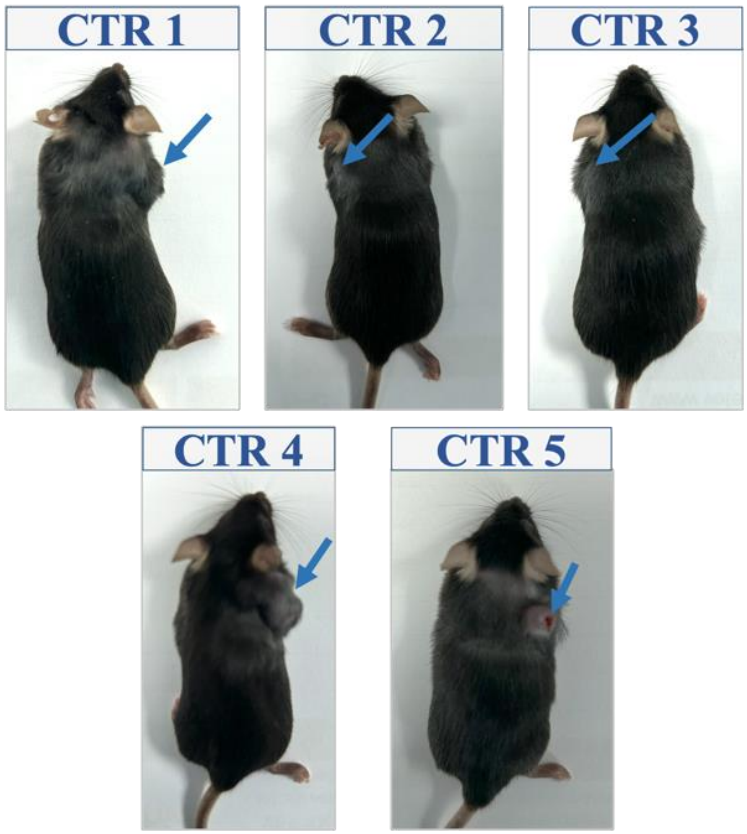

Figure 60: Photos of formed sarcoma tumours (blue arrows) on the 5 tumorgraft mice of the "Control group" taken 7 days after transplantation.

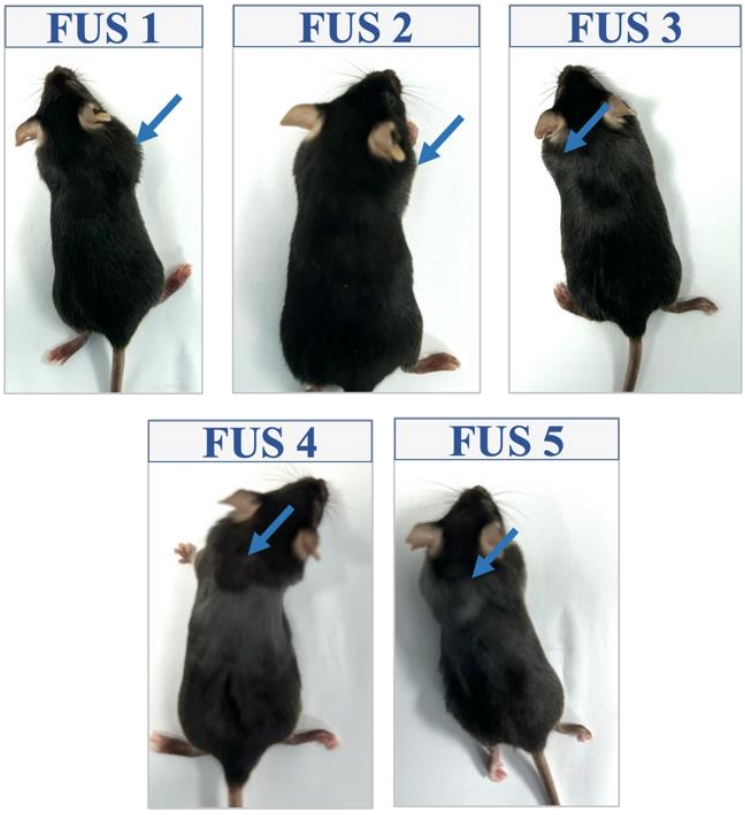

Figure 61: Photos of formed sarcoma tumours (blue arrows) on the 5 tumorgraft mice of the "FUS group" taken 7 days after transplantation.

Table 11: Diameters of tumours as measured for each tumorgraft mouse of the "Control" and "FUS" groups 7 days after transplantation.

Tumour diameters 7 days after transplantation			
"Control group"		***"FUS group"***	
Mouse	**Diameter (mm)**	**Mouse**	**Diameter (mm)**
CTR 1	1	FUS 1	1
CTR 2	6.6	FUS 2	1
CTR 3	1	FUS 3	1
CTR 4	5	FUS 4	1
CTR 5	1	FUS 5	6
Average	***2.92 ± 2.69***	***Average***	***2 ± 2.24***

"Control group"

Throughout the 3-week experimental period, tumour grafts on all mice of the "Control group" invaded the host murine models and naturally grew and increased in size. Photos of the formed sarcoma tumours on the 5 mice (CTR1, CTR2, CTR3, CTR4, and CTR5) of the "Control group" are shown in Figure 62, visually indicating the natural development of the sarcoma tumour grafts over the 21-day period following transplantation.

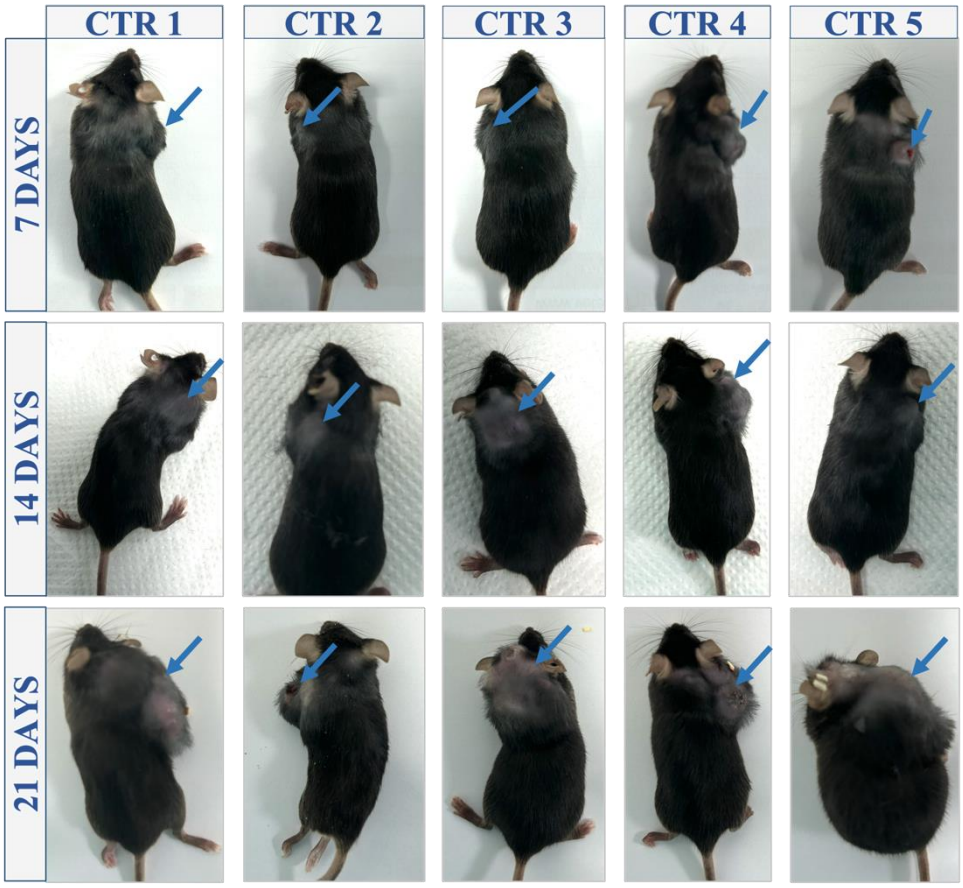

Figure 62: Photos of formed sarcoma tumours (blue arrows) on the 5 tumorgraft mice of the "Control group" taken every 7 days for a duration of 3-weeks after transplantation.

Tumour diameters as measured on the 5 tumorgraft mice of the "Control group" at 7, 10, 14 and 21 days following transplantation are shown in Figure 63. Tumours in all mice of the "Control group" aggressively increased in size during the 21-day period. Monitoring throughout the 3-week period indicated a normal behaviour from all mice. Nevertheless, 22 days after transplantation, the mice stopped eating and drinking probably due to enlarged tumour sizes, thus all mice were humanely euthanised.

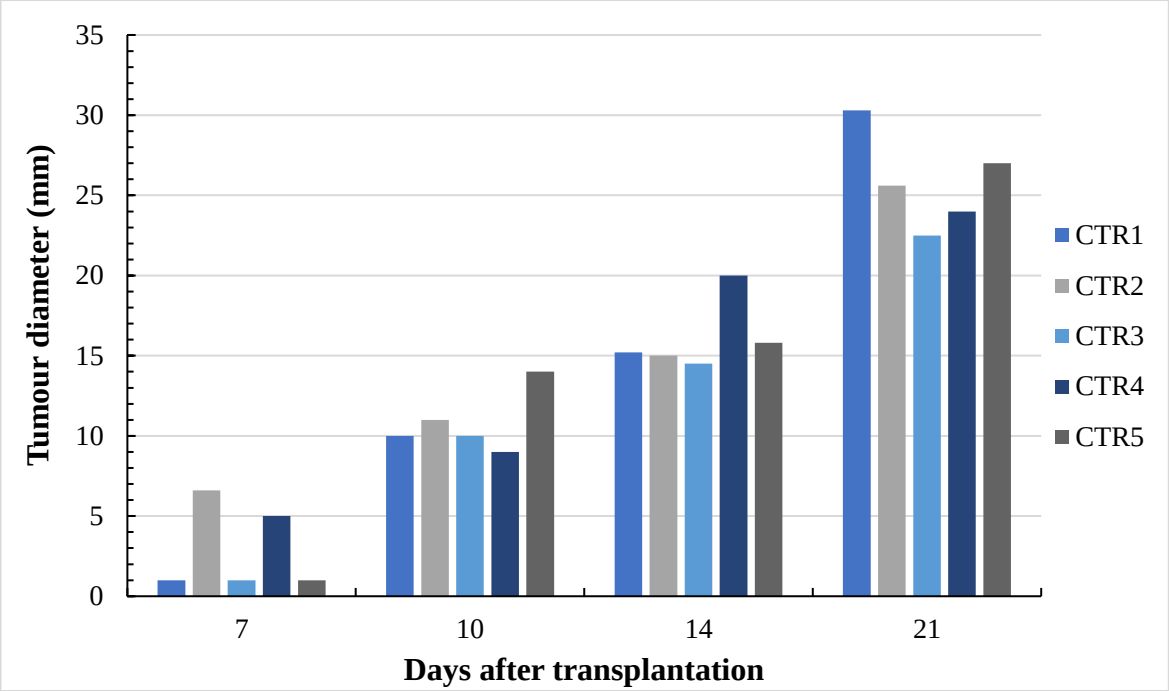

Figure 63: Diameters of tumours as measured for each tumorgraft mouse of the "Control group" at specific timepoints after transplantation.

"FUS group"

Tumours formed on all 5 mice of the "FUS group" were effectively ablated using constant therapeutic protocols (acoustic power of 75 W for a sonication time of 10 s) that were applied in a grid manner (3×3 grid with a 4 mm step) at 7, 14, and 21 days after transplantation. During sonications all mice breathed normally, thus there was no indication of any acute FUS-induced effects present.

Gross examination of the ablated areas of the tumour grafts after the end of each FUS treatment session revealed the formation of visible discrete coagulative lesions on the targeted surface of each tumour. Indicative discrete lesions inflicted on the tumour graft on a mouse from the "FUS group" after FUS ablations are shown in Figure 64. During the 7-day monitoring period following each individual FUS session, normal breathing, motion, eating and drinking habits were exhibited from all mice with no long-term adverse effects indicated. Therefore, the 3 sequential FUS treatment sessions were effectively delivered to all 5 mice.

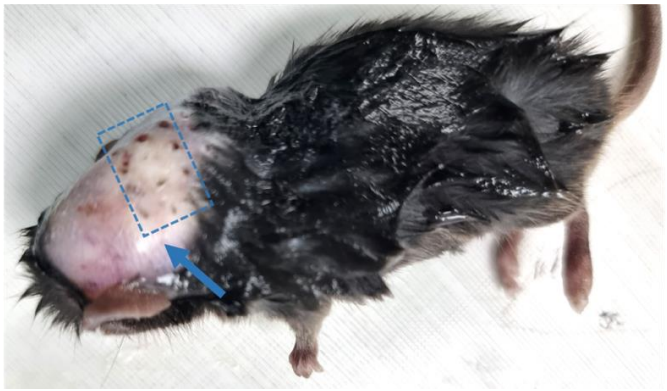

Figure 64: Photo of discrete lesions (blue rectangle) inflicted on a sarcoma tumour graft (blue arrow) on a mouse of the "FUS group" after ablations with the robotic system and a 2.75 MHz transducer (D=50 mm, ROC=65 mm) in a 3×3 grid pattern with a 4 mm step using an acoustic power of 75 W for a sonication time of 10 s.

Figure 65 shows the growth of the transplanted neoplasms on the 5 mice of the "FUS group" (FUS1, FUS2, FUS3, FUS4, and FUS5) over the 21-day period following transplantation. Corresponding tumour diameter measurements obtained at 7, 10, 14 and 21 days after inoculation of the tumour cells for each mouse of the "FUS group" are shown in Figure 66. Similar to the "Control group", tumour sizes substantially increased for all 5 mice of the "FUS group" 21 days after transplantation. After the 3rd FUS treatment session which was delivered on the 21st day, all mice successfully emerged from anaesthesia and continued to behave normally for the following day. However, 2 days after delivery of the final FUS session (23 days after transplantation), the 5 mice were euthanised because they rejected food and water.

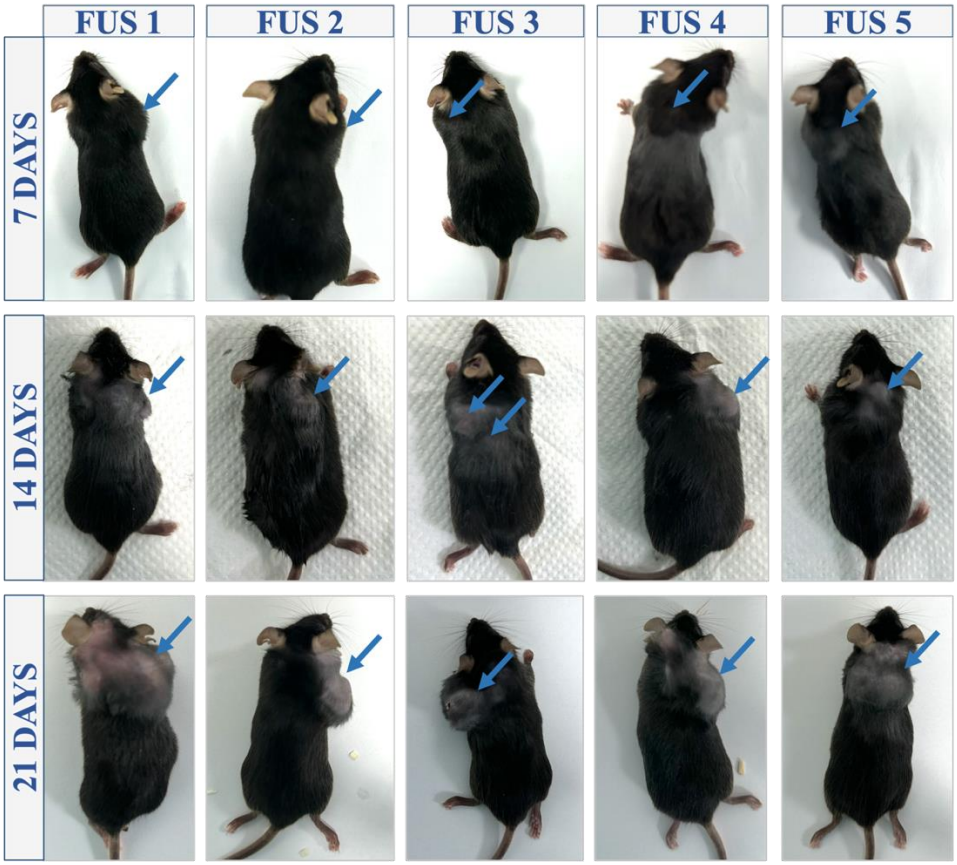

Figure 65: Photos of formed sarcoma tumours (blue arrows) on the 5 tumorgraft mice of the "FUS group" taken every 7 days for a duration of 3-weeks after transplantation.

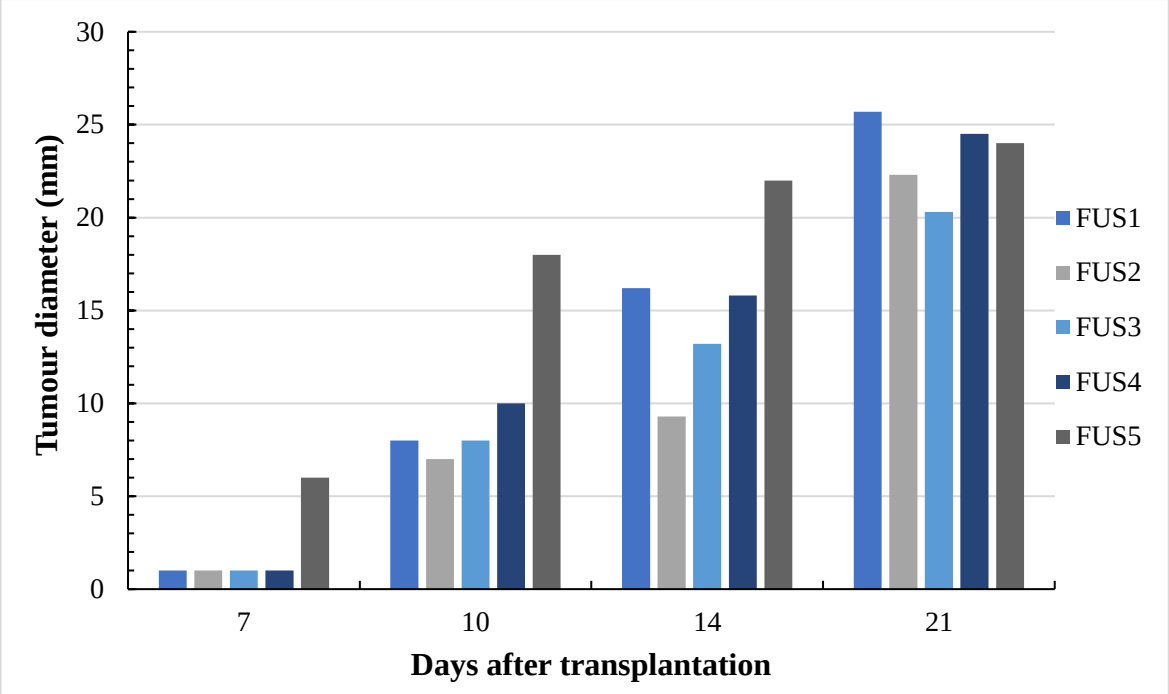

Figure 66: Diameter of tumours as measured for each tumorgraft mouse of the "FUS group" at specific timepoints after transplantation.

Effects of FUS therapy on tumour growth

Measured tumour diameters for the mice of the "Control group" and "FUS group" plotted against the 10- to 21-day period after transplantation are shown in Figure 67, visually showcasing the natural development of tumours on the tumorgraft mice of the "Control group" and the corresponding growth of sequentially FUS-treated tumours on the mice of the "FUS group".

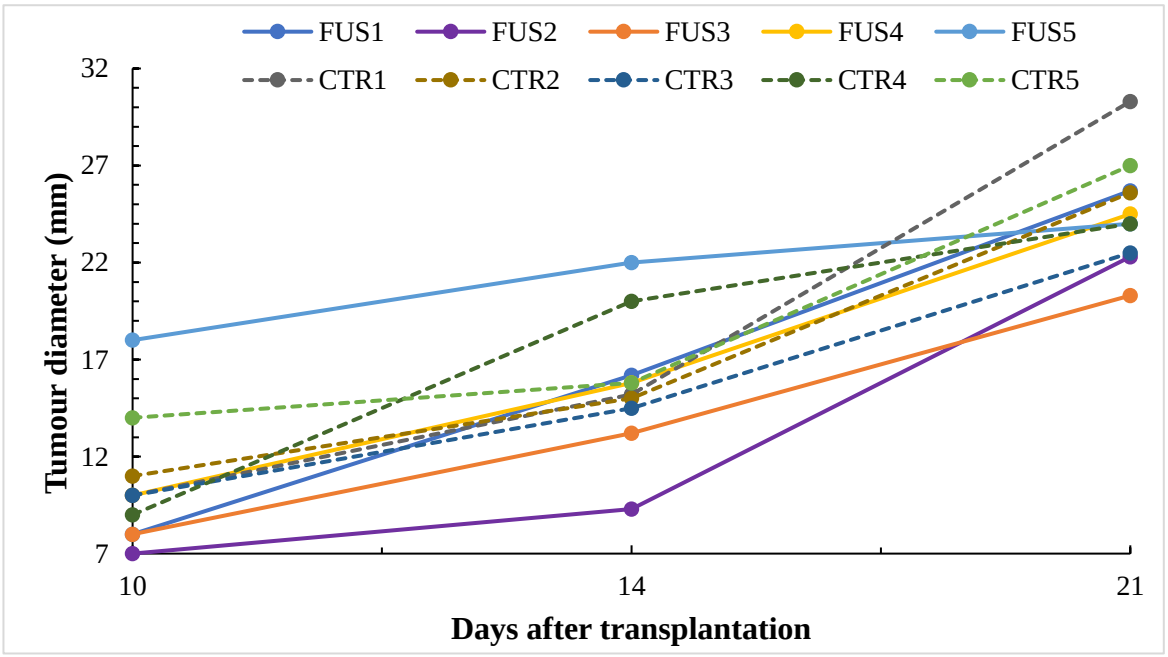

Figure 67: Diameters of tumours as measured for each tumorgraft mouse of the "Control group" (CTR1 to CTR5) and the "FUS group" (FUS1 to FUS5) at different timepoints following transplantation.

Individual tumour diameters as measured for each of the 5 mice of either the "Control group" and "FUS group" at 10 days (3 days after the 1st FUS session), 14 days (7 days after the 1st FUS session) and 21 days (7 days after the 2nd FUS session) after transplantation are listed in Table 12, Table 13, and Table 14, respectively. Comparing tumour size data of the 10th day, the diameters of tumour grafts on mice of the "FUS group" (M=10.2, SD=4.49) were not significantly smaller than those on mice of the "Control group" (M=10.8, SD=1.92, unpaired t-test; t(8)=-0.2744, p=0.3954). Similar results were obtained on the 14th day, wherein application of the 1st FUS session failed to achieve a significantly smaller average tumour diameter in mice of the "FUS group" (M=15.3, SD=4.65) compared to the tumour diameters in mice of the "Control group" (M=16.1, SD=2.23, unpaired t-test; t(8)=-0.3471, p=0.3687) 7 days after treatment. Nevertheless, application of FUS for a 2nd time on the mice of the "FUS group" demonstrated a significantly smaller diameter of the transplanted neoplasms (M=23.36, SD=2.10) compared to tumours on mice of the "Control group" (M=25.88, SD=2.99,unpaired t-test; t(8)=-1.541, p=0.08) one week after treatment delivery.

Table 12: Diameters of tumours as measured for each tumorgraft mouse of the "Control" and "FUS" groups 10 days after transplantation (3 days after the 1st FUS session).

Tumour diameters 10 days after transplantation			
"Control group"		***"FUS group"***	
Mouse	**Diameter (mm)**	**Mouse**	**Diameter (mm)**
CTR 1	10	FUS 1	8
CTR 2	11	FUS 2	7
CTR 3	10	FUS 3	8
CTR 4	9	FUS 4	10
CTR 5	14	FUS 5	18
Average	***10.8 ± 1.92***	***Average***	***10.2 ± 4.49***

Table 13: Diameters of tumours as measured for each tumorgraft mouse of the "Control" and "FUS" groups 14 days after transplantation (7 days after the 1st FUS session).

Tumour diameters 14 days after transplantation			
"Control group"		***"FUS group"***	
Mouse	**Diameter (mm)**	**Mouse**	**Diameter (mm)**
CTR 1	15.2	FUS 1	16.2
CTR 2	15	FUS 2	9.3
CTR 3	14.5	FUS 3	13.2
CTR 4	20	FUS 4	15.8
CTR 5	15.8	FUS 5	22
Average	***16.1 ± 2.23***	***Average***	***15.3 ± 4.65***

Table 14: Diameters of tumours as measured for each tumorgraft mouse of the "Control" and "FUS" groups 21 days after transplantation (7 days after the 2nd FUS session).

Tumour diameters 21 days after transplantation			
"Control group"		***"FUS group"***	
Mouse	**Diameter (mm)**	**Mouse**	**Diameter (mm)**
CTR 1	30.3	FUS 1	25.7
CTR 2	25.6	FUS 2	22.3
CTR 3	22.5	FUS 3	20.3
CTR 4	24	FUS 4	24.5
CTR 5	27	FUS 5	24
Average	***25.88 ± 2.99***	***Average***	***23.36 ± 2.10***

Evaluation on pets with naturally occurring tumours

Generated reports of all experiments are included in Appendix 1. During the 24 months of trials, totally 18 animals were recruited in the study; 16 dogs and 2 cats. Animals were of various ages and presented with different sizes and types of tumours such as mammary, pressure-point comedones, sarcomas, and lipomas. Table 15 lists the age and weight range of the recruited animals as well as the types and volume of their tumours.

Table 15: List of recruited animal and tumour characteristics.

Animal characteristics	
Weight of cats (Kg)	2 – 4
Weight of dogs (Kg)	5 – 40
Age (years)	3 – 13
Tumour characteristics	
Tumour types	Mammary, pressure-point comedones, sarcoma, lipoma
Size of tumour (mm^3)	20×20×30 – 60×50×30

Sonication protocols (acoustical power and sonication time) employed for tumour ablation are summarised in Table 16. In all experiments, irrespective of tumour size, treatment safety was evaluated by applying a constant sonication protocol of low energy (acoustical power of 1.5 W for 10 s duration). In most cases (17 out of 18), high energy single tumour ablations were then executed using a range of sonication protocols (Table 16) that were appropriately selected depending on the tumour volume. In one case (study ID: FUSVET-18), high energy tumour ablations were executed in a grid manner (3×3 grid with 4 mm step) following motion in the PC-controlled X and Y stages of the robotic system.

Table 16: List of sonication protocols employed for tumour ablation.

Sonication protocol	
Acoustical Power (W)	*Pain check:* 1.5 W *Ablation:* 15 - 75 W
Time (s)	*Pain check:* 10 s *Ablation:* 10 - 30 s

In most of the experiments (17 out of 18), gross examination of the tumour after ablations did not reveal a visible lesion on the tumour surface. In one study (study ID: FUSVET-9), gross examination post-sonications revealed the *in-situ* formation of a coagulative lesion at the targeted region as shown in Figure 68. Figure 68A shows a photo of the tumour before FUS ablations, while Figure 68B shows the lesion that was locally inflicted on the tumour after FUS exposure. Histological examination of the inflicted lesion revealed localised loss of the outer skin layer (epidermis) and its replacement with a polymerized fibrin, indicating blood clotting.

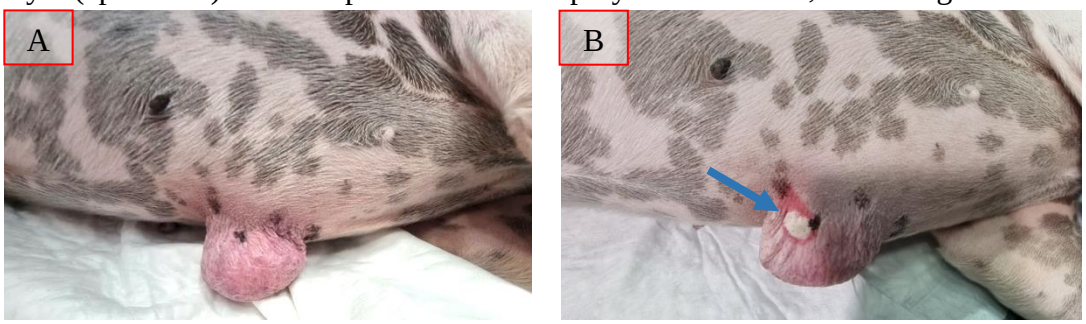

Figure 68: Photo of tumour (pressure-point comedones) in dog. A) Before FUS ablation, and B) After FUS ablations at acoustic power of 75W for 30 s duration showing inflicted lesion (blue arrow).

In all other experiments, FUS-induced necrosis of the sonicated tumour regions was demonstrated by histological examination (H&E staining), as indicatively shown in Figure 69. In untreated areas of the tumours, intact tumour cells were evidenced as shown in Figure 69A. Contrary, at regions treated with FUS, areas with well-defined borders exhibiting disrupted cell architecture and destruction of tumorous cells were revealed as shown in Figure 69B and Figure 69C. In all cases, magnification of the FUS-ablated areas indicated some remnant undamaged tumour cells, while occasionally entrapped areas of blood coagulation were observed as typically shown in Figure 69D.

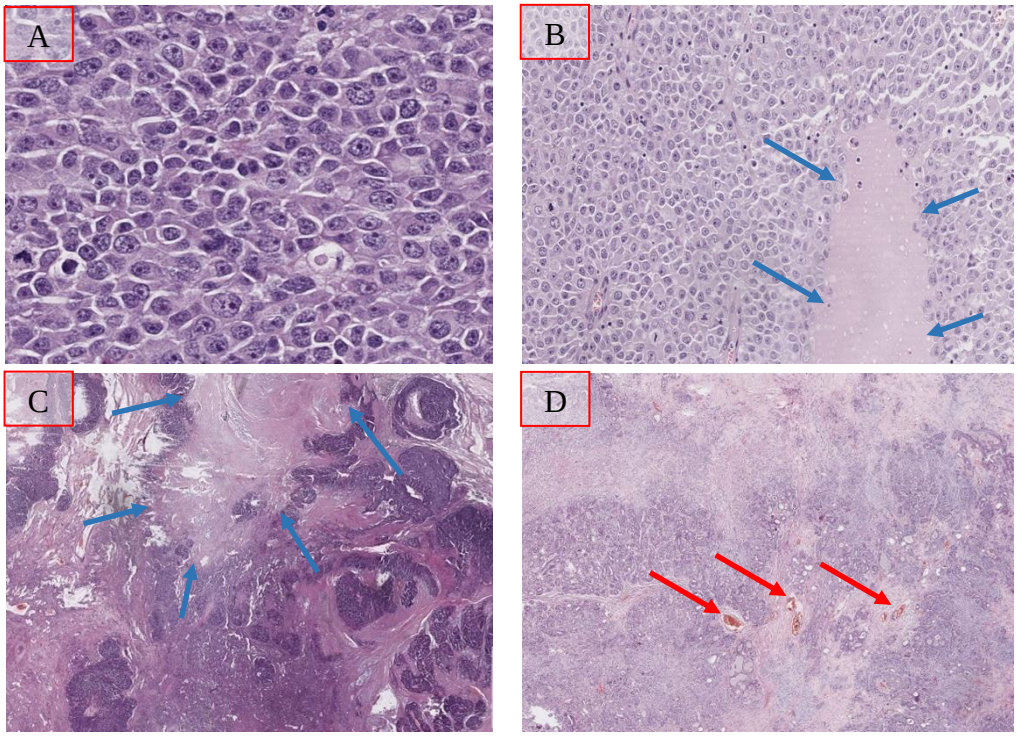

Figure 69: H&E-stained histological slides of resected tumours. A) Magnified untreated tumour area, B-C) FUS-treated tumour regions indicating FUS-induced necrotic areas (blue arrows), and D) Magnified FUS-treated area showing blood coagulation (red arrows).

Discussion

In this deliverable, the robotic system that was developed in the framework of the FUSVET project was extensively evaluated for its MRI compatibility, functionality and reliability on agar-based phantoms, excised pork tissues, tumourgraft murine models and pets with naturally occurring tumours. The robotic system was developed with an integrated single-element focused transducer that operates at a frequency of 2.75 MHz (D=50 mm, ROC=65 mm).

Evaluation on agar-based phantoms, excised pork tissues, and plastic films

Primarily both the robotic system and the integrated transducer were evaluated for their MRI compatibility within a high-field 3 T clinical MRI scanner, while they were also assessed for their thermal heating abilities in laboratory and MRI settings on agar-based phantoms and excised pork tissues. Agar-based phantoms were developed with specific materials (agar, and silicon dioxide) to emulate the acoustic, magnetic, and thermal properties of human soft tissues and provide repeatable measurements, while excised tissues enabled the ability to inflict lesions after high power sonications.

Experiments were initially executed in the laboratory setting to evaluate the heating abilities of the system and assess the motion range of the device. Initially, low power sonications were performed on thin polymer PVC films to evaluate the motion range of the PC-controlled X and Y axes of the robotic system. Single sonications were effectively performed along the origin and end points of each axis, with the film locally melting and successfully forming lesions on each of the 4 points. Distance measurements between the 4 points suggested a motion range of 45 mm in the X-axis and 32 mm in the Y-axis, thus indicating the available range for initiating robotic motion for further evaluation experiments.

Temperature measurements were then recorded using thermocouples in agar-based phantoms and excised tissue during sonications executed at varied acoustical power with the robotic system. Sonications on agar-based phantoms using varied acoustical power of 30-60 W for a constant duration of 60 s induced temperature changes between 20.4-42 ^{o}C, with higher temperature increases recorded at increased applied acoustical power. Similarly, identical sonications (varied acoustical power of 30-60W for a sonication time of 60 s) performed on excised pork tissue, resulted in recorded temperature changes between 35.1-68 ^{o}C. Again, higher acoustical power induced higher temperature change. Notably, tissue sonications at each acoustical power induced temperature changes that were sufficiently high for lesion formation. Lesions inflicted on tissue resulting sonications at varied acoustical power of 30-60 W were formed with increased lengths at higher acoustical power.

Finally, motion of the robotic system was commanded to move the integrated transducer along predetermined grid trajectories during sonications executed on excised pork tissue. Constant sonication protocols (acoustic power of 60 W for a sonication time of 20 s at 25 mm focal depth) were employed, with robotic motion executed along various grid patterns and step sizes for the formation of overlapping or discrete lesions. Overlapping lesions were formed using a 2×2 or 3×3 grid with a 7 mm size between each step.

The MRI compatibility of the robotic system and the integrated transducer was then assessed inside the MRI scanner on an agar-based phantom. Magnitude and phase FLASH images were acquired under different activation configurations of the robotic system (sole presence of the robotic system in the MRI scanner, connection to the motion cables, and activation of the electronic driving system) and the transducer (sole presence of the system in the MRI bore, system connection to the RF cables, amplifier activation, and transducer activation at varied acoustic power of 15-60 W). SNR and signal intensity measurements served as the main metrics for assessing the impact of each activation state of either the robotic system or transducer on the quality of acquired magnitude and phase FLASH images, respectively. Regarding the MRI compatibility of the robotic system, maximum SNR (40.8) was calculated for magnitude FLASH images acquired at the reference condition with only the robotic system present in the MRI scanner. A minor decrease of approximately 8 % from the reference value, was observed in the estimated SNR (37.66) upon connection of the motion cables, while a further 15 % reduction was recorded upon activation of the electronic driving system. Accordingly, maximum signal intensity was calculated on phase images acquired at the reference state with all individual system components disconnected and deactivated. Similar to magnitude images, approximately an 8.3 % reduction in signal intensity was observed when the motion cables were connected to the robotic system. Nevertheless, signal intensity increased from 91.74 % to 99.89 % upon activation of the electronic driving system. Overall, minimal SNR and signal intensity reductions along with no artifacts visible on magnitude or phase images acquired at each different configuration of the robotic system, indicate the MRI compatibility of the robotic system, piezoelectric motors, and optical encoders. In this manner, MR thermometry sequences (FLASH) can be employed for treatment monitoring, with minimal impact on image quality expected during activation of individual system components.

Accordingly, for the various activation states of the ultrasonic transducer, maximum SNR was calculated at the control condition with merely the robotic system present within the MRI scanner. Notably, approximately 30 % and 24 % reductions were noticed in the calculated SNR from the reference value, upon connection of the RF cables and amplifier activation, respectively. Some SNR variations were observed during activation of the transducer at varied acoustic power of 15-60 W. Nevertheless, SNR values as calculated during transducer activation at the varied acoustic power remained between 20-33 % lower than the reference SNR, indicating that transducer activation does not significantly affect the quality of acquired images. Remarkably, signal intensities measured on phase images acquired during system connection with the RF cables, amplifier activation and transducer activation at acoustic power of 15 W and 30 W were slightly higher (2-9 %) than signals measured at the reference condition. On the other hand, signal intensity decreased 10-20 % from the initial signal upon activation of the transducer at acoustic power of 45-60 W, with higher reductions observed at increased acoustic power. Nevertheless, no dramatic changes from the reference state were observed in SNR on magnitude images, or in signal intensity on phase images acquired during the various activation states of the robotic system or transducer. Therefore, both the robotic system and transducer are deemed MRI compatible, with activation of the individual components (electronic driving system, amplifier, or transducer) not affecting the quality of high-resolution MR thermometry sequences.

A series of experiments were then executed on agar-based phantoms and excised pork tissue inside the 3 T MRI scanner to further assess the thermal heating of the system. Temperature increases in both phantoms and tissue, and lesion formation on tissue were monitored using MR thermometry and high-resolution T1-W and T2-W sequences, respectively. High resolution T2-W TSE images of the experimental setting acquired prior ablations, revealed an excellent acoustic coupling between the robotic system and the employed sonication target (agar-based phantom or excised tissue). Initially, ablations were executed on excised tissue using varied acoustical power of 45-60 W for a constant duration of 60 s at a 30 mm focal depth. MR thermometry data (colour-coded thermal maps, and temperature evolution graphs) were successfully generated during sonications, with the thermal heating visualized on the produced thermal maps. Application of an acoustical power of 45 W resulted in a temperature increase of 31.8 ^{o}C recorded in the coronal plane, while application of increased acoustical power of 60 W resulted in high temperature increases recorded in axial (32.3-50.4 ^{o}C) and coronal planes (37.4 ^{o}C) that were sufficient to locally inflict lesions on tissue as evidenced with coronal T2-W TSE images acquired after sonications. Similarly, sonications executed on agar-based phantoms using varied acoustical power of 15-60 W for a constant duration of 30 s were successfully monitored with MR thermometry, with clear thermal maps produced and sufficient temperatures recorded at the focal spot. Higher acoustical power resulted in higher temperature changes recorded in the coronal plane, while application of an acoustical power of 60 W resulted in lower temperature changes induced in an axial plane than corresponding temperature changes resulting identical sonications imaged in the coronal plane.

A series of sonications were then executed on excised tissue using varied sonication parameters to monitor and detect the formation of lesions using T1-W and T2-W sequences. Initially, sonications were commanded along a 3×3 grid pattern with a 10 mm step using an acoustical power of 60 W for a sonication time of 30 s. Lesions inflicted at each sonication point resulting ablations, were clearly visible on coronal T2-W TSE images. Tissue dissection revealed nine thermal discrete lesions successfully formed on the tissue as a result of the sonications. Lesions were formed along an almost square trajectory with approximately equal distances between them, thus indicating the motion accuracy of the robotic device. Moreover, lesions on each grid row were formed with approximately equal diameter and length, thus indicating the delivery of constant acoustic energy by the 2.75 MHz ultrasonic transducer. Nevertheless, some deviations in lesion diameter and length existed between lesions inflicted on different grid rows, that could be attributed to possible presence of fibres within the excised tissue.

Thereafter, single sonications were executed on tissue using an acoustical power of 75 W for a sonication time of 60 s, with T1-W and T2-W TSE sequences utilised to produce high resolution images of the ablated tissue. A series of T2-W TSE images were acquired at certain timeframes after sonications, with the TE value adjusted to assess the ability of detecting the lesion post-ablation. Adjusting the TE at 50 ms resulted in a clearly visible lesion on coronal T2-W TSE images acquired directly after sonications, with the lesion still demarcated on corresponding images obtained 5 minutes after ablations. However, imaging the lesion 5 minutes after ablations with a decreased TE of 48 ms, resulted in a lower contrast between the lesion and the surrounding tissue, thus indicating that the TE of 50 ms is optimal for imaging lesions inflicted on excised tissue for notable timeframes after sonications. Moreover, the T1-

W TSE images of the lesion acquired 5 minutes after sonications had a lower contrast between the lesion and the surrounding tissue than corresponding T2-W images, thus indicating the requirement of employing T2-W TSE images for optimal lesion detection in excised porcine meat.

Overall, from these experiments the developed robotic system and the integrated transducer were proven MRI compatible and able to generate high temperatures on agar-based phantoms and excised pork tissue. Moreover, induced temperatures were of ablative levels and sufficiently high to result in the formation of thermal discrete lesions or well-demarcated areas of overlapping lesions on excised tissue. Generally, lesions were formed with appropriate dimensions according to the applied acoustic energy and along the commanded grid trajectory, thus indicating proper thermal heating abilities and validating the motion accuracy of the robotic system, respectively. However, in cases where lesions under a constant ultrasonic protocol were formed with varied dimensions or in the event that the shape of overlapping lesions deviated from the commanded grid, these were attributed to the presence of fibres, other inhomogeneous structures or bubbles within the excised tissue.

Evaluation on tumorgraft murine models

After successfully validating the proper performance of the system *in-vitro* and *ex-vivo*, the *in-vivo* safety and efficacy of the robotic system and the integrated transducer was evaluated on tumorgraft murine models. Adult male mice of the C57BL/6 strain were employed in the evaluation experiments. A total of 10 mice were inoculated with mouse MCA205 sarcoma cells on one of their shoulders and utilised as tumorgraft models for evaluating the effects of repetitive FUS treatments delivered with the robotic system on the development of tumour grafts. Experiments were carefully designed to obtain accurate results regarding the therapeutic effects of targeted FUS and the occurrence of any FUS-related adverse effects. In this sense, the 10 mice were randomly assigned in an experimental group wherein FUS was consecutively applied to the tumours (“FUS group”, n=5), and a group in which mice received no treatment, thus acting as control (“Control group”, n=5).

The experimental procedure was initiated 7 days after transplantation, when successful formation of tumours was evidenced on all mice of both groups, and lasted for a total period of 2 weeks (21 days after transplantation). Mice were ethically utilised in experiments following a specific workflow that was tailored for each group. Initially, anaesthesia was administered on all mice from both groups according to their weight, and measurements of tumour diameters were acquired. Thereafter, mice in the “Control group” were allowed to naturally recover from the effects of anaesthesia, while mice in the “FUS group” were individually positioned under the acoustic window of the robotic system for targeted delivery of FUS on the tumour grafts. Transplanted tumours on all 5 mice of the “FUS group” were sonicated in an identical grid manner (3×3 grid with 4 mm step) by applying a constant high-power therapeutic protocol (acoustic power of 75 W for a sonication time of 10 s). Treatment parameters were chosen based on the small size of the mice and the initially small tumour sizes at 7 days after transplantation and for consistency, remained identical for subsequent sessions. Following sonications, treated mice of the “FUS group” were also allowed to emerge from anaesthesia.

A 7-day follow-up period was employed wherein mice from both groups were monitored. Mice in the two groups were monitored for different reasons, with those in the "Control group" monitored for the occurrence of any side effects related to natural tumour growth, and those in the "FUS group" monitored to assess the occurrence of any long-term FUS-related adverse events. After the 7-day follow-up period and provided that all mice endured initial experimental conditions, FUS was again delivered on the tumour grafts of the "FUS group" to examine the FUS-related therapeutic effects from sequential FUS sessions on tumour development, while the natural tumour development in control mice continued to be monitored. A total of 3 FUS treatments were consistently delivered at 7, 14, and 21 days after transplantation on the "FUS group", with tumour diameter measurements in both groups acquired at 7, 10, 14 and 21 days.

Throughout the experimental period, all mice in the "Control group" endured experimental conditions (anaesthesia and tumours), while repetitive FUS treatments were effectively applied on every mouse of the "FUS group" with no acute or long-term side effects reported. Gross examination of tumours on tumorgraft mice of the "FUS group" after each FUS session revealed the formation of visible discrete lesions on the tumour surface on all mice, indicating successful coagulative necrosis of the targeted tumour cells. Tumour diameters measured on the 7^{th} day successfully validated similar baseline tumour sizes in the two groups, while diameters taken at 10, 14 and 21 days served as endpoints for evaluating the FUS-related therapeutic effects on tumour development. Notably, data showed that 7 days after application of the 2^{nd} FUS treatment, FUS achieved significantly smaller tumour diameters than tumours that received no treatment ($p<0.1$). The response of tumours to the 3^{rd} FUS treatment was not studied, since all mice from both groups were humanely euthanized shortly after the 21^{st} day (1-2 days) due to distress. Since both groups exhibited the same levels of distress, it was postulated that side effects in mice of the "FUS group" were caused by the grown tumour grafts and not as a consequence of the FUS therapy.

Murine model experiments indicated that application of FUS with the proposed robotic system can successfully coagulate tumour cells and disrupt the natural development of tumours without occurrence of any adverse events. Consequently, the safety and efficacy of the system for veterinary oncological FUS applications was verified. Furthermore, the therapeutic protocol was proven efficient for inducing coagulative tumour necrosis, indicating that similar ultrasonic parameters should be employed for *in-vivo* applications. Overall, results proved that the system can be safely employed for further evaluation on pets (dogs and cats) with naturally occurring cancer, with analogous therapeutic protocols as the ones generated from murine experiments utilised.

Evaluation on pets with naturally occurring tumours

Consequently, dogs and cats presenting with naturally occurring neoplasms were enrolled in the study by following a targeted recruitment strategy. The research team contacted, through phone, veterinarians who previously collaborated with us, while efforts were also made by the principal investigator for a more personal contact of veterinary surgeons through phone calls and personal meetings. As a result of this targeted personal recruitment campaign, a total of 18 pets presenting with various types of tumours and adhering to certain eligibility criteria were enrolled in the study.

All pets were recruited based on conscious informed consent by their owners who maintained the right to remove their animal friend from the trial at any time. Recruited pets were treated following an integrated protocol. Anaesthesia was initially administered to enrolled pets according to their weight and overall health status. Thereafter, the pet was accommodated below the robotic system for targeted treatment of the tumour with FUS, followed by surgical removal of the tumour. The ablated region of the resected tumour was sectioned and sent for histological examination to examine the FUS-related therapeutic effects.

In all experiments, safety of the FUS treatment was initially ensured by applying a constant low energy sonication protocol. Tumours were then sonicated with high power whenever low power sonications were well tolerated by the animal and no pain was felt. Recruited pets (n=18) endured initial safety sonications, making them all eligible for high power tumour ablations. Therapeutic protocols were carefully generated depending on tumour volume. In most of the cases (17/18), high power tumour ablations were executed in a single location, whereas in the last recruited case the tumour was treated in a grid manner (3×3 grid with 3 mm step). Gross examination of the tumours after FUS ablations resulted in inflicted lesions being visible on the tumour surface only in a single case (study ID: FUSVET-9). In all other cases, no lesions were observed on the tumour surface due to entrapped fluid within the tumours that possibly attenuated the ultrasonic beam.

Nevertheless, thermal necrosis of tumour cells was evidenced in all experiments by histopathological examination of the ablated tumour regions. In the only case wherein, the lesion was visible on the tumour surface (study ID: FUSVET-9), histological examination revealed local rupture of multifocal cysts and formation of polymerized fibrin, indicating successful blood coagulation at the sonicated region. In all other tumours, thermal necrosis at the ablated areas was observed on the H&E-stained slides as regions of disrupted cell architecture. Moreover, in sonicated areas, destruction of tumorous cells was revealed. However, magnification identified a small number of remaining intact tumour nuclei, while in some cases blood coagulation within the sonicated area was visible on virtual H&E slides. Nevertheless, from a histopathological viewpoint, tumours were considered completely destroyed by FUS, despite the few residual nuclei. Occasionally, treated tumours were haemorrhagic, while in most cases they included fluid and numerous blood vessels that could potentially attenuate the ultrasonic beam to a great extent, thus possibly resulting in inadequate destruction of all tumour nuclei.

Overall, application of FUS with the proposed robotic system on pets (dogs and cats) presenting with various types of natural tumours resulted in successful coagulative necrosis of targeted tumour cells. Treatments were well tolerated by animals since extensive safety measures were undertaken to ensure animal welfare. As a result, no unintended side effects were reported, with all recruited pets remaining in a good clinical state after trials as verified through regular follow-ups with the referring veterinarians.

These trials established the safety and efficacy of the system for veterinary oncological FUS applications. Experiments verified that small to large-sized animals can be accommodated under the conical water container of the robotic system, while ablation of various types and volumes of tumours can be effectively achieved.

Appendix 1: Reports of experiments on pets with natural tumours

Experiment 1

Date: 19/12/2022

Study ID: FUSVET - 1

Referring veterinarian: [redacted]

Anaesthesia: Dexmedetomidine, Thiopental, Isoflurane

Weight: 6 Kg

Age: 12 years

Species: Dog

Name of owner: [redacted]

Tumour type: Sarcoma

Size of tumour: 30×30×30 mm

Procedure

1) Anaesthesia, 2) Treatment with FUS, 3) Surgical removal of tumour and biopsy

Robot: FUSVET

Transducer: F=2.75 MHz, R=65 mm, D=50 mm

Amplifier: AG1016 (T & C Power Conversion Inc.)

Focal depth: Interface (transducer to membrane distance=60 mm).

Protocol:

Pain check: Acoustic power: 1.5 W, Sonication time: 10 s

Ablation: Acoustic power 60 W, Sonication time: 10 s

Observation: Lesion was not visible on the surface of the tumour. Tumour included fluid inside.

Biopsy procedure: Tissue placed in formalin solution and sent for biopsy (H&E). Histology revealed thermal necrosis.

Anaesthesia/monitoring Record

Date 19/12/2022	**Time** 9:00
Animal ID	FUSVET - 1
Species	Dog
Sex	M
Age (Years)	12
Weight (Kg)	6
Study	CY/EXP/PR.L09/2022
Principal Investigator	K. Alexandros Spanoudes
Time	**Anaesthesia**
9:00	Dexmedetomidine 1 mg/kg, Thiopental 5 mg/Kg, Isoflurane
10:10	Surgery ended

Time	**Heart Rate**	**Resp. Rate**	**Urination** (0 to 3)	**Absence of Movement /Pedal Reflex**	**Temp. (°C)**
9:00	100	16	0	Absent	n/a
9:10	90	19	0	Absent	n/a
9:20	100	18	0	Absent	n/a
9:30	110	20	0	Absent	n/a
9:40	90	15	0	Absent	n/a
9:50	100	17	0	Absent	n/a
10:00	110	19	0	Absent	n/a
10:10	100	14	0	Absent	n/a

Note:

The clinical staff are trained for safe anaesthesia.

The veterinarian considered multiple factors including health status, breed, age, expected pain level, and surgical plan when he planned the anaesthesia for the pet.

An accurate pet weight was obtained on the day of anaesthesia.

Follow-up

The welfare of the animal was followed-up via phone communications with the veterinarian of the pet. Follow-ups are anticipated at 1, 3, 6 and 12 months.

January 18, 2023 – almost 1 month later

Animal is in good condition. No recurrence of the tumour yet.

March (beginning) 2023 – 3-month follow-up

Animal is in good condition. No recurrence of the tumour yet.

June (beginning) 2023 – 6-month follow-up

Animal is in good condition. No recurrence of the tumour yet.

December 2023 – 1 year follow-up

Animal is in good condition. No recurrence of the tumour yet.

FUSVET-1 Fig. 1: System at the veterinary clinic.

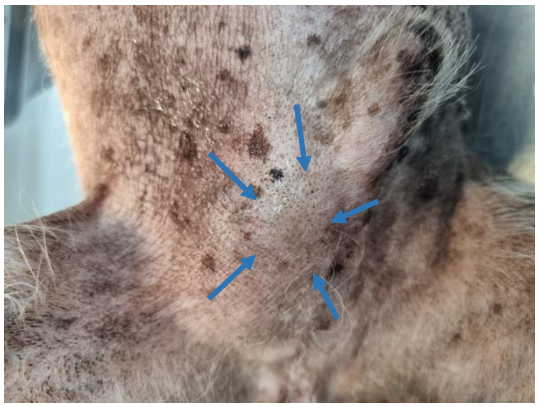

FUSVET-1 Fig. 2: Photo of the tumour (Blue arrows).

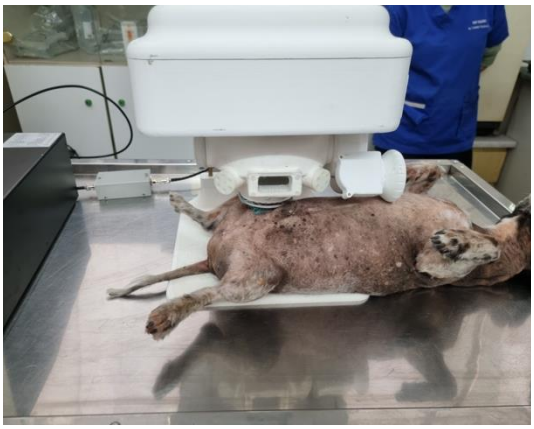

FUSVET-1 Fig. 3: Placement of dog under the system.

FUSVET-1 Fig. 4:Photo of coupling between the robotic system and the tumour.

FUSVET-1 Fig. 5:Photo of the veterinarian and principal investigator.

Histology exams

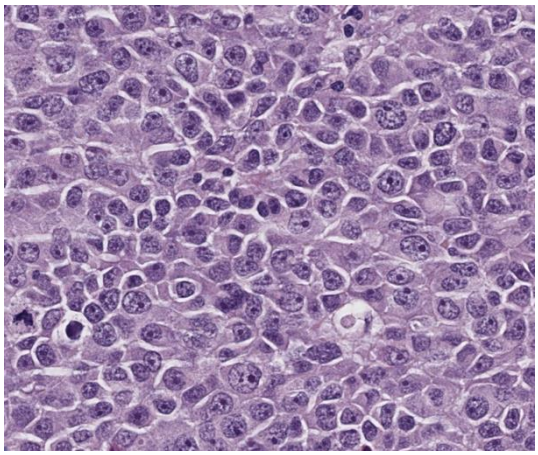

FUSVET-1 Fig. 6: Image of the histology exam.

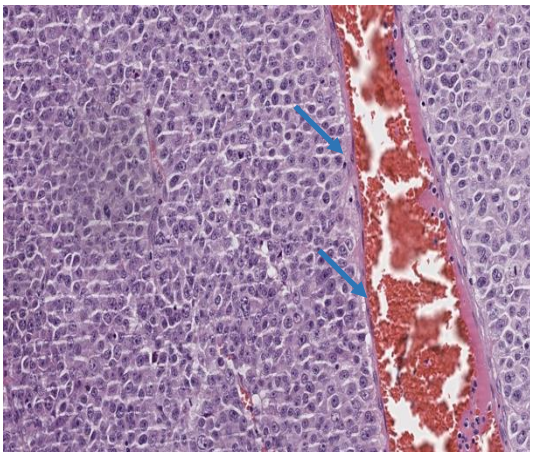

FUSVET-1 Fig. 7: Image of the histology exam. Arrows show haemorrhagic tumour.

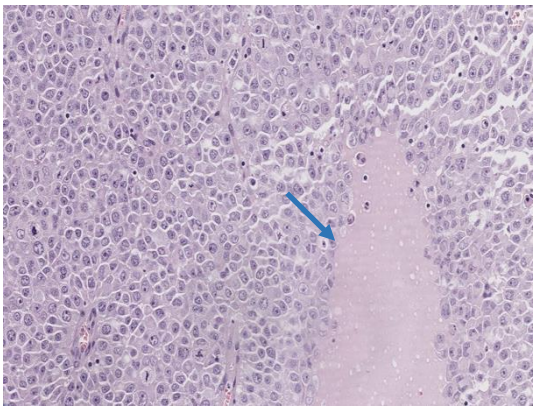

FUSVET-1 Fig. 8: Image of the histology exam. Arrow shows necrosis.

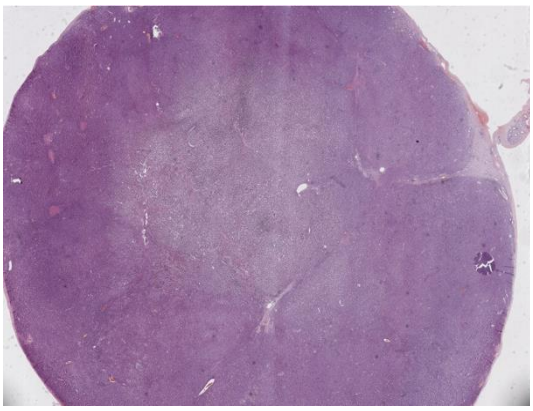

FUSVET-1 Fig. 9: Image of the histology exam.

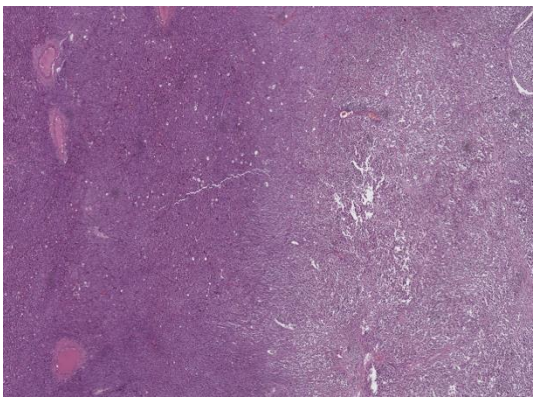

FUSVET-1 Fig. 10: Image of the histology exam.

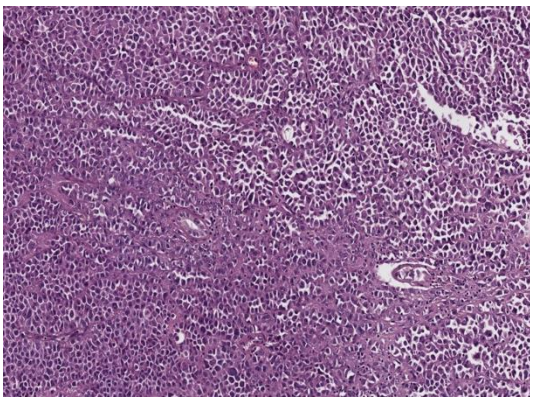

FUSVET-1 Fig. 11: Image of the histology exam.

Conclusions for histology

The architecture of cells is destroyed by thermal ultrasound. In the areas of sonication there was destruction of cancerous nuclei. In magnified areas there is evidence that a few number of nuclei remained (from histology point of view the cancer is considered fully destroyed). The tumour was haemorrhagic. The tumour includes a lot of blood vessels and various ducts and possibly the ultrasound beam is highly attenuated in this cancer type. Attenuation measurements of excised tumour will reveal this hypothesis.

Experiment 2

Date: 28/03/2023

Study ID: FUSVET - 2

Referring veterinarian: [redacted]

Anaesthesia: Dexmedetomidine, Thiopental, Isoflurane

Weight: 4 Kg

Age: 3 years

Species: Cat

Name of owner: [redacted]

Tumour type: Mammary

Size of tumour: 30×20×30 mm

Procedure

1) Anaesthesia, 2) Treatment with FUS, 3) Surgical removal of tumour and biopsy

Robot: FUSVET

Transducer: F=2.75 MHz, R=65 mm, D=50 mm

Amplifier: AG1016 (T & C Power Conversion Inc.).

Focal depth: Interface (transducer to membrane distance=60 mm).

Protocol:

Pain check: Acoustic power: 1.5 W, Sonication time: 10 s

Ablation: Acoustic power: 60 W, Sonication time: 10 s

Observation: Lesion was not visible on the surface of the tumour. Tumour included fluid inside.

Biopsy procedure: Tissue placed in formalin solution and sent for biopsy (H&E). Histology revealed thermal necrosis.

Anaesthesia/monitoring Record

Date 28/03/2023	**Time** 9:00
Animal ID	FUSVET - 2
Species	Cat
Sex	F
Age (Years)	3
Weight (Kg)	4
Study	CY/EXP/PR.L09/2022
Principal Investigator	K. Alexandros Spanoudes
Time	**Anaesthesia**
9:00	Dexmedetomidine 1 mg/kg, Thiopental 5 mg/Kg, Isoflurane
10:10	Surgery ended

Time	**Heart Rate**	**Resp. Rate**	**Urination** (0 to 3)	**Absence of Movement /Pedal Reflex**	**Temp. (°C)**
9:00	100	16	0	Absent	n/a
9:10	90	19	0	Absent	n/a
9:20	100	18	0	Absent	n/a
9:30	110	20	0	Absent	n/a
9:40	90	15	0	Absent	n/a
9:50	100	17	0	Absent	n/a
10:00	110	19	0	Absent	n/a
10:10	100	14	0	Absent	n/a

Note:

The clinical staff are trained for safe anaesthesia.

The veterinarian considered multiple factors including health status, breed, age, expected pain level, and surgical plan when he planned the anaesthesia for the pet.

An accurate pet weight was obtained on the day of anaesthesia.

Follow-up

The welfare of the animal was followed-up via phone communications with the veterinarian of the pet. Follow-ups are anticipated at 1, 3, 6 and 12 months.

April 28, 2023 – almost 1 month later

Animal is in good condition. No recurrence of the tumour yet.

July (beginning) 2023 – 3-month follow-up

Animal is in good condition. No recurrence of the tumour yet.

September (beginning) 2023 – 6-month follow-up

Animal is in good condition. No recurrence of the tumour yet.

March 2024 – 1 year follow-up

Animal is in good condition. No recurrence of the tumour yet.

FUSVET-2 Fig. 1: System at the veterinary clinic.

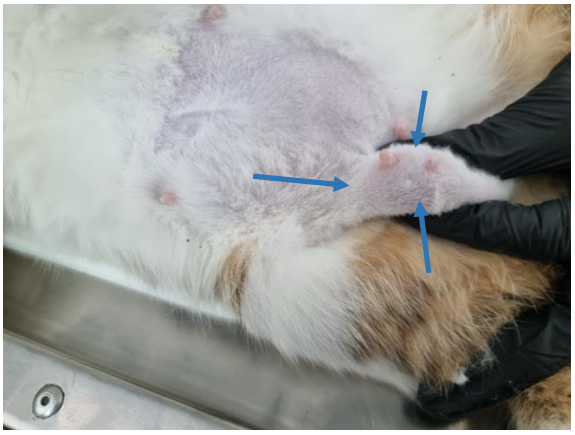

FUSVET-2 Fig. 2: Photo of the tumour (Blue arrows).

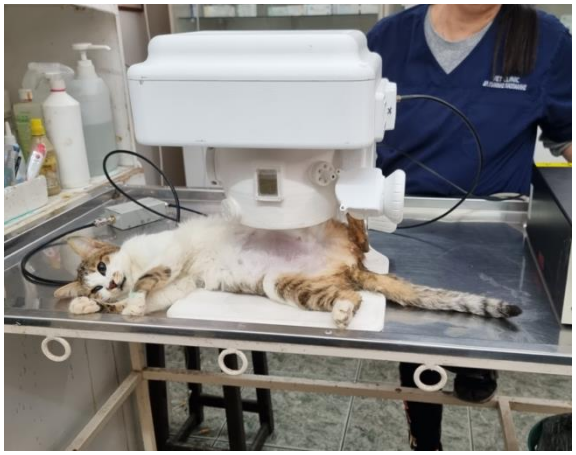

FUSVET-2 Fig. 3: Placement of cat under the system.

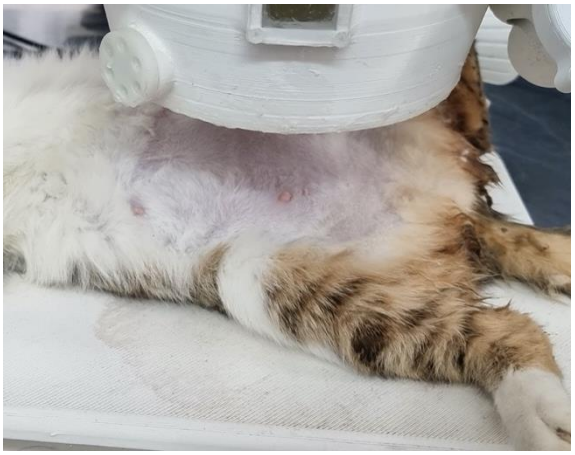

FUSVET-2 Fig. 4: Photo of coupling between the robotic system and the tumour.

FUSVET-2 Fig. 5:Photo of the veterinarian and principal investigator.

Histology exams

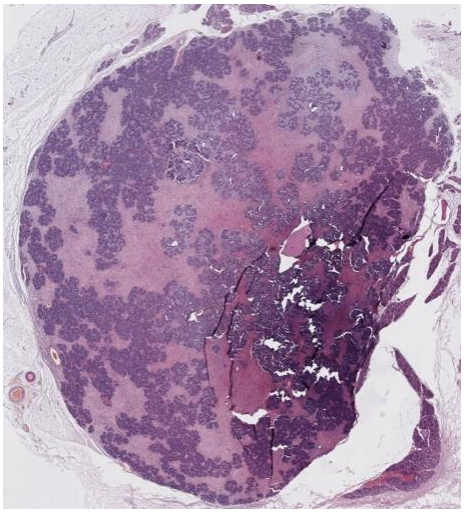

FUSVET-2 Fig. 6: Image of the histology exam.

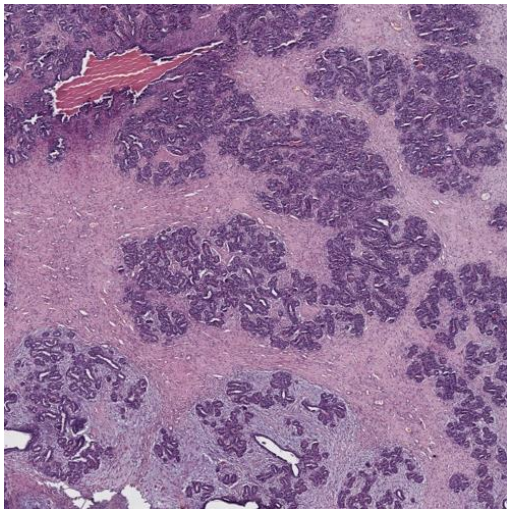

FUSVET-2 Fig. 7: Image of the histology exam.

Conclusions for histology

The architecture of cells is destroyed by thermal ultrasound. In the areas of sonication there was destruction of cancerous nuclei. In magnified areas there is evidence that a few number of nuclei remained (from histology point of view the cancer is considered fully destroyed). The tumour includes a lot of blood vessels and various ducts and possibly the ultrasound beam is highly attenuated in this cancer type. Attenuation measurements of excised tumour will reveal this hypothesis.

Experiment 3

Date: 11/04/2023

Study ID: FUSVET - 3

Referring veterinarian: [redacted]

Anaesthesia: Dexmedetomidine, Thiopental, Isoflurane

Weight: 9 Kg

Age: 8 years

Species: Dog

Name of owner: [redacted]

Tumour type: Mammary

Size of tumour: 60×50×30 mm

Procedure

1) Anaesthesia, 2) Treatment with FUS, 3) Surgical removal of tumour and biopsy

Robot: FUSVET

Transducer: F=2.75 MHz, R=65 mm, D=50 mm

Amplifier: AG1016 (T & C Power Conversion Inc.).

Focal depth: Interface (transducer to membrane distance=60 mm).

Protocol:

Pain check: Acoustic power: 1.5 W, Sonication time: 10 s

Ablation: Acoustic power: 60 W, Sonication time: 30 s

Observation: Lesion was not visible on the surface of the tumour. Tumour included fluid inside.

Biopsy procedure: Tissue placed in formalin solution and sent for biopsy (H&E). Histology revealed thermal necrosis.

Anaesthesia/monitoring Record

Date 11/04/2023	**Time** 9:00
Animal ID	FUSVET - 3
Species	Dog
Sex	F
Age (Years)	8
Weight (Kg)	9
Study	CY/EXP/PR.L09/2022
Principal Investigator	K. Alexandros Spanoudes
Time	**Anaesthesia**
9:00	Dexmedetomidine 1 mg/kg, Thiopental 5 mg/Kg, Isoflurane
10:10	Surgery ended

Time	**Heart Rate**	**Resp. Rate**	**Urination** (0 to 3)	**Absence of Movement /Pedal Reflex**	**Temp. (°C)**
9:00	100	16	0	Absent	n/a
9:10	90	19	0	Absent	n/a
9:20	100	18	0	Absent	n/a
9:30	110	20	0	Absent	n/a
9:40	90	15	0	Absent	n/a
9:50	100	17	0	Absent	n/a
10:00	110	19	0	Absent	n/a
10:10	100	14	0	Absent	n/a

Note:

The clinical staff are trained for safe anaesthesia.

The veterinarian considered multiple factors including health status, breed, age, expected pain level, and surgical plan when he planned the anaesthesia for the pet.

An accurate pet weight was obtained on the day of anaesthesia.

Follow-up

The welfare of the animal was followed-up via phone communications with the veterinarian of the pet. Follow-ups are anticipated at 1, 3, 6 and 12 months.

May 11, 2023 – almost 1 month later

Animal is in good condition. No recurrence of the tumour yet.

July (beginning) 2023 – 3-month follow-up

Animal is in good condition. No recurrence of the tumour yet.

October (beginning) 2023 – 6-month follow-up

Animal is in good condition. No recurrence of the tumour yet.

April 2024 – 1 year follow-up

Animal is in good condition. No recurrence of the tumour yet.

FUSVET-3 Fig. 1: System at the veterinary clinic.

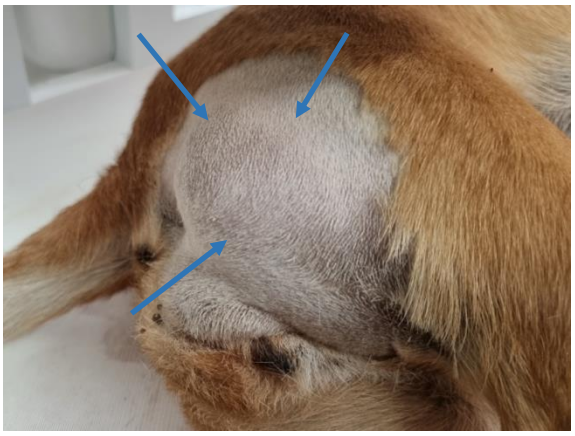

FUSVET-3 Fig. 2: Photo of the tumour (Blue arrows).

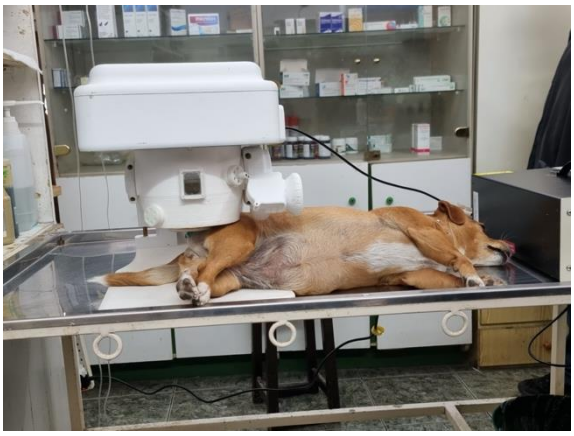

FUSVET-3 Fig. 3: Placement of dog under the system.

FUSVET-3 Fig. 4: Photo of coupling between the robotic system and the tumour.

FUSVET-3 Fig. 5: Photo of the veterinarian and principal investigator.

Histology exams

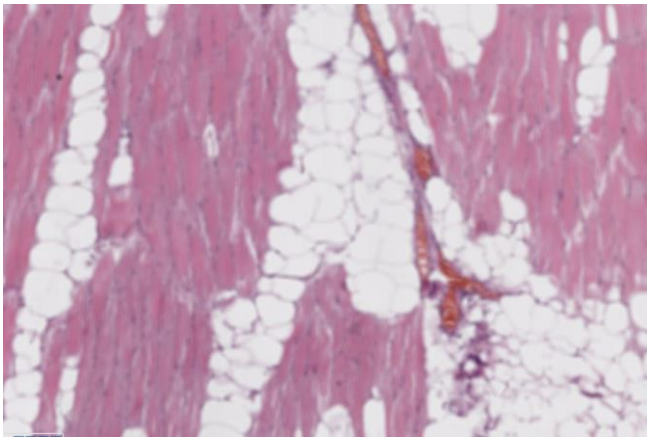

FUSVET-3 Fig. 6: Image of the histology exam.

Conclusions for histology

The architecture of cells is destroyed by thermal ultrasound. In the areas of sonication there was destruction of cancerous nuclei. In magnified areas there is evidence that a few number of nuclei remained (from histology point of view the cancer is considered fully destroyed). The tumour includes a lot of blood vessels and various ducts and possibly the ultrasound beam is highly attenuated in this cancer type. Attenuation measurements of excised tumour will reveal this hypothesis.

Experiment 4

Date: 17/04/2023

Study ID: FUSVET - 4

Referring veterinarian: [redacted]

Anaesthesia: Dexmedetomidine, Thiopental, Isoflurane

Weight: 5 Kg

Age: 12 years

Species: Dog

Name of owner: [redacted]

Tumour type: Mammary

Size of tumour: 20×30×30 mm

Procedure

1) Anaesthesia, 2) Treatment with FUS, 3) Surgical removal of tumour and biopsy

Robot: FUSVET

Transducer: F=2.75 MHz, R=65 mm, D=50 mm

Amplifier: AG1016 (T & C Power Conversion Inc.).

Focal depth: Interface (transducer to membrane distance=60 mm).

Protocol:

Pain check: Acoustic power: 1.5 W, Sonication time: 10 s

Ablation: Acoustic power: 45 W, Sonication time: 30 s

Observation: Lesion was not visible on the surface of the tumour. Tumour included fluid inside.

Biopsy procedure: Tissue placed in formalin solution and sent for biopsy (H&E). Histology revealed thermal necrosis.

Anaesthesia/monitoring Record

Date 17/04/2023	**Time** 9:00
Animal ID	FUSVET - 4
Species	Dog
Sex	F
Age (Years)	12
Weight (Kg)	5
Study	CY/EXP/PR.L09/2022
Principal Investigator	K. Alexandros Spanoudes
Time	**Anaesthesia**
9:00	Dexmedetomidine 1 mg/kg, Thiopental 5 mg/Kg, Isoflurane
10:10	Surgery ended

Time	**Heart Rate**	**Resp. Rate**	**Urination** (0 to 3)	**Absence of Movement /Pedal Reflex**	**Temp. (°C)**
9:00	100	16	0	Absent	n/a
9:10	90	19	0	Absent	n/a
9:20	100	18	0	Absent	n/a
9:30	110	20	0	Absent	n/a
9:40	90	15	0	Absent	n/a
9:50	100	17	0	Absent	n/a
10:00	110	19	0	Absent	n/a
10:10	100	14	0	Absent	n/a

Note:

The clinical staff are trained for safe anaesthesia.

The veterinarian considered multiple factors including health status, breed, age, expected pain level, and surgical plan when he planned the anaesthesia for the pet.

An accurate pet weight was obtained on the day of anaesthesia.

Follow-up

The welfare of the animal was followed-up via phone communications with the veterinarian of the pet. Follow-ups are anticipated at 1, 3, 6 and 12 months.

June 17, 2023 – almost 1 month later

Animal is in good condition. No recurrence of the tumour yet.

August (beginning) 2023 – 3-month follow-up

Animal is in good condition. No recurrence of the tumour yet.

November (beginning) 2023 – 6-month follow-up

Animal is in good condition. No recurrence of the tumour yet.

May 2024 – 1 year follow-up

Animal is in good condition. No recurrence of the tumour yet.

FUSVET-4 Fig. 1: System at the veterinary clinic.

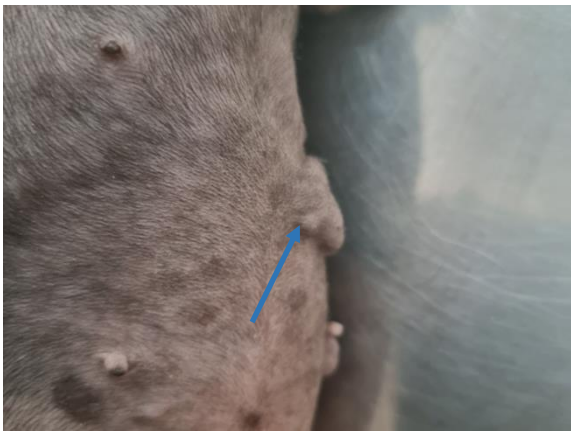

FUSVET-4 Fig. 2: Photo of the tumour (Blue arrow).

FUSVET-4 Fig. 3: Placement of dog under the system.

FUSVET-4 Fig. 4: Photo of coupling between the robotic system and the tumour.

FUSVET-4 Fig. 5: Photo of the veterinarian and principal investigator.

Histology exams

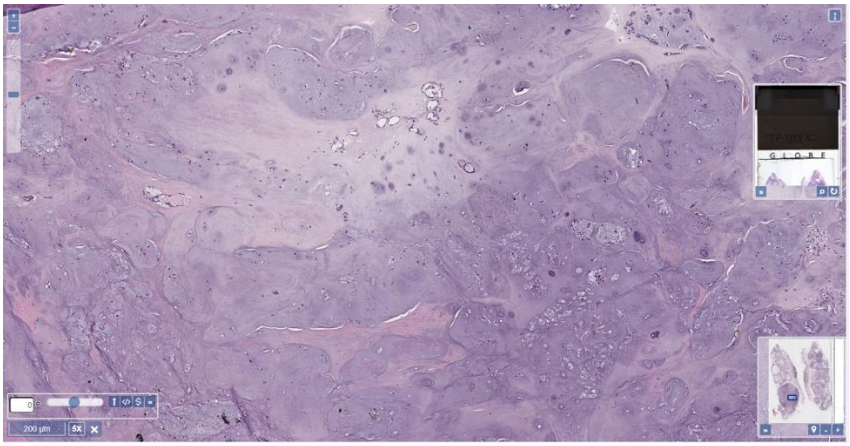

FUSVET-4 Fig. 6: Image of the histology exam.

Conclusions for histology

The architecture of cells is destroyed by thermal ultrasound. In the areas of sonication there was destruction of cancerous nuclei. In magnified areas there is evidence that a few number of nuclei remained (from histology point of view the cancer is considered fully destroyed). The tumour includes a lot of blood vessels and various ducts and possibly the ultrasound beam is highly attenuated in this cancer type. Attenuation measurements of excised tumour will reveal this hypothesis.

Experiment 5

Date: 23/05/2023

Study ID: FUSVET - 5

Referring veterinarian: [redacted]

Anaesthesia: Dexmedetomidine, Thiopental, Isoflurane

Weight: 14 Kg

Age: 10 years

Species: Dog

Name of owner: [redacted]

Tumour type: Mammary

Size of tumour: 30×30×35 mm

Procedure

1) Anaesthesia, 2) Treatment with FUS, 3) Surgical removal of tumour and biopsy

Robot: FUSVET

Transducer: F=2.75 MHz, R=65 mm, D=50 mm

Amplifier: AG1016 (T & C Power Conversion Inc.).

Focal depth: Interface (transducer to membrane distance=60 mm).

Protocol:

Pain check: Acoustic power: 1.5 W, Sonication time: 10 s

Ablation: Acoustic power: 75 W, Sonication time: 30 s

Observation: Lesion was not visible on the surface of the tumour. Tumour included fluid inside.

Biopsy procedure: Tissue placed in formalin solution and sent for biopsy (H&E). Histology revealed thermal necrosis.

Anaesthesia/monitoring Record

Date 23/05/2023	**Time** 9:00
Animal ID	FUSVET - 5
Species	Dog
Sex	F
Age (Years)	10
Weight (Kg)	14
Study	CY/EXP/PR.L09/2022
Principal Investigator	K. Alexandros Spanoudes
Time	**Anaesthesia**
9:00	Dexmedetomidine 1 mg/kg, Thiopental 5 mg/Kg, Isoflurane
10:10	Surgery ended

Time	**Heart Rate**	**Resp. Rate**	**Urination** (0 to 3)	**Absence of Movement /Pedal Reflex**	**Temp. (°C)**
9:00	100	16	0	Absent	n/a
9:10	90	19	0	Absent	n/a
9:20	100	18	0	Absent	n/a
9:30	110	20	0	Absent	n/a
9:40	90	15	0	Absent	n/a
9:50	100	17	0	Absent	n/a
10:00	110	19	0	Absent	n/a
10:10	100	14	0	Absent	n/a

Note:

The clinical staff are trained for safe anaesthesia.

The veterinarian considered multiple factors including health status, breed, age, expected pain level, and surgical plan when he planned the anaesthesia for the pet.

An accurate pet weight was obtained on the day of anaesthesia.

Follow-up

The welfare of the animal was followed-up via phone communications with the veterinarian of the pet. Follow-ups are anticipated at 1, 3, 6 and 12 months.

June 23, 2023 – almost 1 month later

Animal is in good condition. No recurrence of the tumour yet.

August (beginning) 2023 – 3-month follow-up

Animal is in good condition. No recurrence of the tumour yet.

November (beginning) 2023 – 6-month follow-up

Animal is in good condition. No recurrence of the tumour yet.

May 2024 – 1 year follow-up

Animal is in good condition. No recurrence of the tumour yet.

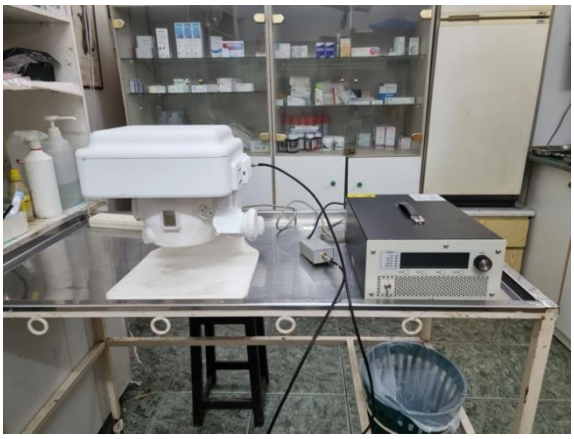

FUSVET-5 Fig. 1: System at the veterinary clinic.

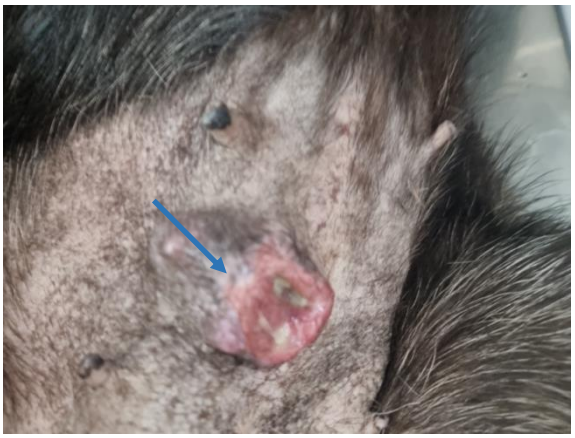

FUSVET-5 Fig. 2: Photo of the tumour (Blue arrow).

FUSVET-5 Fig. 3: Placement of dog under the system.

FUSVET-5 Fig. 4: Photo of the veterinarian and principal investigator.

Histology exams

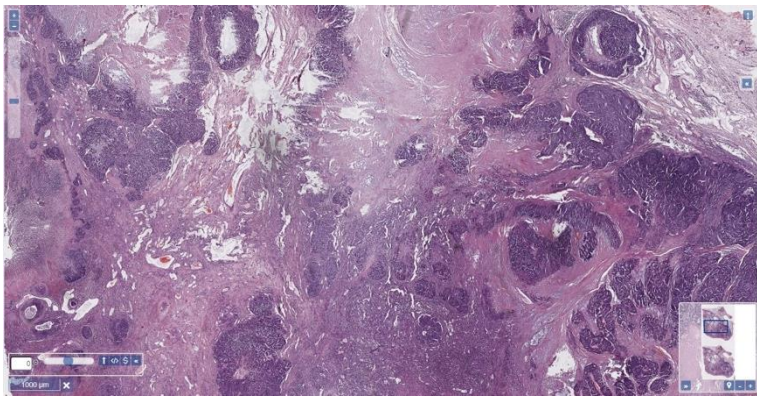

FUSVET-5 Fig. 5: Image of the histology exam.

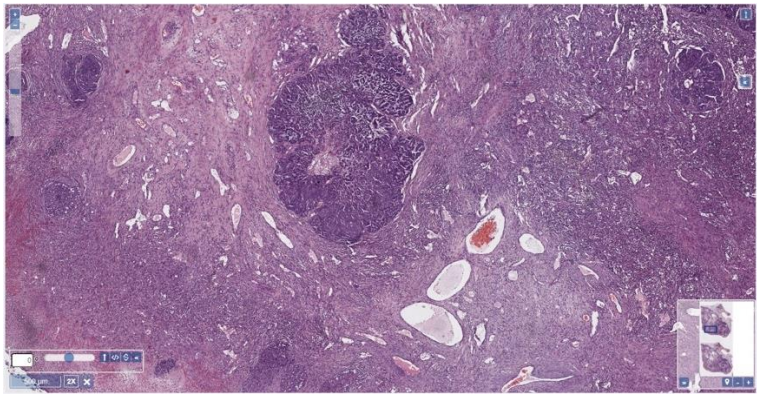

FUSVET-5 Fig. 6: Image of the histology exam.

Conclusions for histology

The architecture of cells is destroyed by thermal ultrasound. In the areas of sonication there was destruction of cancerous nuclei. In magnified areas there is evidence that a few number of nuclei remained (from histology point of view the cancer is considered fully destroyed). The tumour includes a lot of blood vessels and various ducts and possibly the ultrasound beam is highly attenuated in this cancer type. Attenuation measurements of excised tumour will reveal this hypothesis.

Experiment 6

Date: 06/06/2023

Study ID: FUSVET - 6

Referring veterinarian: [redacted]

Anaesthesia: Dexmedetomidine, Thiopental, Isoflurane

Weight: 40 Kg

Age: 9 years

Species: Dog

Name of owner: [redacted]

Tumour type: Mammary

Size of tumour: 20×20×30 mm

Procedure

1) Anaesthesia, 2) Treatment with FUS, 3) Surgical removal of tumour and biopsy

Robot: FUSVET

Transducer: F=2.75 MHz, R=65 mm, D=50 mm

Amplifier: AG1016 (T & C Power Conversion Inc.).

Focal depth: Interface (transducer to membrane distance=60 mm).

Protocol:

Pain check: Acoustic power: 1.5 W, Sonication time: 10 s

Ablation: Acoustic power: 75 W, Sonication time: 30 s

Observation: Lesion was not visible on the surface of the tumour. Tumour included fluid inside.

Biopsy procedure: Tissue placed in formalin solution and sent for biopsy (H&E). Histology revealed thermal necrosis.

Anaesthesia/monitoring Record

Date 06/06/2023	**Time** 15:30
Animal ID	FUSVET - 6
Species	Dog
Sex	F
Age (Years)	9
Weight (Kg)	40
Study	CY/EXP/PR.L09/2022
Principal Investigator	K. Alexandros Spanoudes
Time	**Anaesthesia**
15:30	Dexmedetomidine 1 mg/kg, Thiopental 5 mg/Kg, Isoflurane
16:40	Surgery ended

Time	**Heart Rate**	**Resp. Rate**	**Urination** (0 to 3)	**Absence of Movement /Pedal Reflex**	**Temp. (°C)**
15:30	100	16	0	Absent	n/a
15:40	90	19	0	Absent	n/a
15:50	100	18	0	Absent	n/a
16:00	110	20	0	Absent	n/a
16:10	90	15	0	Absent	n/a
16:20	100	17	0	Absent	n/a
16:30	110	19	0	Absent	n/a
16:40	100	14	0	Absent	n/a

Note:

The clinical staff are trained for safe anaesthesia.

The veterinarian considered multiple factors including health status, breed, age, expected pain level, and surgical plan when he planned the anaesthesia for the pet.

An accurate pet weight was obtained on the day of anaesthesia.

Follow-up

The welfare of the animal was followed-up via phone communications with the veterinarian of the pet. Follow-ups are anticipated at 1, 3, 6 and 12 months.

July 23, 2023 – almost 1 month later

Animal is in good condition. No recurrence of the tumour yet.

September (beginning) 2023 – 3-month follow-up

Animal is in good condition. No recurrence of the tumour yet.

December (beginning) 2023 – 6-month follow-up

Animal is in good condition. No recurrence of the tumour yet.

June 2024 –1 year follow-up

Animal is in good condition. No recurrence of the tumour yet.

FUSVET-6 Fig. 1: System at the veterinary clinic.

FUSVET-6 Fig. 2: Photo of the tumour (Blue arrow).

FUSVET-6 Fig. 3: Placement of dog under the system.

FUSVET-6 Fig. 4: Photo of coupling between the robotic system and the tumour.

FUSVET-6 Fig. 5: Photo of the veterinarian and principal investigator.

Histology exams

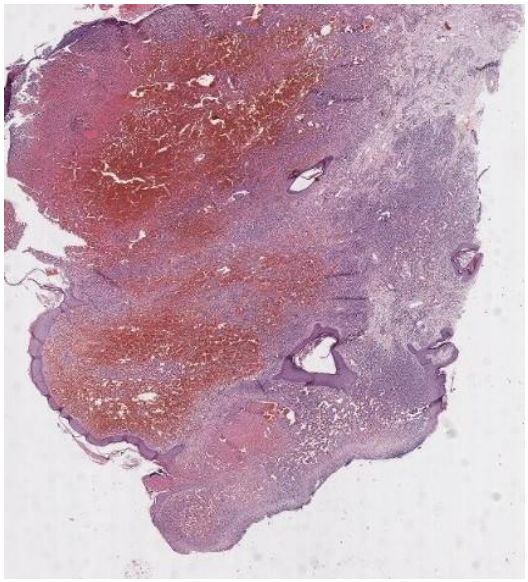

FUSVET-6 Fig. 6: Image of the histology exam.

Conclusions for histology

The architecture of cells is destroyed by thermal ultrasound. In the areas of sonication there was destruction of cancerous nuclei. In magnified areas there is evidence that a few number of nuclei remained (from histology point of view the cancer is considered fully destroyed). The tumour includes a lot of blood vessels and various ducts and possibly the ultrasound beam is highly attenuated in this cancer type. Attenuation measurements of excised tumour will reveal this hypothesis.

Experiment 7

Date: 28/06/2023

Study ID: FUSVET - 7

Referring veterinarian: [redacted]

Anaesthesia: Dexmedetomidine, Thiopental, Isoflurane

Weight: 25 Kg

Age: 8.5 years

Species: Dog

Name of owner: [redacted]

Tumour type: Mammary

Size of tumour: 30×25×30 mm

Procedure

1) Anaesthesia, 2) Treatment with FUS, 3) Surgical removal of tumour and biopsy

Robot: FUSVET

Transducer: F=2.75 MHz, R=65 mm, D=50 mm

Amplifier: AG1016 (T & C Power Conversion Inc.).

Focal depth: Interface (transducer to membrane distance=60 mm).

Protocol:

Pain check: Acoustic power: 1.5 W, Sonication time: 10 s

Ablation: Acoustic power: 75 W, Sonication time: 30 s

Observation: Lesion was not visible on the surface of the tumour. Tumour included fluid inside.

Biopsy procedure: Tissue placed in formalin solution and sent for biopsy (H&E). Histology revealed thermal necrosis.

Anaesthesia/monitoring Record

Date 28/06/2023	**Time** 09:00
Animal ID	FUSVET - 7
Species	Dog
Sex	F
Age (Years)	8.5
Weight (Kg)	25
Study	CY/EXP/PR.L09/2022
Principal Investigator	K. Alexandros Spanoudes
Time	**Anaesthesia**
9:00	Dexmedetomidine 1 mg/kg, Thiopental 5 mg/Kg, Isoflurane
10:10	Surgery ended

Time	**Heart Rate**	**Resp. Rate**	**Urination** (0 to 3)	**Absence of Movement /Pedal Reflex**	**Temp. (°C)**
9:00	100	16	0	Absent	n/a
9:10	90	19	0	Absent	n/a
9:20	100	18	0	Absent	n/a
9:30	110	20	0	Absent	n/a
9:40	90	15	0	Absent	n/a
9:50	100	17	0	Absent	n/a
10:00	110	19	0	Absent	n/a
10:10	100	14	0	Absent	n/a

Note:

The clinical staff are trained for safe anaesthesia.

The veterinarian considered multiple factors including health status, breed, age, expected pain level, and surgical plan when he planned the anaesthesia for the pet.

An accurate pet weight was obtained on the day of anaesthesia.

Follow-up

The welfare of the animal was followed-up via phone communications with the veterinarian of the pet. Follow-ups are anticipated at 1, 3, 6 and 12 months.

July 2023 – almost 1 month later

Animal is in good condition. No recurrence of the tumour yet.

September (beginning) 2023 – 3-month follow-up

Animal is in good condition. No recurrence of the tumour yet.

December (beginning) 2023 – 6-month follow-up

Animal is in good condition. No recurrence of the tumour yet.

June 2024 – 1 year follow-up

Animal is in good condition. No recurrence of the tumour yet.

FUSVET-7 Fig. 1: System at the veterinary clinic.

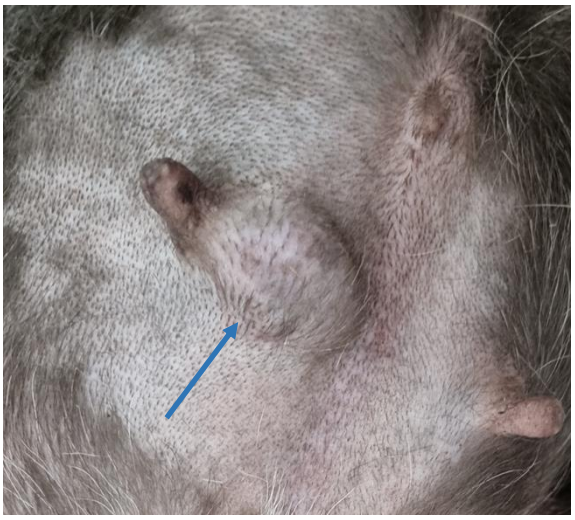

FUSVET-7 Fig. 2: Photo of the tumour (Blue arrow).

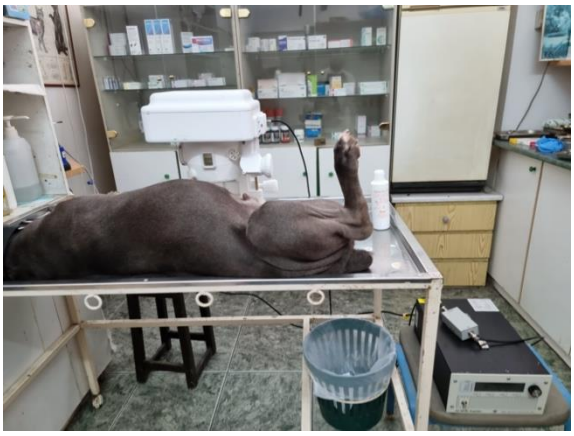

FUSVET-7 Fig. 3: Placement of dog under the system.

FUSVET-7 Fig. 4: Photo of coupling between the tumour and robotic system.

FUSVET-7 Fig. 5: Photo of the veterinarian and principal investigator.

Histology exams

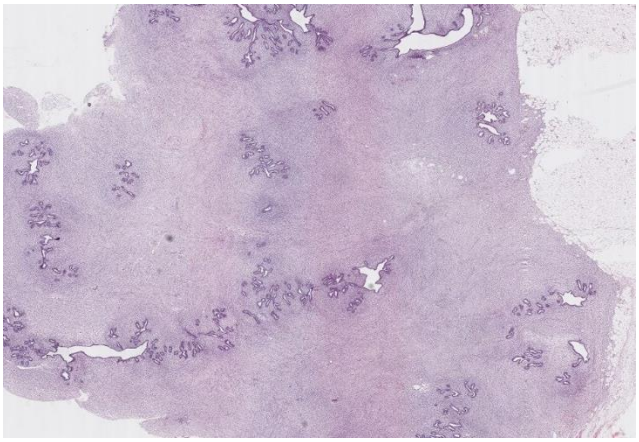

FUSVET-7 Fig. 6: Image of the histology exam.

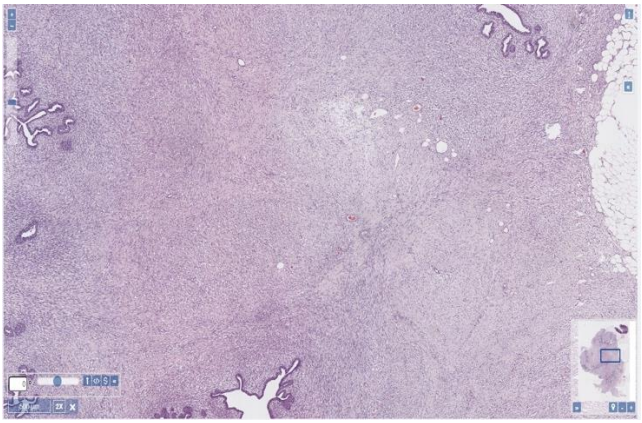

FUSVET-7 Fig. 7: Image of the histology exam.

Conclusions for histology

The architecture of cells is destroyed by thermal ultrasound. In the areas of sonication there was destruction of cancerous nuclei. In magnified areas there is evidence that a few number of nuclei remained (from histology point of view the cancer is considered fully destroyed). The tumour includes a lot of blood vessels and various ducts and possibly the ultrasound beam is highly attenuated in this cancer type. Attenuation measurements of excised tumour will reveal this hypothesis.

Experiment 8

Date: 30/06/2023

Study ID: FUSVET - 8

Referring veterinarian: [redacted]

Anaesthesia: Dexmedetomidine, Thiopental, Isoflurane

Weight: 2 Kg

Age: 10 years

Species: Cat

Name of owner: [redacted]

Tumour type: Mammary

Size of tumour: 40×40×30 mm

Procedure

1) Anaesthesia, 2) Treatment with FUS, 3) Surgical removal of tumour and biopsy

Robot: FUSVET

Transducer: F=2.75 MHz, R=65 mm, D=50 mm

Amplifier: AG1016 (T & C Power Conversion Inc.).

Focal depth: Interface (transducer to membrane distance=60 mm).

Protocol:

Pain check: Acoustic power: 1.5 W, Sonication time: 10 s

Ablation: Acoustic power: 60 W, Sonication time: 20 s

Observation: Lesion was not visible on the surface of the tumour. Tumour included fluid inside.

Biopsy procedure: Tissue placed in formalin solution and sent for biopsy (H&E). Histology revealed thermal necrosis.

Anaesthesia/monitoring Record

Date 30/06/2023	**Time** 09:00
Animal ID	FUSVET - 8
Species	Cat
Sex	F
Age (Years)	10
Weight (Kg)	2
Study	CY/EXP/PR.L09/2022
Principal Investigator	K. Alexandros Spanoudes
Time	**Anaesthesia**
9:00	Dexmedetomidine 1 mg/kg, Thiopental 5 mg/Kg, Isoflurane
10:10	Surgery ended

Time	**Heart Rate**	**Resp. Rate**	**Urination** (0 to 3)	**Absence of Movement /Pedal Reflex**	**Temp. (°C)**
9:00	100	16	0	Absent	n/a
9:10	90	19	0	Absent	n/a
9:20	100	18	0	Absent	n/a
9:30	110	20	0	Absent	n/a
9:40	90	15	0	Absent	n/a
9:50	100	17	0	Absent	n/a
10:00	110	19	0	Absent	n/a
10:10	100	14	0	Absent	n/a

Note:

The clinical staff are trained for safe anaesthesia.

The veterinarian considered multiple factors including health status, breed, age, expected pain level, and surgical plan when he planned the anaesthesia for the pet.

An accurate pet weight was obtained on the day of anaesthesia.

Follow-up

The welfare of the animal was followed-up via phone communications with the veterinarian of the pet. Follow-ups are anticipated at 1, 3, 6 and 12 months.

July 2023 – almost 1 month later

Animal is in good condition. No recurrence of the tumour yet.

September (beginning) 2023 – 3-month follow-up

Animal is in good condition. No recurrence of the tumour yet.

December (beginning) 2023 – 6-month follow-up

Animal is in good condition. No recurrence of the tumour yet.

June 2024 – 1 year follow-up

Animal is in good condition. No recurrence of the tumour yet.

FUSVET-8 Fig. 1: System at the veterinary clinic.

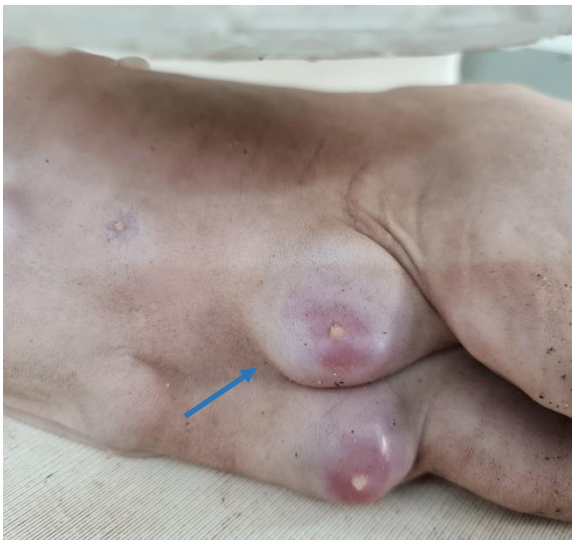

FUSVET-8 Fig. 2: Photo of the tumour (Blue arrow).

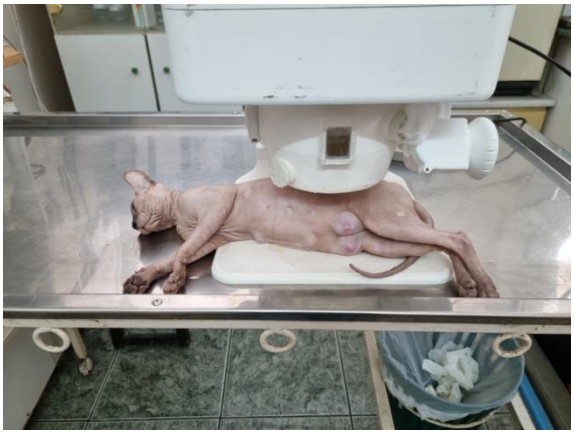

FUSVET-8 Fig. 3: Placement of cat under the system.

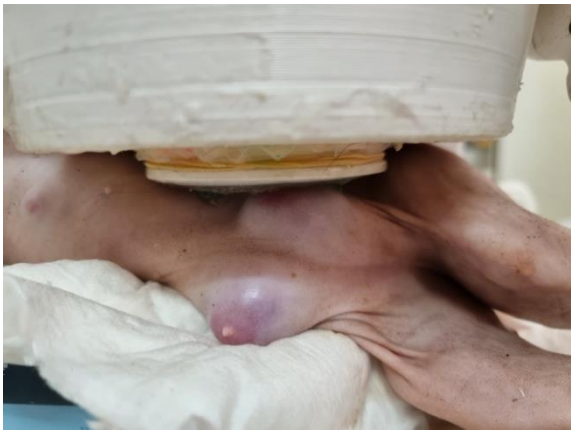

FUSVET-8 Fig. 4: Photo of coupling between the robotic system and tumour.

FUSVET-8 Fig. 5: Photo of the veterinarian and principal investigator.

Histology exams

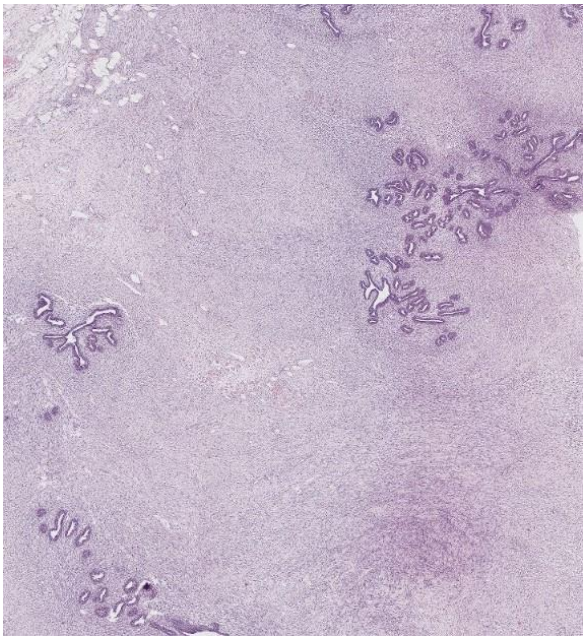

FUSVET-8 Fig. 6: Image of the histology exam.

Conclusions for histology

The architecture of cells is destroyed by thermal ultrasound. In the areas of sonication there was destruction of cancerous nuclei. In magnified areas there is evidence that a few number of nuclei remained (from histology point of view the cancer is considered fully destroyed). The tumour includes a lot of blood vessels and various ducts and possibly the ultrasound beam is highly attenuated in this cancer type. Attenuation measurements of excised tumour will reveal this hypothesis.

Experiment 9

Date: 28/07/2023

Study ID: FUSVET - 9

Referring veterinarian: [redacted]

Anaesthesia: Dexmedetomidine, Thiopental, Isoflurane

Weight: 15 Kg

Age: 6 years

Species: Dog

Name of owner: [redacted]

Tumour type: pressure-point comedones

Size of tumour: 40×40×30 mm

Procedure

1) Anaesthesia, 2) Treatment with FUS, 3) Surgical removal of tumour and biopsy

Robot: FUSVET

Transducer: F=2.75 MHz, R=65 mm, D=50 mm

Amplifier: AG1016 (T & C Power Conversion Inc.).

Focal depth: Interface (transducer to membrane distance=60 mm).

Protocol:

Pain check: Acoustic power: 1.5 W, Sonication time: 10 s

Ablation: Acoustic power: 75 W, Sonication time: 30 s

Observation: Lesion was visible on the surface of the tumour.

Biopsy procedure: Tissue placed in formalin solution and sent for biopsy (H&E). Histology revealed thermal necrosis.

Anaesthesia/monitoring Record

Date 28/07/2023	**Time** 12:00
Animal ID	FUSVET - 9
Species	Dog
Sex	M
Age (Years)	6
Weight (Kg)	15
Study	CY/EXP/PR.L09/2022
Principal Investigator	K. Alexandros Spanoudes
Time	**Anaesthesia**
12:00	Dexmedetomidine 1 mg/kg, Thiopental 5 mg/Kg, Isoflurane
13:10	Surgery ended

Time	**Heart Rate**	**Resp. Rate**	**Urination** (0 to 3)	**Absence of Movement /Pedal Reflex**	**Temp. (°C)**
12:00	100	16	0	Absent	n/a
12:10	90	19	0	Absent	n/a
12:20	100	18	0	Absent	n/a
12:30	110	20	0	Absent	n/a
12:40	90	15	0	Absent	n/a
12:50	100	17	0	Absent	n/a
13:00	110	19	0	Absent	n/a
13:10	100	14	0	Absent	n/a

Note:

The clinical staff are trained for safe anaesthesia.

The veterinarian considered multiple factors including health status, breed, age, expected pain level, and surgical plan when he planned the anaesthesia for the pet.

An accurate pet weight was obtained on the day of anaesthesia.

Follow-up

The welfare of the animal was followed-up via phone communications with the veterinarian of the pet. Follow-ups are anticipated at 1, 3, 6 and 12 months.

July 2023 – almost 1 month later

Animal is in good condition. No recurrence of the tumour yet.

September (beginning) 2023 – 3-month follow-up

Animal is in good condition. No recurrence of the tumour yet.

December (beginning) 2023 – 6-month follow-up

Animal is in good condition. No recurrence of the tumour yet.

June 2024 – 1 year follow-up

Animal is in good condition. No recurrence of the tumour yet.

FUSVET-9 Fig. 1: System at the veterinary clinic.

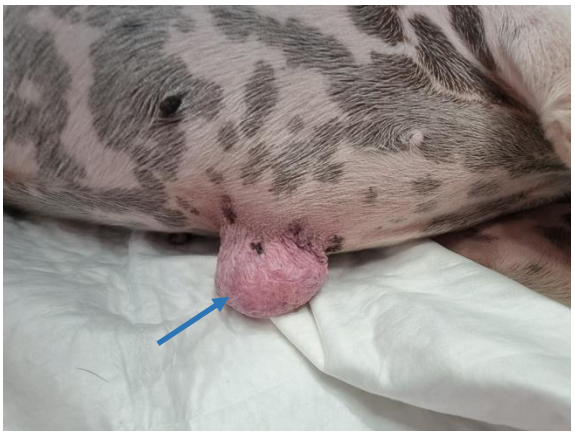

FUSVET-9 Fig. 2: Photo of the tumour (Blue arrow).

FUSVET-9 Fig. 3: Placement of dog under the system.

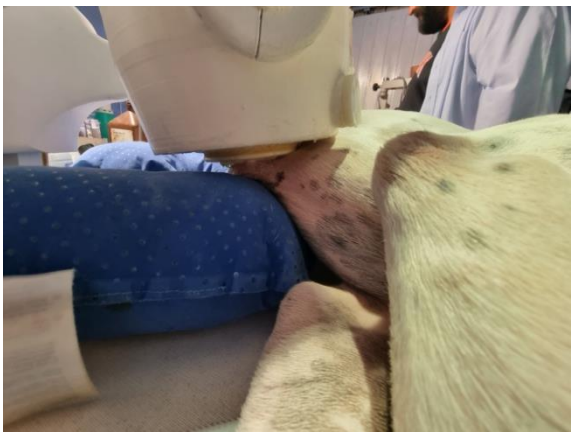

FUSVET-9 Fig. 4: Photo of coupling between the tumour and the robotic system.

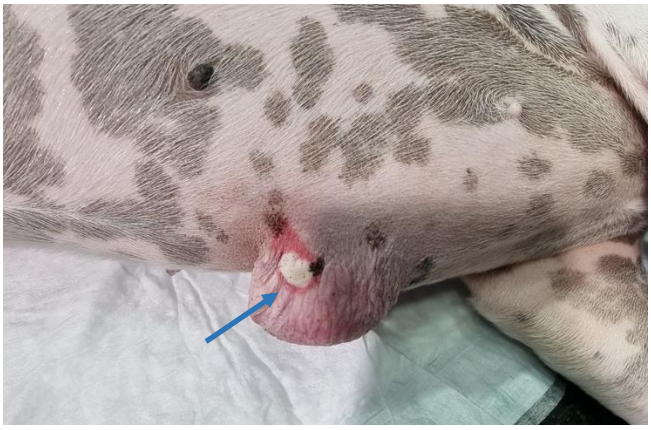

FUSVET-9 Fig. 5: Photo of the tumour after sonication showing inflicted lesion (Blue arrow).

Histology report

Page 1 of 2

N.G.N. Veterinary Pathology Consulting

Veterinary Laboratory Services
Surgical Pathology Report

GROSS DESCRIPTION

One sample of haired skin (~4.5x5x4 cm), exhibiting a soft, ulcerated paracentral mass (~4 cm in diameter)

- x1 in cassette.

HISTOLOGY

Haired skin: The dermis and subcutis are focally effaced by multiple well-demarcated, not encapsulated, expansive cystic masses. The cyst walls are composed of stratified squamous epithelium and the lumina of the cysts are filled with keratin admixed with variable numbers of degenerated cells and occasional hair shafts. The dermis between the cysts is severely thickened by the fibroblasts and deposition of collagen (fibrosis), as well as by the infiltration of a few lymphocytes and macrophages and a few plasma cells. Multifocally cysts are ruptured and, in these areas, there is severe infiltration by numerous macrophages exhibiting an eosinophilic cytoplasm and a vesicular nucleus (epithelioid). Multifocal haemorrhage is present. The epidermis covering the lesion is focally lost and replaced by polymerized fibrin entrapping erythrocytes and neutrophils (ulceration). The remaining of the epidermis is thickened with the formation of deep ridges projecting into the dermis (acanthosis) and it is covered by thick keratin (hyperkeratosis).

MORPHOLOGICAL DIAGNOSIS

Pressure-point comedones

Page 2 of 2

COMMENT

The histological changes are representing pressure-point comedones. Pressure-point comedones are common lesions in dogs resting on hard areas. Deep-chested pointers are very prone to develop such lesions. The process in this case is completely excised and the prognosis is good.

Experiment 10

Date: 29/11/2023

Study ID: FUSVET - 10

Referring veterinarian: [redacted]

Anaesthesia: Dexmedetomidine, Thiopental, Isoflurane

Weight: 9 Kg

Age: 12 years

Species: Dog

Name of owner: [redacted]

Tumour type: Sarcoma

Size of tumour: 20×20×30 mm

Procedure

1) Anaesthesia, 2) Treatment with FUS, 3) Surgical removal of tumour and biopsy

Robot: FUSVET

Transducer: F=2.75 MHz, R=65 mm, D=50 mm

Amplifier: AG1016 (T & C Power Conversion, Inc.).

Focal depth: Interface (transducer to membrane distance=60 mm).

Protocol:

Pain check: Acoustic power: 1.5 W, Sonication time: 10 s

Ablation: Acoustic power: 75 W, Sonication time: 20 s

Observation: Lesion was not visible on the surface of the tumour. Tumour included fluid inside.

Biopsy procedure: Tissue placed in formalin solution and sent for biopsy (H&E). Histology revealed thermal necrosis.

Anaesthesia/monitoring Record

Date 29/11/2023	**Time** 09:00
Animal ID	FUSVET - 10
Species	Dog
Sex	M
Age (Years)	12
Weight (Kg)	9
Study	CY/EXP/PR.L09/2022
Principal Investigator	K. Alexandros Spanoudes
Time	**Anaesthesia**
9:00	Dexmedetomidine 1 mg/kg, Thiopental 5 mg/Kg, Isoflurane
10:10	Surgery ended

Time	**Heart Rate**	**Resp. Rate**	**Urination** (0 to 3)	**Absence of Movement /Pedal Reflex**	**Temp. (°C)**
9:00	100	16	0	Absent	n/a
9:10	90	19	0	Absent	n/a
9:20	100	18	0	Absent	n/a
9:30	110	20	0	Absent	n/a
9:40	90	15	0	Absent	n/a
9:50	100	17	0	Absent	n/a
10:00	110	19	0	Absent	n/a
10:10	100	14	0	Absent	n/a

Note:

The clinical staff are trained for safe anaesthesia.

The veterinarian considered multiple factors including health status, breed, age, expected pain level, and surgical plan when he planned the anaesthesia for the pet.

An accurate pet weight was obtained on the day of anaesthesia.

Follow-up

The welfare of the animal was followed-up via phone communications with the veterinarian of the pet. Follow-ups are anticipated at 1, 3, 6 and 12 months.

December 30, 2023 – almost 1 month later

Animal is in good condition. No recurrence of the tumour yet.

February 2024 – 3 month follow-up

Animal is in good condition. No recurrence of the tumour yet.

May 2024 – 6 month follow-up

Animal is in good condition. No recurrence of the tumour yet.

November 2024 – 1 year follow-up

Animal is in good condition. No recurrence of the tumour yet.

FUSVET-10 Fig. 1: System at the veterinary clinic.

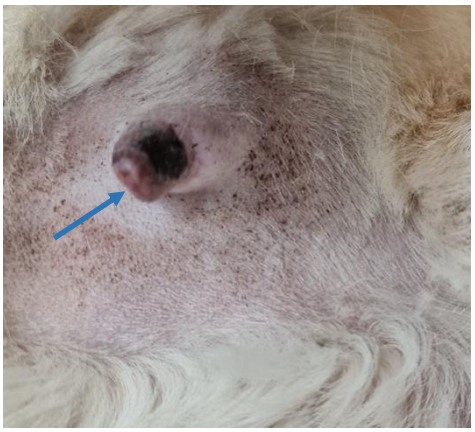

FUSVET-10 Fig. 2: Photo of the tumour (blue arrow).

FUSVET-10 Fig. 3: Placement of dog under the system.

FUSVET-10 Fig. 4: Photo of coupling between the tumour and the robotic system.

Histology exams

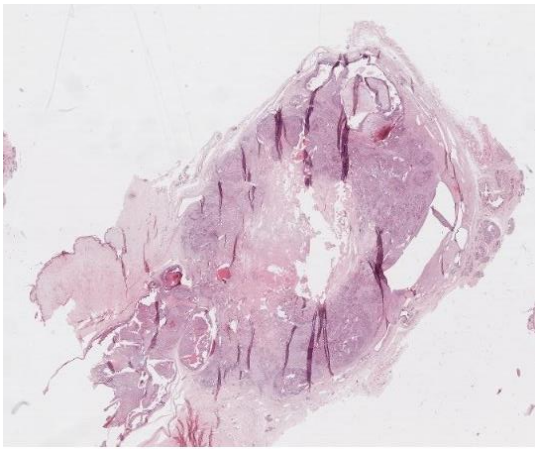

FUSVET-10 Fig. 5: Image of the histology exam.

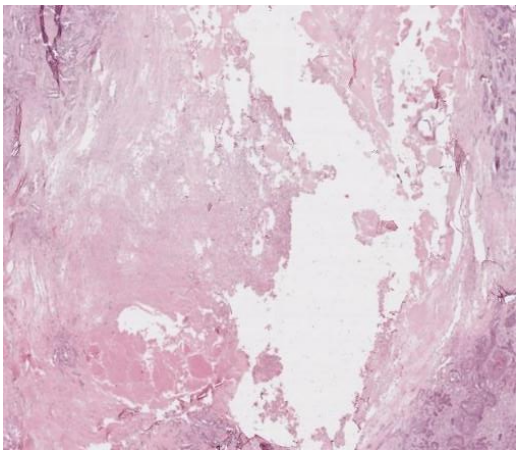

FUSVET-10 Fig. 6: Image of the histology exam.

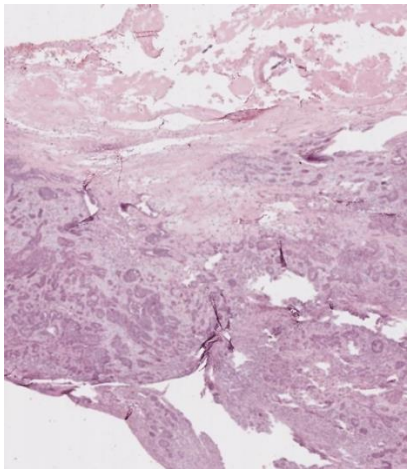

FUSVET-10 Fig. 7: Image of the histology exam.

Conclusions for histology

The architecture of cells is destroyed by thermal ultrasound. In the areas of sonication there was destruction of cancerous nuclei. In magnified areas there is evidence that a few number of nuclei remained (from histology point of view the cancer is considered fully destroyed). The tumour includes a lot of blood vessels and various ducts and possibly the ultrasound beam is highly attenuated in this cancer type. Attenuation measurements of excised tumour will reveal this hypothesis.

Experiment 11

Date: 03/01/2024

Study ID: FUSVET - 11

Referring veterinarian: [redacted]

Anaesthesia: Dexmedetomidine, Thiopental, Isoflurane

Weight: 7 Kg

Age: 10 years

Species: Dog

Name of owner: [redacted]

Tumour type: Sarcoma

Size of tumour: 20×20×30 mm

Procedure

1) Anaesthesia, 2) Treatment with FUS, 3) Surgical removal of tumour and biopsy

Robot: FUSVET

Transducer: F=2.75 MHz, R=65 mm, D=50 mm

Amplifier: AG1016 (T & C Power Conversion, Inc.).

Focal depth: Interface (transducer to membrane distance=60 mm).

Protocol:

Pain check: Acoustic power: 1.5 W, Sonication time: 10 s

Ablation: Acoustic power: 60 W, Sonication time: 15 s

Observation: Lesion was not visible on the surface of the tumour. Tumour included fluid inside.

Biopsy procedure: Tissue placed in formalin solution and sent for biopsy (H&E). Histology revealed thermal necrosis.

Anaesthesia/monitoring Record

Date 03/01/2024	**Time** 09:00
Animal ID	FUSVET - 11
Species	Dog
Sex	F
Age (Years)	10
Weight (Kg)	7
Study	CY/EXP/PR.L09/2022
Principal Investigator	K. Alexandros Spanoudes
Time	**Anaesthesia**
9:00	Dexmedetomidine 1 mg/kg, Thiopental 5 mg/Kg, Isoflurane
10:10	Surgery ended

Time	**Heart Rate**	**Resp. Rate**	**Urination** (0 to 3)	**Absence of Movement /Pedal Reflex**	**Temp. (°C)**
9:00	100	16	0	Absent	n/a
9:10	90	19	0	Absent	n/a
9:20	100	18	0	Absent	n/a
9:30	110	20	0	Absent	n/a
9:40	90	15	0	Absent	n/a
9:50	100	17	0	Absent	n/a
10:00	110	19	0	Absent	n/a
10:10	100	14	0	Absent	n/a

Note:

The clinical staff are trained for safe anaesthesia.

The veterinarian considered multiple factors including health status, breed, age, expected pain level, and surgical plan when he planned the anaesthesia for the pet.

An accurate pet weight was obtained on the day of anaesthesia.

Follow-up

The welfare of the animal was followed-up via phone communications with the veterinarian of the pet. Follow-ups are anticipated at 1, 3, 6 and 12 months.

February, 2024 – almost 1 month later

Animal is in good condition. No recurrence of the tumour yet.

April 2024 – 3 month follow-up

Animal is in good condition. No recurrence of the tumour yet.

July 2024 – 6 month follow-up

Animal is in good condition. No recurrence of the tumour yet.

January 2025 – 1 year follow-up

Animal is in good condition. No recurrence of the tumour yet.

FUSVET-11 Fig. 1: System at the veterinary clinic.

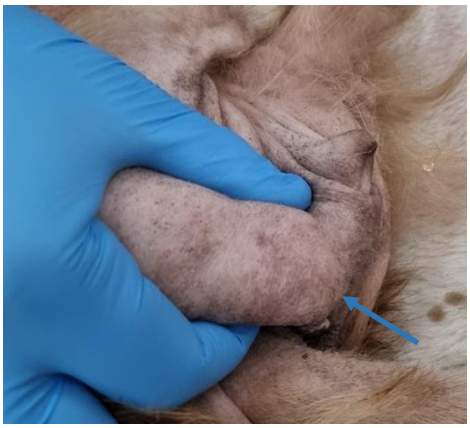

FUSVET-11 Fig. 2: Photo of the tumour (blue arrow).

FUSVET-11 Fig. 3: Placement of dog under the system.

FUSVET-11 Fig. 4: Photo of coupling between the tumour and the robotic system.

Histology exams

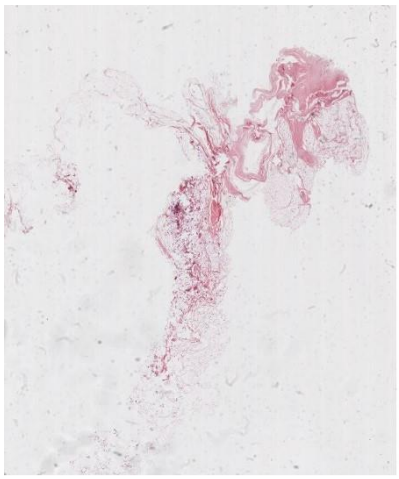

FUSVET-11 Fig. 5: Image of the histology exam.

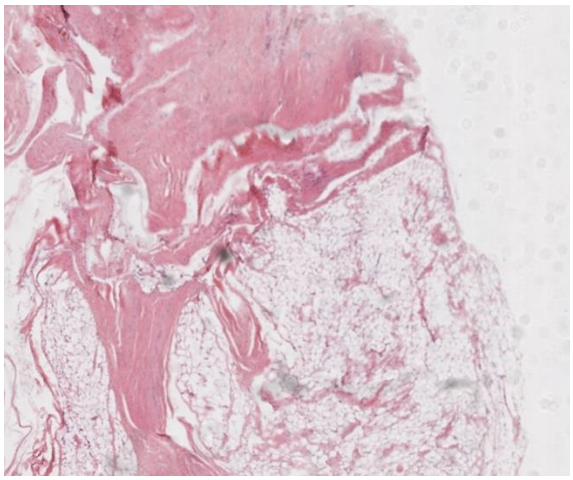

FUSVET-11 Fig. 6: Image of the histology exam.

Conclusions for histology

The architecture of cells is destroyed by thermal ultrasound. In the areas of sonication there was destruction of cancerous nuclei. In magnified areas there is evidence that a few number of nuclei remained (from histology point of view the cancer is considered fully destroyed). The tumour includes a lot of blood vessels and various ducts and possibly the ultrasound beam is highly attenuated in this cancer type. Attenuation measurements of excised tumour will reveal this hypothesis.

Experiment 12

Date: 29/01/2024

Study ID: FUSVET - 12

Referring veterinarian: [redacted]

Anaesthesia: Dexmedetomidine, Thiopental, Isoflurane

Weight: 16 Kg

Age: 11 years

Species: Dog

Name of owner: [redacted]

Tumour type: Mammary

Size of tumour: 20×40×30 mm

Procedure

1) Anaesthesia, 2) Treatment with FUS, 3) Surgical removal of tumour and biopsy

Robot: FUSVET

Transducer: F=2.75 MHz, R=65 mm, D=50 mm

Amplifier: AG1016 (T & C Power Conversion, Inc.).

Focal depth: Interface (transducer to membrane distance=60 mm).

Protocol:

Pain check: Acoustic power: 1.5 W, Sonication time: 10 s

Ablation: Acoustic power: 60 W, Sonication time: 30 s

Observation: Lesion was not visible on the surface of the tumour. Tumour included fluid inside.

Biopsy procedure: Tissue placed in formalin solution and sent for biopsy (H&E). Histology revealed thermal necrosis.

Anaesthesia/monitoring Record

Date 29/01/2024	**Time** 09:00
Animal ID	FUSVET - 12
Species	Dog
Sex	F
Age (Years)	11
Weight (Kg)	16
Study	CY/EXP/PR.L09/2022
Principal Investigator	K. Alexandros Spanoudes
Time	**Anaesthesia**
9:00	Dexmedetomidine 1 mg/kg, Thiopental 5 mg/Kg, Isoflurane
10:10	Surgery ended

Time	**Heart Rate**	**Resp. Rate**	**Urination** (0 to 3)	**Absence of Movement /Pedal Reflex**	**Temp. (°C)**
9:00	100	16	0	Absent	n/a
9:10	90	19	0	Absent	n/a
9:20	100	18	0	Absent	n/a
9:30	110	20	0	Absent	n/a
9:40	90	15	0	Absent	n/a
9:50	100	17	0	Absent	n/a
10:00	110	19	0	Absent	n/a
10:10	100	14	0	Absent	n/a

Note:

The clinical staff are trained for safe anaesthesia.

The veterinarian considered multiple factors including health status, breed, age, expected pain level, and surgical plan when he planned the anaesthesia for the pet.

An accurate pet weight was obtained on the day of anaesthesia.

Follow-up

The welfare of the animal was followed-up via phone communications with the veterinarian of the pet. Follow-ups are anticipated at 1, 3, and 6 months.

February, 2024 – almost 1 month later

Animal is in good condition. No recurrence of the tumour yet.

April 2024 – 3 month follow-up

Animal is in good condition. No recurrence of the tumour yet.

July 2024 – 6 month follow-up

Animal is in good condition. No recurrence of the tumour yet.

FUSVET-12 Fig. 1: System at the veterinary clinic.

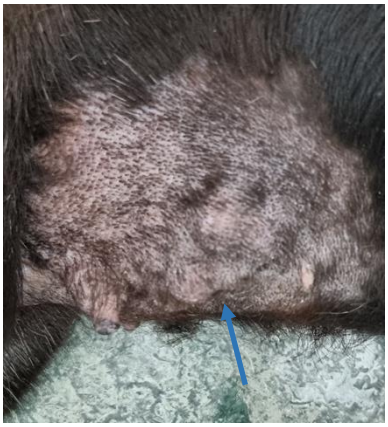

FUSVET-12 Fig. 2: Photo of the tumour (blue arrow).

FUSVET-12 Fig. 3: Placement of dog under the system.

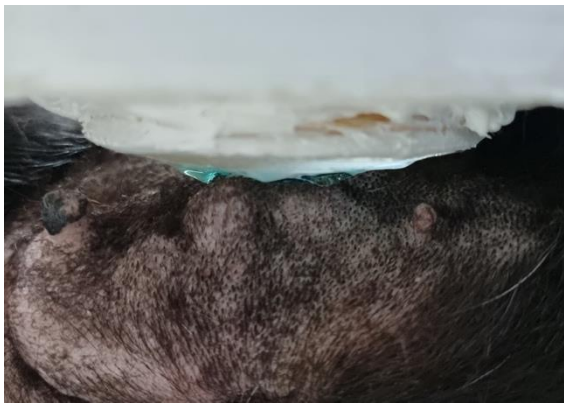

FUSVET-12 Fig. 4: Photo of coupling between the tumour and the robotic system.

Histology exams

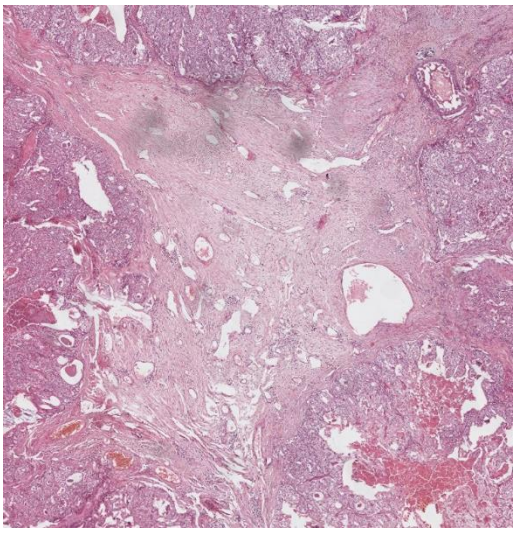

FUSVET-12 Fig. 5: Image of the histology exam.

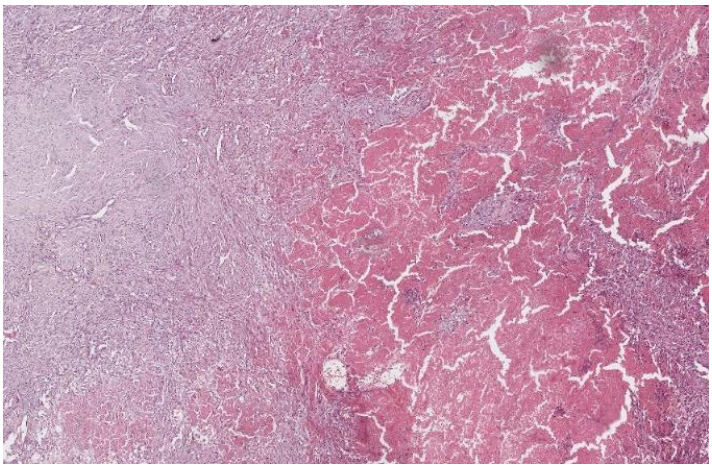

FUSVET-12 Fig. 6: Image of the histology exam.

Conclusions for histology

The architecture of cells is destroyed by thermal ultrasound. In the areas of sonication there was destruction of cancerous nuclei. In magnified areas there is evidence that a few number of nuclei remained (from histology point of view the cancer is considered fully destroyed). The tumour includes a lot of blood vessels and various ducts and possibly the ultrasound beam is highly attenuated in this cancer type. Attenuation of excised tumour will reveal this hypothesis.

Experiment 13

Date: 12/02/2024

Study ID: FUSVET - 13

Referring veterinarian: [redacted]

Anaesthesia: Dexmedetomidine, Thiopental, Isoflurane

Weight: 8 Kg

Age: 12 years

Species: Dog

Name of owner: [redacted]

Tumour type: Sarcoma

Size of tumour: 20×40×30 mm

Procedure

1) Anaesthesia, 2) Treatment with FUS, 3) Surgical removal of tumour and biopsy

Robot: FUSVET

Transducer: F=2.75 MHz, R=65 mm, D=50 mm

Amplifier: AG1016 (T & C Power Conversion Inc.).

Focal depth: Interface (transducer to membrane distance=60 mm).

Protocol:

Pain check: Acoustic power: 1.5 W, Sonication time: 10 s

Ablation: Acoustic power: 15 W, Sonication time: 20 s

Observation: Lesion was not visible on the surface of the tumour. Tumour included fluid inside.

Biopsy procedure: Tissue placed in formalin solution and sent for biopsy (H&E). Histology revealed thermal necrosis.

Anaesthesia/monitoring Record

Date 12/02/2024	**Time** 09:00
Animal ID	FUSVET - 13
Species	Dog
Sex	F
Age (Years)	12
Weight (Kg)	8
Study	CY/EXP/PR.L09/2022
Principal Investigator	K. Alexandros Spanoudes
Time	**Anaesthesia**
9:00	Dexmedetomidine 1 mg/kg, Thiopental 5 mg/Kg, Isoflurane
10:10	Surgery ended

Time	**Heart Rate**	**Resp. Rate**	**Urination** (0 to 3)	**Absence of Movement /Pedal Reflex**	**Temp. (°C)**
9:00	100	16	0	Absent	n/a
9:10	90	19	0	Absent	n/a
9:20	100	18	0	Absent	n/a
9:30	110	20	0	Absent	n/a
9:40	90	15	0	Absent	n/a
9:50	100	17	0	Absent	n/a
10:00	110	19	0	Absent	n/a
10:10	100	14	0	Absent	n/a

Note:

The clinical staff are trained for safe anaesthesia.

The veterinarian considered multiple factors including health status, breed, age, expected pain level, and surgical plan when he planned the anaesthesia for the pet.

An accurate pet weight was obtained on the day of anaesthesia.

Follow-up

The welfare of the animal was followed-up via phone communications with the veterinarian of the pet. Follow-ups are anticipated at 1, 3 and 6 months.

March 2024 – almost 1 month later

Animal is in good condition. No recurrence of the tumour yet.

May 2024 – 3 month follow-up

Animal is in good condition. No recurrence of the tumour yet.

August 2024 – 6 month follow-up

Animal is in good condition. No recurrence of the tumour yet.

FUSVET-13 Fig. 1: System at the veterinary clinic.

FUSVET-13 Fig. 2: Photo of the tumour (blue arrow).

FUSVET-13 Fig. 3: Placement of dog under the system.

FUSVET-13 Fig. 4: Photo of coupling between the tumour and the robotic system.

Histology exams

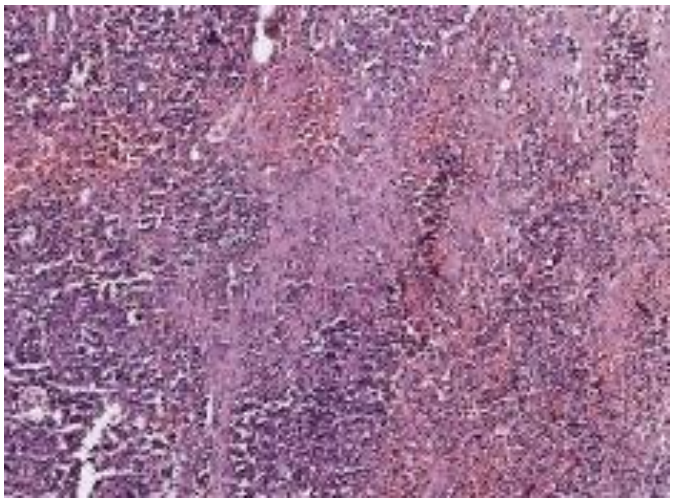

FUSVET-13 Fig. 5: Image of the histology exam.

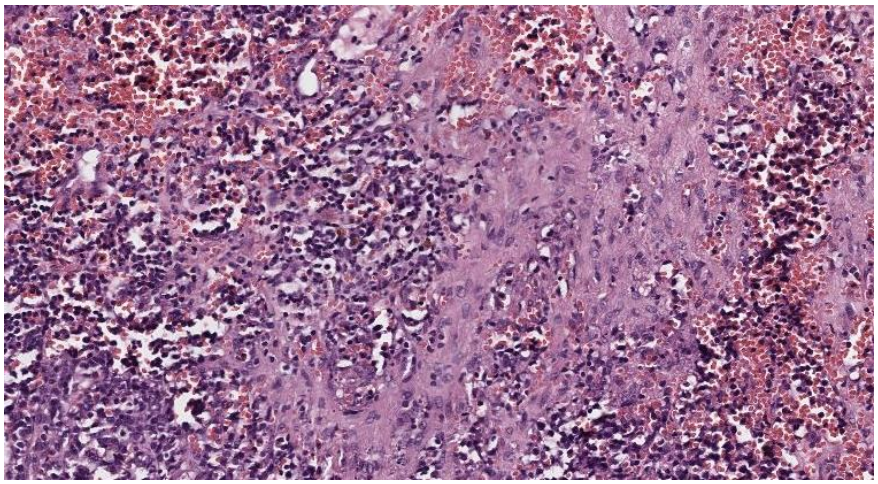

FUSVET-13 Fig. 6: Image of the histology exam.

Conclusions for histology

The architecture of cells is destroyed by thermal ultrasound. In the areas of sonication there was destruction of cancerous nuclei. In magnified areas there is evidence that a few number of nuclei remained (from histology point of view the cancer is considered fully destroyed). The tumour includes a lot of blood vessels and various ducts and possibly the ultrasound beam is highly attenuated in this cancer type. Attenuation measurements of excised tumour will reveal this hypothesis.

Experiment 14

Date: 26/03/2024

Study ID: FUSVET - 14

Referring veterinarian: [redacted]

Anaesthesia: Dexmedetomidine, Thiopental, Isoflurane

Weight: 11 Kg

Age: 10 years

Species: Dog

Name of owner: [redacted]

Tumour type: Mammary

Size of tumour: 30×20×30 mm

Procedure

1) Anaesthesia, 2) Treatment with FUS, 3) Surgical removal of tumour and biopsy

Robot: FUSVET

Transducer: F=2.75 MHz, R=65 mm, D=50 mm

Amplifier: AG1016 (T & C Power Conversion, Inc.).

Focal depth: Interface (transducer to membrane distance=60 mm).

Protocol:

Pain check: Acoustic power: 1.5 W, Sonication time: 10 s

Ablation: Acoustic power: 60 W, Sonication time: 20 s

Observation: Lesion was not visible on the surface of the tumour. Tumour included fluid inside.

Biopsy procedure: Tissue placed in formalin solution and sent for biopsy (H&E). Histology revealed thermal necrosis.

Anaesthesia/monitoring Record

Date 26/03/2024	**Time** 09:00
Animal ID	FUSVET - 14
Species	Dog
Sex	F
Age (Years)	10
Weight (Kg)	11
Study	CY/EXP/PR.L09/2022
Principal Investigator	K. Alexandros Spanoudes
Time	**Anaesthesia**
9:00	Dexmedetomidine 1 mg/kg, Thiopental 5 mg/Kg, Isoflurane
10:10	Surgery ended

Time	**Heart Rate**	**Resp. Rate**	**Urination** (0 to 3)	**Absence of Movement /Pedal Reflex**	**Temp. (°C)**
9:00	100	16	0	Absent	n/a
9:10	90	19	0	Absent	n/a
9:20	100	18	0	Absent	n/a
9:30	110	20	0	Absent	n/a
9:40	90	15	0	Absent	n/a
9:50	100	17	0	Absent	n/a
10:00	110	19	0	Absent	n/a
10:10	100	14	0	Absent	n/a

Note:

The clinical staff are trained for safe anaesthesia.

The veterinarian considered multiple factors including health status, breed, age, expected pain level, and surgical plan when he planned the anaesthesia for the pet.

An accurate pet weight was obtained on the day of anaesthesia.

Follow-up

The welfare of the animal was followed-up via phone communications with the veterinarian of the pet. Follow-ups are anticipated at 1, 3 and 6 months.

April 2024 – almost 1 month later

Animal is in good condition. No recurrence of the tumour yet.

June 2024 – 3 month follow-up

Animal is in good condition. No recurrence of the tumour yet.

September 2024 – 6 month follow-up

Animal is in good condition. No recurrence of the tumour yet.

FUSVET-14 Fig. 1: System at the veterinary clinic.

FUSVET-14 Fig. 2: Photo of the tumour (blue arrow).

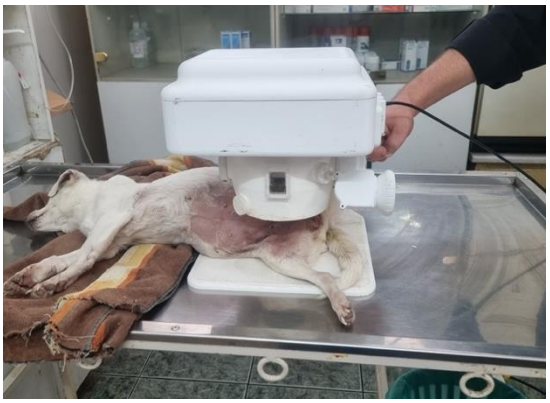

FUSVET-14 Fig. 3: Photo of dog under the system.

FUSVET-14 Fig. 4: Photo of coupling between the tumour and the robotic system.

Histology exams

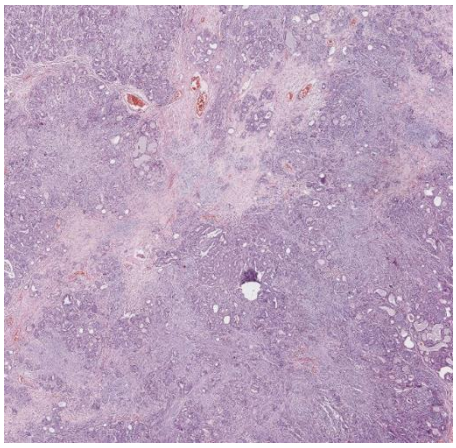

FUSVET-14 Fig. 5: Image of the histology exam.

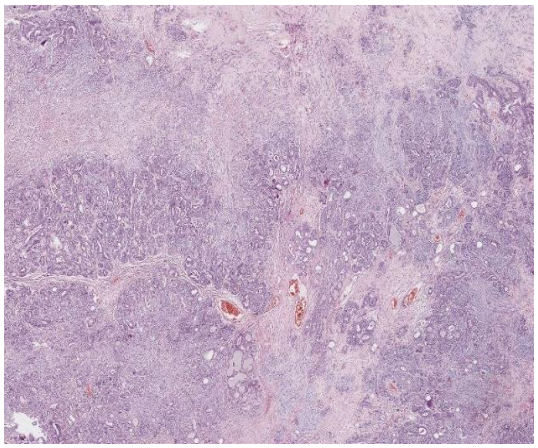

FUSVET-14 Fig. 6: Image of the histology exam.

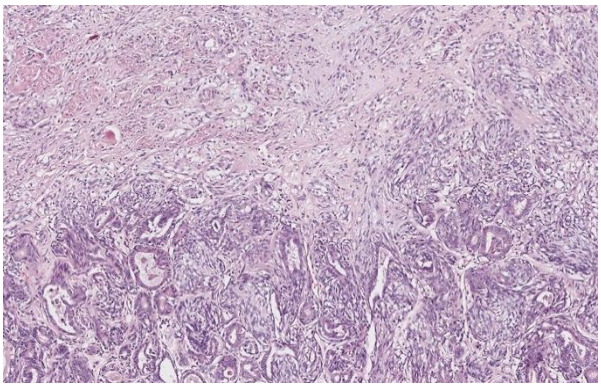

FUSVET-14 Fig. 7: Image of the histology exam.

Conclusions for histology

The architecture of cells is destroyed by thermal ultrasound. In the areas of sonication there was destruction of cancerous nuclei. In magnified areas there is evidence that a few number of nuclei remained (from histology point of view the cancer is considered fully destroyed). The tumour includes a lot of blood vessels and various ducts and possibly the ultrasound beam is highly attenuated in this cancer type. Attenuation measurements of excised tumour will reveal this hypothesis.

Experiment 15

Date: 07/05/2024

Study ID: FUSVET - 15

Referring veterinarian: [redacted]

Anaesthesia: Dexmedetomidine, Thiopental, Isoflurane

Weight: 8 Kg

Age: 6 years

Species: Dog

Name of owner: [redacted]

Tumour type: Lipoma

Size of tumour: 60×45×30 mm

Procedure

1) Anaesthesia, 2) Treatment with FUS, 3) Surgical removal of tumour and biopsy

Robot: FUSVET

Transducer: F=2.75 MHz, R=65 mm, D=50 mm

Amplifier: AG1016 (T & C Power Conversion, Inc.).

Focal depth: Interface (transducer to membrane distance=60 mm).

Protocol:

Pain check: Acoustic power: 1.5 W, Sonication time: 10 s

Ablation: Acoustic power: 60 W, Sonication time: 20 s

Observation: Lesion was not visible on the surface of the tumour. Tumour included fluid inside.

Biopsy procedure: Tissue placed in formalin solution and sent for biopsy (H&E). Histology revealed thermal necrosis.

Anaesthesia/monitoring Record

Date 07/05/2024	**Time** 09:00
Animal ID	FUSVET - 15
Species	Dog
Sex	M
Age (Years)	6
Weight (Kg)	8
Study	CY/EXP/PR.L09/2022
Principal Investigator	K. Alexandros Spanoudes
Time	**Anaesthesia**
9:00	Dexmedetomidine 1 mg/kg, Thiopental 5 mg/Kg, Isoflurane
10:10	Surgery ended

Time	**Heart Rate**	**Resp. Rate**	**Urination** (0 to 3)	**Absence of Movement /Pedal Reflex**	**Temp. (°C)**
9:00	100	16	0	Absent	n/a
9:10	90	19	0	Absent	n/a
9:20	100	18	0	Absent	n/a
9:30	110	20	0	Absent	n/a
9:40	90	15	0	Absent	n/a
9:50	100	17	0	Absent	n/a
10:00	110	19	0	Absent	n/a
10:10	100	14	0	Absent	n/a

Note:

The clinical staff are trained for safe anaesthesia.

The veterinarian considered multiple factors including health status, breed, age, expected pain level, and surgical plan when he planned the anaesthesia for the pet.

An accurate pet weight was obtained on the day of anaesthesia.

Follow-up

The welfare of the animal was followed-up via phone communications with the veterinarian of the pet. Follow-ups are anticipated at 1, 3 and 6 months.

May 2024 – almost 1 month later

Animal is in good condition. No recurrence of the tumour yet.

July 2024 – 3 month follow-up

Animal is in good condition. No recurrence of the tumour yet.

October 2024 – 6 month follow-up

Animal is in good condition. No recurrence of the tumour yet.

FUSVET-15 Fig. 1: System at the veterinary clinic.

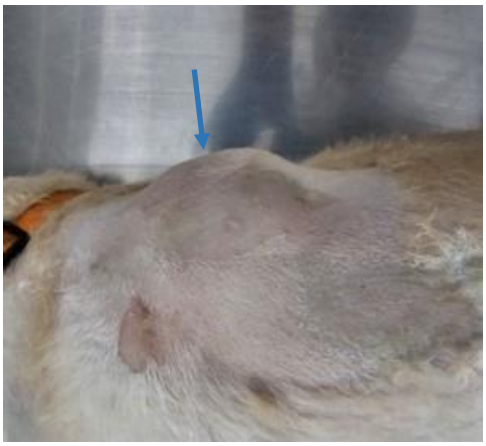

FUSVET-15 Fig. 2: Photo of the tumour (blue arrow).

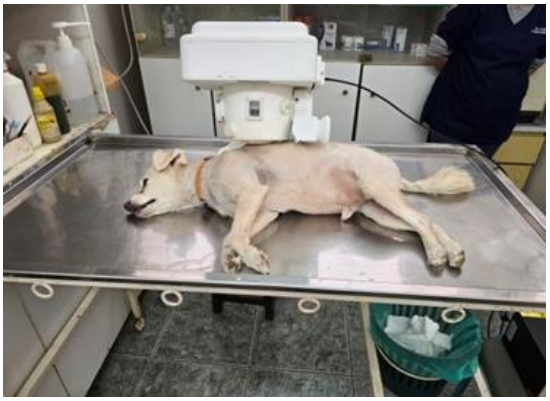

FUSVET-15 Fig. 3: Photo of dog under the system.

FUSVET-15 Fig. 4: Photo of coupling between the tumour and the robotic system.

Histology exams

FUSVET-15 Fig. 5: Image of the histology exam.

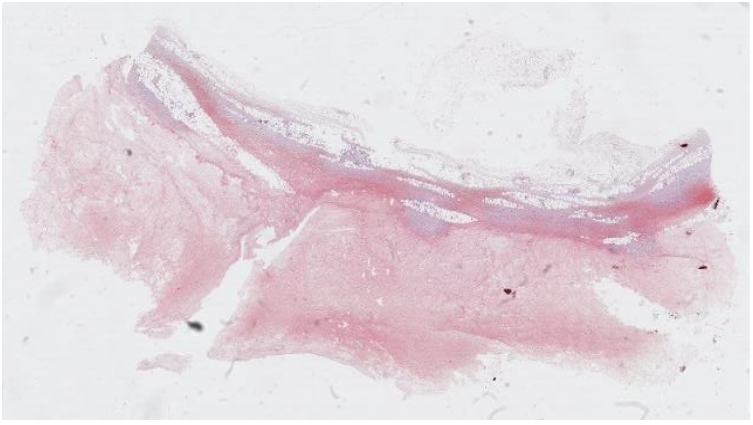

FUSVET-15 Fig. 6: Image of the histology exam.

Conclusions for histology

The architecture of cells is destroyed by thermal ultrasound. In the areas of sonication there was destruction of cancerous nuclei. In magnified areas there is evidence that a few number of nuclei remained (from histology point of view the cancer is considered fully destroyed). The tumour includes a lot of blood vessels and various ducts and possibly the ultrasound beam is highly attenuated in this cancer type. Attenuation measurements of excised tumour will reveal this hypothesis.

Experiment 16

Date: 18/07/2024

Study ID: FUSVET - 16

Referring veterinarian: [redacted]

Anaesthesia: Dexmedetomidine, Thiopental, Isoflurane

Weight: 10 Kg

Age: 10 years

Species: Dog

Name of owner: [redacted]

Tumour type: Lipoma

Size of tumour: 30×20×30 mm

Procedure

1) Anaesthesia, 2) Treatment with FUS, 3) Surgical removal of tumour and biopsy

Robot: FUSVET

Transducer: F=2.75 MHz, R=65 mm, D=50 mm

Amplifier: AG1016 (T & C Power Conversion, Inc.).

Focal depth: Interface (transducer to membrane distance=60 mm).

Protocol:

Pain check: Acoustic power: 1.5 W, Sonication time: 10 s

Ablation: Acoustic power: 60 W, Sonication time: 20 s

Observation: Lesion was not visible on the surface of the tumour. Tumour included fluid inside.

Biopsy procedure: Tissue placed in formalin solution and sent for biopsy (H&E). Histology revealed thermal necrosis.

Anaesthesia/monitoring Record

Date 18/07/2024	**Time** 09:00
Animal ID	FUSVET - 16
Species	Dog
Sex	M
Age (Years)	10
Weight (Kg)	10
Study	CY/EXP/PR.L09/2022
Principal Investigator	K. Alexandros Spanoudes
Time	**Anaesthesia**
9:00	Dexmedetomidine 1 mg/kg, Thiopental 5 mg/Kg, Isoflurane
10:10	Surgery ended

Time	**Heart Rate**	**Resp. Rate**	**Urination** (0 to 3)	**Absence of Movement /Pedal Reflex**	**Temp. (°C)**
9:00	100	16	0	Absent	n/a
9:10	90	19	0	Absent	n/a
9:20	100	18	0	Absent	n/a
9:30	110	20	0	Absent	n/a
9:40	90	15	0	Absent	n/a
9:50	100	17	0	Absent	n/a
10:00	110	19	0	Absent	n/a
10:10	100	14	0	Absent	n/a

Note:

The clinical staff are trained for safe anaesthesia.

The veterinarian considered multiple factors including health status, breed, age, expected pain level, and surgical plan when he planned the anaesthesia for the pet.

An accurate pet weight was obtained on the day of anaesthesia.

Follow-up

The welfare of the animal was followed-up via phone communications with the veterinarian of the pet. Follow-ups are anticipated at 1, 3 and 6 months.

May 2024 – almost 1 month later

Animal is in good condition. No recurrence of the tumour yet.

July 2024 – 3 month follow-up

Animal is in good condition. No recurrence of the tumour yet.

October 2024 – 6 month follow-up

Animal is in good condition. No recurrence of the tumour yet.

FUSVET-16 Fig. 1: System at the veterinary clinic.

FUSVET-16 Fig. 2: Photo of the tumour (blue arrow).

FUSVET-16 Fig. 3: Photo of dog under the system.

FUSVET-16 Fig. 4: Photo of coupling between the tumour and the robotic system.

Histology exams

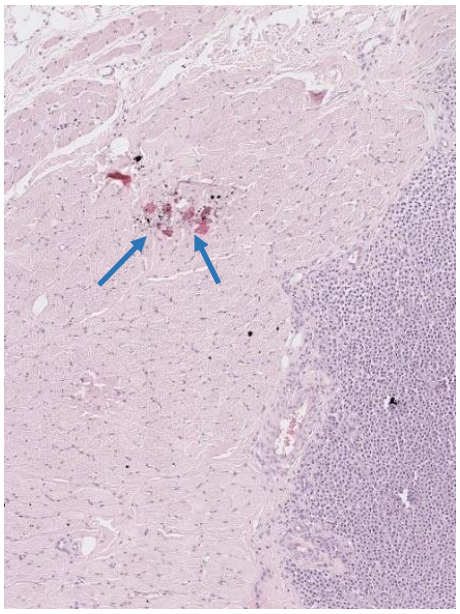

FUSVET-16 Fig. 5: Image of the histology exam. Arrows show blood coagulation within necrotic area.

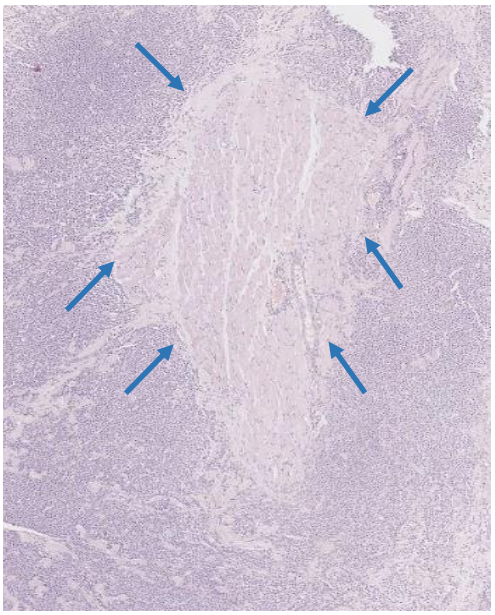

FUSVET-16 Fig. 6: Image of the histology exam. Arrows show necrosis.

Conclusions for histology

The architecture of cells is destroyed by thermal ultrasound. In the areas of sonication there was destruction of cancerous nuclei. In magnified areas there is evidence that a few number of nuclei remained (from histology point of view the cancer is considered fully destroyed). The tumour includes a lot of blood vessels and various ducts and possibly the ultrasound beam is highly attenuated in this cancer type. Attenuation measurements of excised tumour will reveal this hypothesis.

Experiment 17

Date: 17/10/2024

Study ID: FUSVET - 17

Referring veterinarian: [redacted]

Anaesthesia: Dexmedetomidine, Thiopental, Isoflurane

Weight: 10 Kg

Age: 13 years

Species: Dog

Name of owner: [redacted]

Tumour type: Lipoma

Size of tumour: 30×25×30 mm

Procedure

1) Anaesthesia, 2) Treatment with FUS, 3) Surgical removal of tumour and biopsy

Robot: FUSVET

Transducer: F=2.75 MHz, R=65 mm, D=50 mm

Amplifier: AG1016 (T & C Power Conversion, Inc.).

Focal depth: Interface (transducer to membrane distance=60 mm).

Protocol:

Pain check: Acoustic power: 1.5 W, Sonication time: 10 s

Ablation: Acoustic power: 60 W, Sonication time: 20 s

Observation: Lesion was not visible on the surface of the tumour. Tumour included fluid inside.

Biopsy procedure: Tissue placed in formalin solution and sent for biopsy (H&E). Histology revealed thermal necrosis.

Anaesthesia/monitoring Record

Date 17/10/2024	**Time** 09:00
Animal ID	FUSVET - 17
Species	Dog
Sex	M
Age (Years)	13
Weight (Kg)	10
Study	CY/EXP/PR.L09/2022
Principal Investigator	K. Alexandros Spanoudes
Time	**Anaesthesia**
09:00	Dexmedetomidine 1 mg/kg, Thiopental 5 mg/Kg, Isoflurane
10:10	Surgery ended

Time	**Heart Rate**	**Resp. Rate**	**Urination** (0 to 3)	**Absence of Movement /Pedal Reflex**	**Temp. (°C)**
09:00	100	16	0	Absent	n/a
09:10	90	19	0	Absent	n/a
09:20	100	18	0	Absent	n/a
09:30	110	20	0	Absent	n/a
09:40	90	15	0	Absent	n/a
09:50	100	17	0	Absent	n/a
09:00	110	19	0	Absent	n/a
10:10	100	14	0	Absent	n/a

Note:

The clinical staff are trained for safe anaesthesia.

The veterinarian considered multiple factors including health status, breed, age, expected pain level, and surgical plan when he planned the anaesthesia for the pet.

An accurate pet weight was obtained on the day of anaesthesia.

Follow-up

The welfare of the animal was followed-up via phone communications with the veterinarian of the pet. Follow-ups are anticipated at 1 and 3 months.

November 2024 – almost 1 month later

Animal is in good condition. No recurrence of the tumour yet.

January 2025 – 3 month follow-up

Animal is in good condition. No recurrence of the tumour yet.

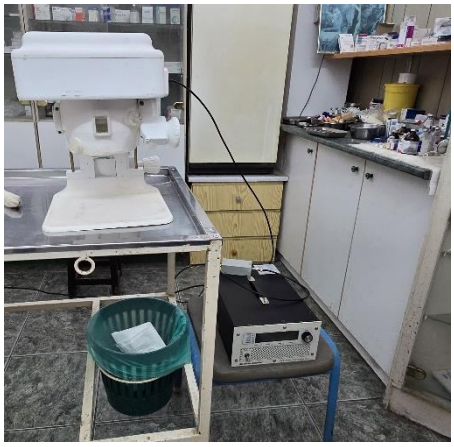

FUSVET-17 Fig. 1: System at the veterinary clinic.

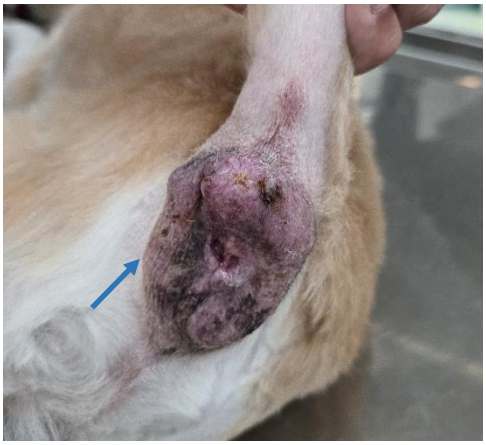

FUSVET-17 Fig. 2: Photo of the tumour (blue arrow).

FUSVET-17 Fig. 3: Photo of dog under the system.

FUSVET-17 Fig. 4: Photo of coupling between the tumour and the robotic system.

Histology exams

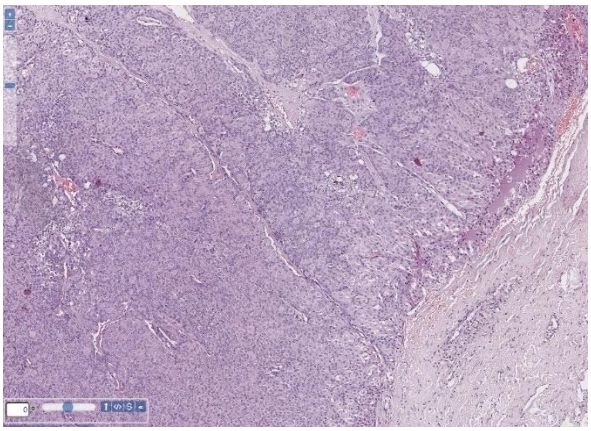

FUSVET-17 Fig. 5: Image of the histology exam.

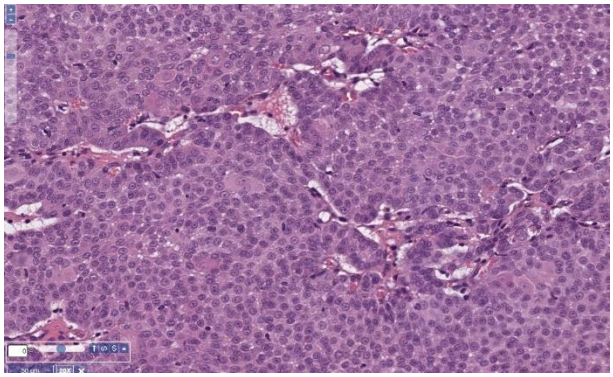

FUSVET-17 Fig. 6: Image of the histology exam.

Conclusions for histology

The architecture of cells is destroyed by thermal ultrasound. In the areas of sonication there was destruction of cancerous nuclei. In magnified areas there is evidence that a few number of nuclei remained (from histology point of view the cancer is considered fully destroyed). The tumour includes a lot of blood vessels and various ducts and possibly the ultrasound beam is highly attenuated in this cancer type. Attenuation measurements of excised tumour will reveal this hypothesis.

Experiment 18

Date: 11/12/2024

Study ID: FUSVET - 18

Referring veterinarian: [redacted]

Anaesthesia: Dexmedetomidine, Thiopental, Isoflurane

Weight: 11 Kg

Age: 12 years

Species: Dog

Name of owner: [redacted]

Tumour type: Lipoma

Size of tumour: 30×40×30 mm

Procedure

1) Anaesthesia, 2) Treatment with FUS, 3) Surgical removal of tumour and biopsy

Robot: FUSVET

Transducer: F=2.75 MHz, R=65 mm, D=50 mm

Amplifier: AG1016 (T & C Power Conversion, Inc.).

Driving system: Electronic driving system

Focal depth: Interface (transducer to membrane distance=60 mm).

Protocol:

Pain check: Acoustic power: 1.5 W, Sonication time: 10 s

Ablation: Grid: 3×3, Step: 3 mm, Acoustic power: 60 W, Sonication time: 30 s, Delay: 60s

Observation: Lesion was not visible on the surface of the tumour. Tumour included fluid inside.

Biopsy procedure: Tissue placed in formalin solution and sent for biopsy (H&E). Histology revealed thermal necrosis.

Anaesthesia/monitoring Record

Date 11/12/2024	**Time** 09:00
Animal ID	FUSVET - 18
Species	Dog
Sex	M
Age (Years)	12
Weight (Kg)	11
Study	CY/EXP/PR.L09/2022
Principal Investigator	K. Alexandros Spanoudes
Time	**Anaesthesia**
09:00	Dexmedetomidine 1 mg/kg, Thiopental 5 mg/Kg, Isoflurane
10:10	Surgery ended

Time	**Heart Rate**	**Resp. Rate**	**Urination** (0 to 3)	**Absence of Movement /Pedal Reflex**	**Temp. (°C)**
09:00	100	16	0	Absent	n/a
09:10	90	19	0	Absent	n/a
09:20	100	18	0	Absent	n/a
09:30	110	20	0	Absent	n/a
09:40	90	15	0	Absent	n/a
09:50	100	17	0	Absent	n/a
10:00	110	19	0	Absent	n/a
10:10	100	14	0	Absent	n/a

Note:

The clinical staff are trained for safe anaesthesia.

The veterinarian considered multiple factors including health status, breed, age, expected pain level, and surgical plan when he planned the anaesthesia for the pet.

An accurate pet weight was obtained on the day of anaesthesia.

Follow-up

The welfare of the animal was followed-up via phone communications with the veterinarian of the pet. Follow-ups are anticipated at 1 month.

January 2025 – almost 1 month later

Animal is in good condition. No recurrence of the tumour yet.

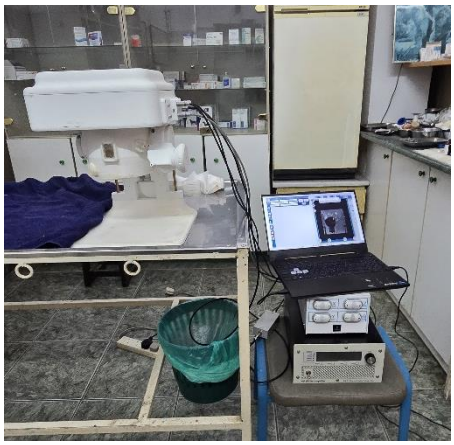

FUSVET-18 Fig. 1: System at the veterinary clinic.

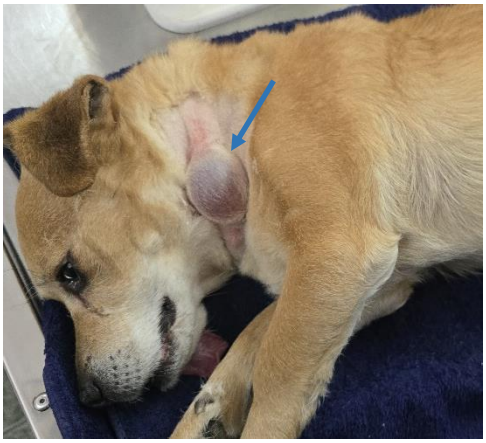

FUSVET-18 Fig. 2: Photo of the tumour (blue arrow).

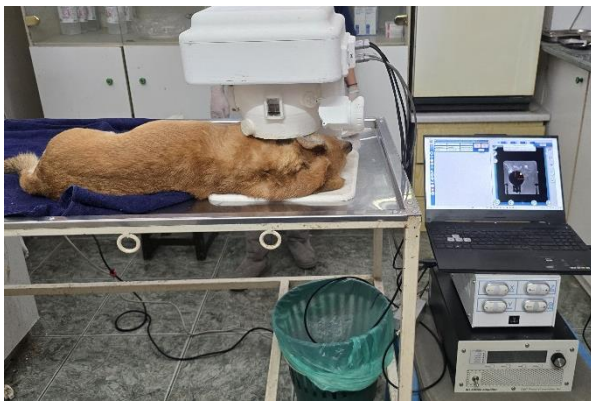

FUSVET-18 Fig. 3: Photo of dog under the system.

FUSVET-18 Fig. 4: Photo of coupling between the tumour and the robotic system.

Histology exams

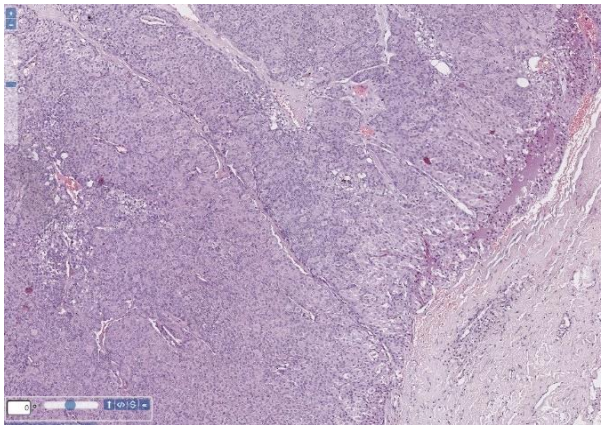

FUSVET-18 Fig. 5: Image of the histology exam.

Conclusions for histology

The architecture of cells is destroyed by thermal ultrasound. In the areas of sonication, there was destruction of cancerous nuclei. In magnified areas there is evidence that a few number of nuclei remained (from histology point of view the cancer is considered fully destroyed). The tumour includes a lot of blood vessels and various ducts and possibly the ultrasound beam is highly attenuated in this cancer type. Attenuation measurements of excised tumour will reveal this hypothesis.